الجمهورية
الجزائرية الديمقراطية الشعبية

PEOPLE'S DEMOCRATIC REPUBLIC OF ALGERIA

وزارة التعليم العالي
و البحث العلمي

MINISTRY OF HIGHER EDUCATION AND SCIENTIFIC RESEARCH

جامعة أبي بكر بلقايد –
تلمسان –

UNIVERSITY OF ABOU-BEKR BELKAID, TLEMCEN

FACULTY OF TECHNOLOGY

THESIS

Presented for the obtaining of a **Master’s Degree**

In: Civil Engineering

Specialty: Transportation and Public Works

By: Nthoka Scolasticah Mutheu

MASTER’S THESIS THEME:

THE DESIGN AND THE STUDY OF A PRE-STRESSED CONCRETE BEAM BRIDGE PK7

Publicly defended, on, 15th September, 2024. In front of a jury composed of:

Dr. Moulay Idris TABET DERRAZ	University of Tlemcen	President
Dr. Fatima AYAD	University of Tlemcen	Examiner
Dr. Nadia HAMIMED	University of Tlemcen	Supervisor
Mr. Ismail BABA AHMED	University of Tlemcen	Co-Supervisor

Academic Year: 2023 /2024

ACKNOWLEDGEMENTS

I wish to earnestly, express my gratitude to my supervisor Dr. Nadia HAMIMED, for her unending support, for her patience, for her motivation to keep going always and for staying positive throughout this journey. I also want to sincerely thank Mr. Ismail Chems Eddine BABA AHMED, the co-supervisor, for his perpetual efforts and invaluable technical help on my thesis research.

To the SEROR fraternity, especially Engineer Chiali Nadir, their assistance and guidance on this project were really valuable and of great aid to my project.

To the professors at the University of Tlemcen, Mr. Boumechra Nadir and our year head, Dr. Fethi Hamzoui, I would like to express my appreciation for their support while writing this thesis.

To the University of Tlemcen fraternity and all the professors, especially in the civil engineering department, I would like to sincerely thank them for their support throughout my studies and for shaping my academic life.

To my classmates, the class of 2023/2024, I would like to genuinely appreciate them for their unwavering support, motivation, love and friendship, which kept us going.

Lastly, I would like to wholeheartedly thank my family and friends for their support and encouragement during this journey and for believing in me.

DEDICATION

I would like to thank the Almighty God for this thesis research and therefore i dedicate it to:

My parents Mr. Nicholas Nthoka Ndambuki and Mrs. Zipporah Nduki Daniel.

My siblings Neema, Bill and Winnie.

My friends and professors who encouraged me during the writing of this thesis.

ABSTRACT

The focus of this Master's thesis is the design and study of a pre-stressed concrete beam bridge located in the El-Bayadh Wilaya in Algeria, PK7. There are two crossing conditions, but in our thesis study, we shall focus on the crossing condition where the bridge passes over a railway line and not under it because of the natural flooding risks in the region. The bridge has a single span of 33.40m. This thesis research has several chapters, which talk about the project's presentation, the characteristics of the construction materials used, the pre-sizing of the beam, the lowering of loads, prestressing, and a few others. The SAP software, together with other civil engineering principles such as 'guyon-massonet' and Algerian/French guidelines were used in this thesis from the dimensioning to the evaluation of the results to verify the project's viability.

Keywords: *Pre-stressed Beam, Single-Span Bridge, Reinforced Concrete, Dead Loads, Live-Loads, Pre-stressing Cables*.

RÉSUMÉ

L'objet de ce mémoire de master porte sur la conception et l'étude d'un pont à poutres en béton précontraint situé dans la wilaya d'El-Bayadh en Algérie, PK7. Il existe deux conditions de franchissement, mais dans notre étude de thèse, nous nous concentrerons sur la condition de franchissement où le pont passe au-dessus d'une voie ferrée et non en dessous en raison des risques naturels d'inondation dans la région. Le pont a une travée unique de 33,40 m. Cette thèse de recherche comporte plusieurs chapitres, qui parlent de la présentation du projet, des caractéristiques des matériaux de construction utilisés, du prédimensionnement de la poutre, de l'abaissement des charges, de la précontrainte, des appuis et quelques autres. Le logiciel SAP, ainsi que d'autres principes du génie civil tels que « guyon-massonet » et les directives algériennes/françaises ont été utilisés dans cette thèse depuis le dimensionnement jusqu'à l'évaluation des résultats afin de vérifier la viabilité de ce projet.

Mots clés: *Poutre précontrainte, pont à travée unique, béton armé, charges permanentes, surcharges , câbles de précontrainte.*

خلاصة

تهدف هذه المذكرة إلى تصميم ودراسة جسر عوارض خرسانية مسبقة الصنع يقع بولاية البيض بالجزائر على طريق PK7. هناك حالتان للعبور، ولكن في دراستنا سنركز على الحالة التي يمر فيها الجسر فوق سكة حديدية بدلاً من مروره تحتها بسبب مخاطر الفيضانات الطبيعية في المنطقة .يتكون الجسر من امتداد واحد يبلغ 33.40 مترًا .تتضمن أطروحة البحث هذه عدة فصول، تتحدث عن عرض المشروع، وخصائص مواد البناء المستخدمة، والتصميم الأولي للعارضة، والأحمال، والتجهيز المسبق، والدعامات، وبعض المواضيع الأخرى .تم استخدام برنامج SAP بالإضافة إلى مبادئ الهندسة المدنية مثل « Guyon-Massonet » في هذه الأطروحة من الفرنسية/ والمعايير الجزائرية التصميم إلى تقييم النتائج للتحقق من جدوى هذا المشروع.

الكلمات المفتاحية : عوارض مسبقة الإجهاد، جسر ذو امتداد واحد، خرسانة مسلحة، أحمال ميتة، أحمال حية، كابلات مسبقة الإجهاد..

Table of Contents

Table of Contents

Table of Contents

Table of Contents

List of Figures

List of Figures

List of Tables

The bridge-building technology traces back to the Romans, the Babylonians, the ancient Egyptians and ever since, the bridge construction has revolutionized. The soul-purpose of this technology has been the same, to facilitate the crossing over an obstacle. There are many types of bridges such as suspension bridges, cable-stayed bridges and many others.

In the wilaya of El Bayadh, a bridge had to be constructed to facilitate the crossing of a railway line heading towards Mechria and El-Bayadh. The bridge is linked to a roadway running from Goulet Sendel to Tousmouline.

Figure 0.1: A map showing El Bayadh Wilaya

Source: www.mapsofindia.com

In this thesis, we shall explore a prestressed post-tensioned beam bridge, which was constructed to curb the crossing conditions of a railway track. To understand more details on this bridge, a study and the design of this bridge was done.

Chapters in this thesis include:

- The presentation of the project
- The materials used
- The pre-sizing and lowering of loads

- The prestressing
- The reinforcement of the beam
- The study of the slab

Each chapter is detailed with a discussion, starting with an introduction, relevant sub-chapters with tables and figures for better comprehension and a conclusion.

It is important to note that this project was realized by SEROR, under the request of DTP. The necessary steps to execute this project were carried out from the feasibility, surveys to the commissioning of the project, with different parties playing their respective roles

Chapter 1:
The Presentation of the Project

1.1 Introduction

A bridge is a spanning structure carrying a road, a path, or a railway, that facilitates the crossing of a physical obstacle like a railway line, a river, or a road (Designing Buildings 2015). In our project, the bridge carries a roadway across an obstacle which is a railway. This chapter entails various topics that will help to understand our project better from various perspectives that will enable us in the detailed study of our chosen solution.

1.2 Presentation of the Structure

This project is about a prestressed concrete beam bridge that passes over a railway line. The bridge is located in the El Bayadh Wilaya, while the 130-km railway line runs between the wilaya of Mechria and El Bayadh. The bridge is a single-span bridge with a length of 33.4m and a width of 10.5m.

1.3 Crossing Condition

The point of intersection between the railway and the bridge creates a black point, which is to be avoided. This led to the search for an optimal solution that meets the technical, economic, and environmental aspects. There were two proposed options for the intersection point, whereby:

- The road could pass under the railway track.
- The road could pass over the railway track.

The DTP rejected the first option of the road passing under the bridge because the site is prone to flooding risks. Therefore, the second option of the road passing over the railway track was adopted, hence the need for a bridge to facilitate the crossing.

1.4 Functional Data

The functional data is necessary to ensure that all the essential characteristics of the bridge design are taken into consideration to make sure that it serves its intended purpose. To characterize the geometry of the bridge track, we need three key elements which are;

- The plan layout,
- The longitudinal profile

- The cross profile.

1.4.1 The Plan Layout

This layout enables us to establish the alignment of the track axis of the bridge. In most cases, the alignment is to be straight and not curved. In our case, we have a curved alignment but straight girders were used in the bridge construction.

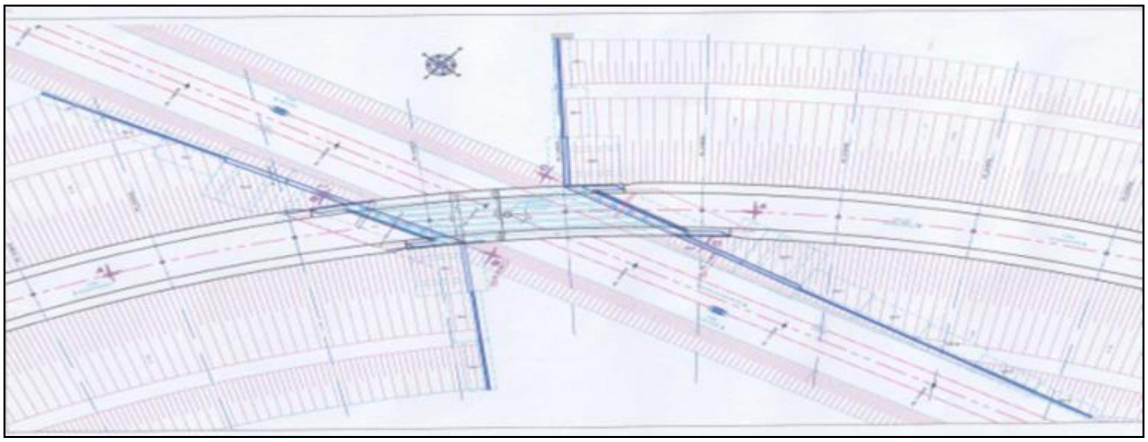

Figure 0.2: The plan layout from the Top view

1.4.2 The Longitudinal Profile

From the side view or elevation view, we can see the longitudinal profile of the bridge as a long geometric line track with altimetry differences. It is deduced from a couple of factors which are: the different altitudes, partial distances, cumulative distances, slopes, alignments and curves. The earth layout influences the longitudinal profile plan.

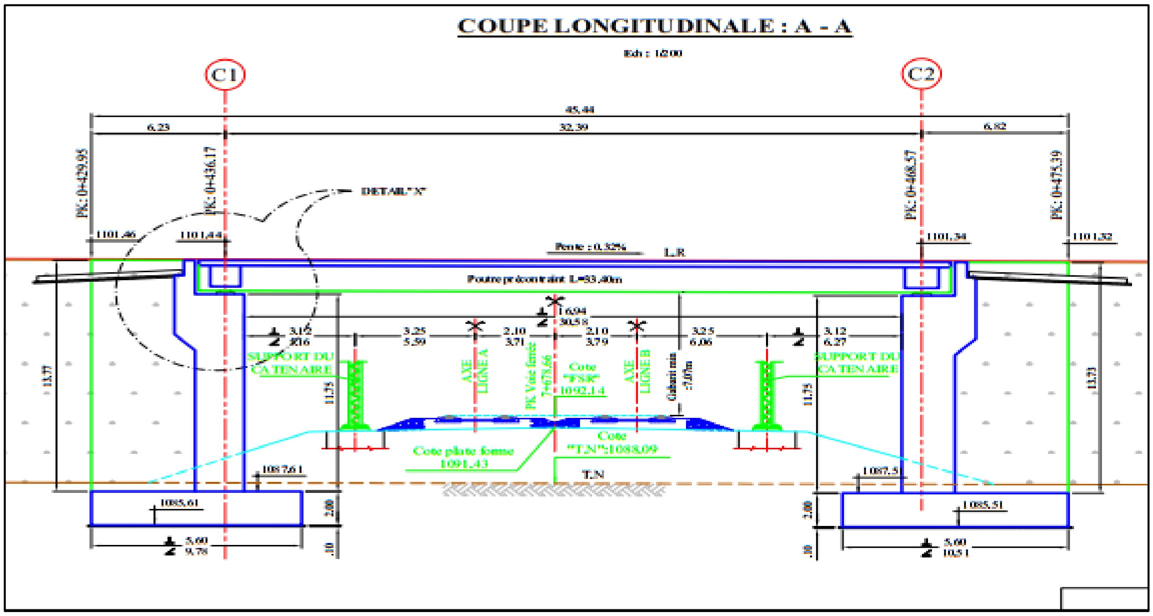

Figure 0.3: Side view

1.4.3 The Cross Profile

This profile plan defines the transversal geometry of the bridge track, making the different layers and composition of the deck visible. It cuts across the longitudinal profile.

The cross profile of this bridge case study is defined by:

- Total road width = 10.50m
- Road width, Lc = 7.00m
- Number of traffic lanes = 2 lanes
- Sidewalk width: 1.25m
- The superelevation: 2.5%

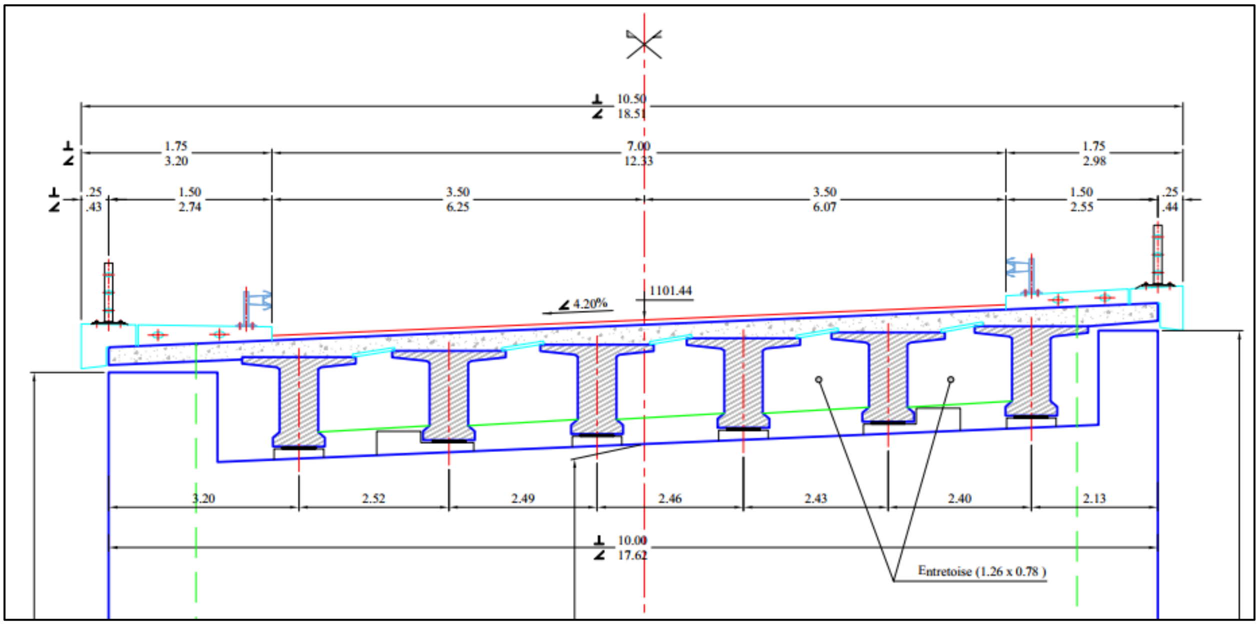

Figure 0.4: Cross-profile-B-B over abutment C1

1.5 Natural Data

1.5.1 Geotechnical Data

In the construction world, geotechnical study is one of the most fundamental studies to be carried out at a site (Afric Memoire 2024). The geotechnical data is essential in determining the foundation type to be used for the structure. It also helps in the reconnaissance of the natural terrain, like:

- The bearing capacity of the soil
- The rheological factors (elasticity of soil, which influences settlement and creep)
- The permeability of the soil
- The water table in the site

1.5.2 The Hydraulic Data

El Bayadh Wilaya is prone to flooding risks (Hafnaoui M et al 2022); hence, necessary safety precautions have to be considered during the construction of the longitudinal profile of the bridge. This is due to the constant immersion of bridge parts, which might lead to some deterioration.

1.5.3 Lithology Data

This data helps us to know the different layers of the soil composition on the site from the different surveys carried out.

1.5.4 Topographical Data

A topographical survey helps us study the natural terrain surface and the different altitudes present. The natural terrain surface of the site is sloping and curvy; hence, C1 is at PK: 0+436.17 and C2 is at PK: 0+460.00, with different altitudes.

1.5.5 Climate Data

- The Algerian Seismic Design Code classifies El Bayadh Wilaya as a Zone 1 meaning that it experiences low seismicity with a gravity acceleration of 0.12 to 0.15.
- El Bayadh Wilaya experiences a dry sub-Saharan climate.
- The maximum rainfall recorded was 109.3mm.
- Sirocco is a type of wind experienced in the region. It's characterized as hot and dry, blowing Northwards from the Sahara Desert (Karima et al 2014).

1.6 The Choice of the Structure

Certain aspects influence the choice of the structure, such as:

- The structure's elements have to be dimensioned concerning the regulations of the B.A.E.L., B.P.E.L., and R.P.A
- How does it integrate with the surroundings?
- The production duration of the structure until its commissioning
- The economic and technical capacity of the companies and design offices involved.

Below is a table used to determine the span or choice of the structure.

Table 0.1: The span length and the possible solution (Oussadit and Hadj 2016)

The Span Length	The Possible Solution
< 20m	A Slab bridge in reinforced concrete or prestressed concrete
20m to 50m	A Slab bridge corbel Mixed bridge with metallic beams Prestressed concrete girder bridge
50m to 300m	Prestressed concrete bridge built in corbel A Slab Bridge in Corbel Cable-stayed bridge
>300m	Suspension bridge Cable-stayed bridge

1.7 Conclusion

From this chapter, we can conclude that an engineer must collect the preliminary data to help them gain more knowledge about the natural state of the terrain, that is the geological facts and also to gain more insight on the functional data. The presentation of the project gives the Engineer a clue of where the project is located and what various factors to consider for the crossing conditions.

Chapter 2 :

Material Characteristics

Chapter 2 : Material Characteristics

2

2.1 Introduction

In this chapter, we are going to study the characteristics of the main materials which are required for the design and construction of a bridge. These materials are concrete, active steel and passive steel. The choice of the characteristics of these materials plays a huge role in the realization of this project.

2.2 Concrete

Concrete is one of the most used building materials in the world. It is a solid-like mass mixture which is made up of different proportions of cement, water, sand, gravel and admixtures. The different proportions determine the concrete's strength and quality.

At the age of 28 days, the concrete gains a compression strength, which is used to characterize the strength of the concrete. It is denoted as $\mathbf{f_{c28}}$.

2.2.1 Density

The density of a standard reinforced concrete is **2.5t/m³**.

2.2.2 Characteristic Compressive Strength

From the B.A.E.L and B.P.E.L guidelines, we have two formulas which enable us to calculate the compression strength of concrete on certain days concerning the $\mathbf{f_{c28}}$. These formulas are:

- If $f_{c28} \leq 40MPa$

  $f_{cj}=f_{c28}\times \left(\frac{j}{4.76+0.83j}\right)$

- If $f_{c28} > 40MPa$

  $f_{cj}=f_{c28}\times \left(\frac{j}{1.4+0.95j}\right)$

Therefore, the concrete used for this project was f_{c28} = 30Mpa for the superstructures and f_{c28} = 35Mpa for the infrastructure, according to the B.P.E.L guideline.

2.2.3 Characteristic Tensile Strength

Generally, concrete has a low tensile strength. The tensile strength still relies on the compressive strength even though tensile and compression stresses are two independent types of stresses. The B.A.E.L and B.P.E.L guidelines grant us a formula to calculate the tensile strength which is; $\mathbf{f_{t28}=0.6+0.06f_{c28}}$

$\mathbf{f_{t28}=2.4Mpa.}$

2.2.4 Permissible Stress

These are allowable stresses, which act as limits to concrete stresses for safety reasons.

- **Permissible stress for ultimate limit state (ULS)**

  $$f_{bu} = \frac{0{,}85\ fcj}{\theta \times \gamma b}$$

  with:

  q=1 when the probable duration of application of the combined action is greater than 24hrs

  q=0.9, when the duration is between 1 hour to 24hours

  q=0.85, when the duration is less than 1hour

  $_{\gamma b}$=1.5 for sustainable situations

  $_{\gamma b}$=1.15 for accidental situations

- **Permissible stress for serviceability limit state (SLS)**

  In Henry Thornier prestressing book, the permissible stresses defined under class II are applicable for this project. The permissible stresses were verified at 14 days and 28 days.

  The permissible stresses at **14 days**, which takes place during the **construction phase,** are in respect to the tensile and compressive strength of the concrete at 14 days.

  Thus f_{c14}=25.64MPa and f_{t14}=2.1384MPa.

  - In compression;

σ_{cs}= 0.6×f_{c14}=15.384MPa

σ_{ci}= 0.6×f_{c14}=15.384MPa

- In tensile;

σ_{ts}= -1.5×f_{t14}=-3.2076MPa

σ_{ti}= -1×f_{t14}=-2.1384MPa

The figure 5 shows an elaborate diagram of the permissible stress limits.

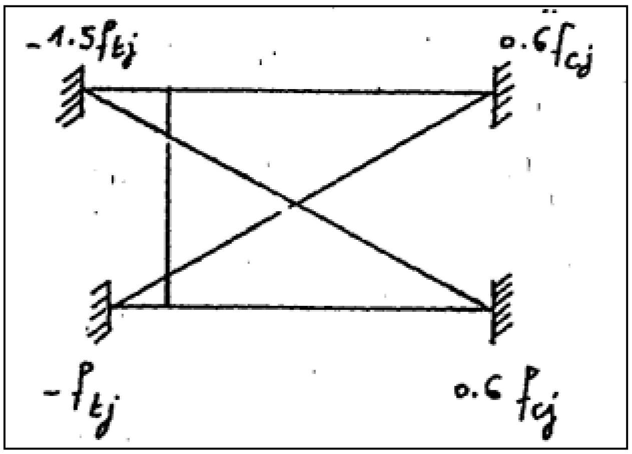

Figure 2.1: Permissible stress limits at 14days.

The permissible stress limits at **28 days** which takes place in the **commissioning phase** are in respect to the tensile and compressive strength of the concrete at 28 days under the rare combination. Therefore:

- In compression;

σ_{cs}= 0.6×f_{c28}=18MPa

σ_{ci}= 0.6×f_{c28}=18MPa

- In tensile;

σ_{ts}= -1.5×f_{t28}=-3.6MPa

σ_{ti}= -1×f_{t28}=-2.4MPa

The diagram below, shows an elaborately the permissible stress limits.

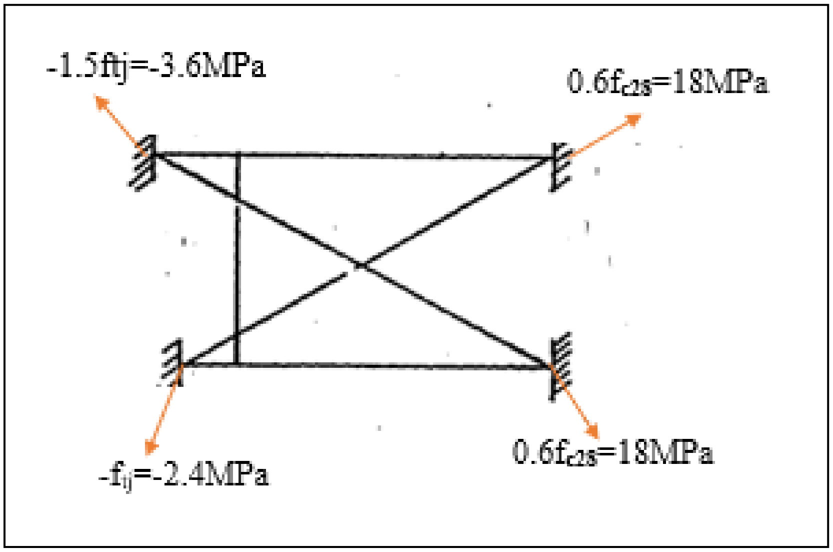

Figure 2.2: The permissible stress limits at 28 days

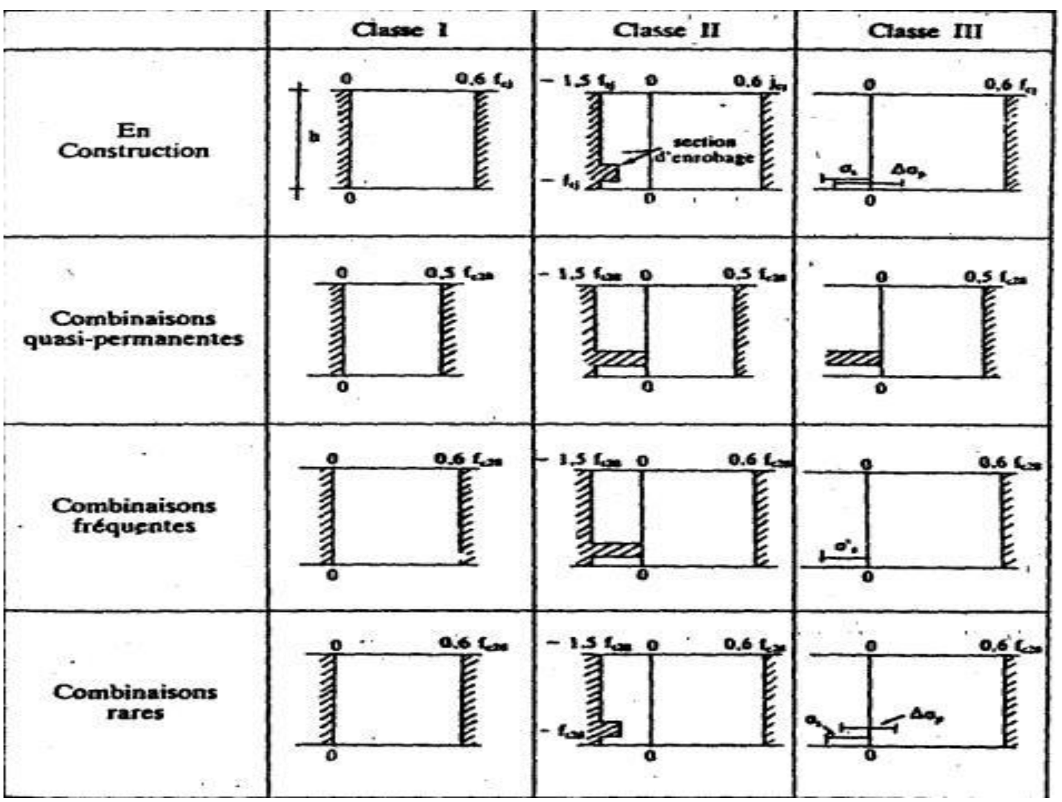

Figure 2.3: The Permissible Stress Limit Guideline from the B.P.E.L

2.2.5 Poisson Ratio

This is the ratio of lateral strain and longitudinal strain due to axial stress. Generally, the Poisson ratio recommended by the B.A.E.L and B.P.E.L guidelines is:

- $\nu=0.2$, for uncracked concrete
- $\nu=0$, for cracked concrete

2.2.6 Longitudinal Deformation Modulus of Concrete, E

The B.A.E.L and B.P.E.L guidelines outline the longitudinal deformation modulus, to be used as follows:

- ✓ Instantaneous deformation modulus for a short duration of less than 24 hours.
  $E_{ij}=11000\sqrt[3]{f_{cj}}$ en MPa
- ✓ Delayed deformation modulus for a long duration.
  $E_{ij}=3700\sqrt[3]{f_{cj}}$ in MPa

2.2.7 Transversal Deformation Modulus

$$G = \frac{E}{2(1+\nu)}$$

The above formula is used to calculate the transversal modulus.

2.3 Steel

Steel is a versatile metal which is widely used in bridge construction, especially in beams. Due to its mechanical properties, steel is combined with other construction materials such as concrete to complement each other (C Miki et al,2002). In the prestressed beam bridge, steel is used in two different forms; passive and active.

2.3.1 Passive Steel

In order, to limit the cracking in concrete, the passive steel takes up the shear forces. High adhesion steel of class FeE400 is used, with an elastic limit of FeE400 which remains the same in both compression and tension.

- Characteristic resistance of steel to ULS (fsu) and SLS(σs)
  a) For damaging cracking cases; σs = fe/$_{\gamma s}$
  $_{\gamma s}$ is the weighting coefficient value taken as 1.15
  $\bar{\sigma}_{st} \leq \mathrm{Inf}\left([\frac{2}{3}fe; 110\sqrt{\eta \cdot f_{tj}}]\right)$ With, η=1 for RL and η=1.6 HA
  b) For very damaging cracking cases in SLS;
  $\bar{\sigma}_{st} \leq \mathrm{Inf}\left([fe/2; 90\sqrt{\eta \cdot f_{tj}}]\right)$

2.3.2 Active Steel

High tensile strength steel reinforcements are used in the prestressed concrete works by pre-tension or post-tension.

Characteristics of the cables used according to the **FREYSSINET**:

- Prestressing unit: 19 strands
- Linear friction coefficient:0.002m^{-1}
- Angular friction coefficient: 0.2 rad^{-1}
- Cross-Sectional area: 1668mm^2
- Sheath diameter: 100mm
- Nominal breaking force:25.21tons
- Maximum force under anchorage:24.13tons
- The permissible limit in tension is σ0≤min(0.8fprg,0.9fpeg)

fprg: 1860MPa

fpeg :1640MPa

With: fprg is the guaranteed breaking limit of the prestressing steels.

fpeg is the yield strength of the prestressing steel.

- **Young's Modulus (E)**

It is also referred to as the longitudinal modulus of elasticity of active steel which is around 200000Mpa under tension or compression. The young's modulus is expressed from the ratio of stress to strain. (Team Xometry 2023)

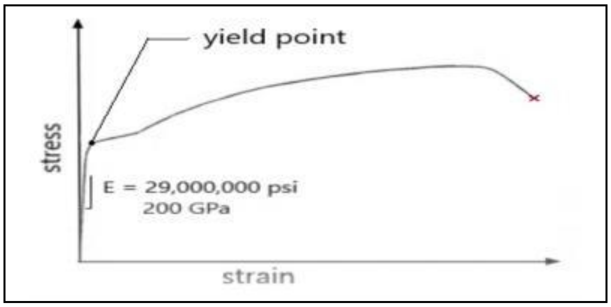

Figure 2.4: Stress-strain steel curve

2.4 Conclusion

In this chapter, we have gone through two prerequisite materials, that is, concrete and steel. It is of the essence for an engineer to be knowledgeable on how the materials behave under different stresses, their elasticity, and the stress limits of these materials. Therefore, in the later stages of the design and study of this project, the engineer will have sufficient data on the mechanical properties of these materials and consider them including the different calculation formulas which are provided by the B.A.E.L and B.P.E.L guidelines.

Chapter 3:
Pre-sizing of the Beam
and
Lowering of Loads

3

3.1 Introduction

A bridge is composed of numerous members such as the apron, deck, beams, columns, sidewalks, piers and others. In this chapter, we are going to pre-size the beams, and the deck using the B.P.E.L and the S.E.T.R.A guide. Followed by, identifying and calculating the different types of loads involved, using the Fascicule standard guidelines.

3.2 Pre-Sizing of a Deck

A deck is a horizontal flat surface that allows vehicles, passengers and others to access the bridge.

3.2.1 The Width of the Deck

The prestressed beam bridge is characterized by a width of 10.50m on the perpendicular view, and 18.51m on the angular view. The deck has two lanes, each lane is 3.5m. The passable platform is 7.00m on the perpendicular view and 12.33m on the angular view. Using the perpendicular view, the total length of the cornices, 2 sidewalks and 2 sills add up to 3.50m.

3.2.2 The Span Length

The bridge has a single span length of 33.40m.

3.2.3 The Thickness of the Deck, H0

The spacing between beams influences the thickness of the deck for instance, the bigger the spacing, the thicker the thickness. The thickness of the slab under compression has to be between the following bounds of $0.20m \leq ed \leq 0,30m$ using the S.E.T.R.A guide. In this project, a thickness of 30cm was used.

3.3 Pre-Sizing of a Beam

The sizing of a beam depends on the bridge spans and the distribution of loads acting on the span. Therefore, in this chapter, we are going to use the S.E.T.R.A guide to pre-size the prestressed beams.

3.3.1 The Height of the Beam, Hp

The B.P.E.L guide grants us limits to determine the beam's height. The limits are; L/15 and L/18.

L: The span length of the beam = 33.40m.

$$\frac{L}{18} \le H_t \le \frac{L}{15}$$

1.8m≤Ht≤2.2m

H_t is the total height of the beam and the slab, which is 30cm.

Hence, the beam height used is 1.5m

3.3.2 The Width of the Deck under Compression, b

According to the B.P.E.L guide:

0.5Hp< b ≤0.7Hp

Hp: Height of the beam

Thus 0.75m< b ≤1.05m, we take b as 1.03m

3.3.3 The Thickness of the Deck under Compression, e

e=11cm

According to the S.E.T.R.A guide, the thickness of the deck has to be more than 10cm.

3.3.4 The Number of Beams, N

In this project, 6 beams were used.

$N= \frac{La}{E} +1 = \frac{7}{1.4} +1 = 6$

La: rollable width

E: automated spacing from SAP2000

3.3.5 The Spacing of the Beams, E

The beam spacing between axes is 1.4m

3.3.6 The Thickness of the Web, b0

According to the S.E.T.R.A guide the thickness of the web;

On the extreme beam section, b_0=0.35m due to the fact that 0.25m ≤ b0≥0.35m.

On the middle beam section, b_0=0.18m due to the fact that 0.16m ≤ b0≥0.22m.

3.3.7 The Width of the Heel, bt

The formula below is provided by the S.E.T.R.A guide, for the heel's width calculation.

$$b_t \geq \frac{l \times L^2}{K_t \times h_t^2}$$

Whereby:

I: Width of the deck

L: span length of the beam

ht: Total height of the (beam + slab) =1.5+0.3+0.005+0.08=1.885m

K: coefficient without dimension 1100≤K≤1300, we take K=1200

bt≥(10.5×33.4^2)/ (1200×1.885^2) = 2.747m

bt/6=0.4578, thus bt=0.47m

3.3.8 The Thickness of the Heel, et

The S.E.T.R.A guide permits us, to find the heel's thickness using the following limits: 10cm≤et≤20cm, ergo the et=0.15m

3.3.9 The Gusset

It is a triangular piece made from metal or concrete. It connects different members, that is, the flange and the web, making sure that the stability of the I beam is achieved.

3.3.10 The Compression Deck Gusset

For the beam section on the extreme:

Thickness: $\alpha = 56.3^\circ$ for e3=0.07m

Width: $\alpha = 56.3^\circ$ for 0.34m

For the beam section on the intermediary:

Thickness: $\alpha = 56.3^\circ$ for e3=0.06m

Width: $\alpha = 56.3^\circ$ for 0.395m

Thickness $\alpha = 33.7^\circ$ for e4=0.03m

Width $\alpha = 33.7^\circ$ for 0.03m

3.3.10.1 The Heel Gussets

For the extreme beam section: $\alpha = 56.3^\circ$, thickness =0.09m with a width of 0.06m.

For the intermediary beam section: $\alpha = 56.6^\circ$, thickness =0.22m with a width of 0.145m.

3.4 The Geometric Characteristics of the Beam

Beams exist in different structural cross-section shapes such as the T shape, I shape, and circular shape among others. They satisfy different civil engineering needs for instance:

- The T-shaped beam participates in the taking up of the shear forces which occur.
- The I-shaped beam is advantageous, for the fact that less concrete is used hence making the beam lighter. This project uses an I-shaped beam.

The beam cross-section area is divided into simpler shapes such as triangles and rectangles to aid in the calculation of the geometric characteristics of the beam which are:

- Bi: gross cross-sectional area; $B_i = b_i \times h_i$
- Zi: distance from the centre of gravity of section (i) to the base of the beam.
- Ii: moment of inertia of section I relative to the base of the beam.
- Si: static moment of the section: $S_i = B_i \times Z_i$

- V: distance from the centre of gravity of the total section to the upper fibre.

  $V = \frac{\sum Bi \times Zi}{\sum Bi}$

- V': distance from the centre of gravity of the total section to the lower fibre.

  V'=h-v

- IG': moment of inertia specific to the section considered

  For the triangular section: $IG' = bh^3/36$

  For the rectangular section: $IG' = bh^3/12$

- IG: moment of inertia relative to the center of gravity of the total section

  $IG = (I0 + Bi \times Zi^2) - (\sum Bi \times V^2)$

- Wi: modulus of inertia of the section relative to the upper fibre
- Ws: modulus of inertia of the section relative to the lower fibre
- i: radius of gyration of the section

  $i^2 = \frac{I_G}{B}$

- ρ: section efficiency coefficient $\rho = \frac{I_B}{s_B \times V \times V'_B}$

In our project, the beam section has two different cross-sections of the form I specifically on the longitudinal extremes of the beams and the intermediary sections. The significant difference between the two cross-sections is the width of the web, which transforms from 35cm to 18cm. The width of the web is reduced for economical purposes and to reduce the self-weight of the beam in general.

3.4.1 The Geometric Characteristics of the Extreme Cross-Section of the Beam

Below is a figure of a cross-section of the extreme beam section.

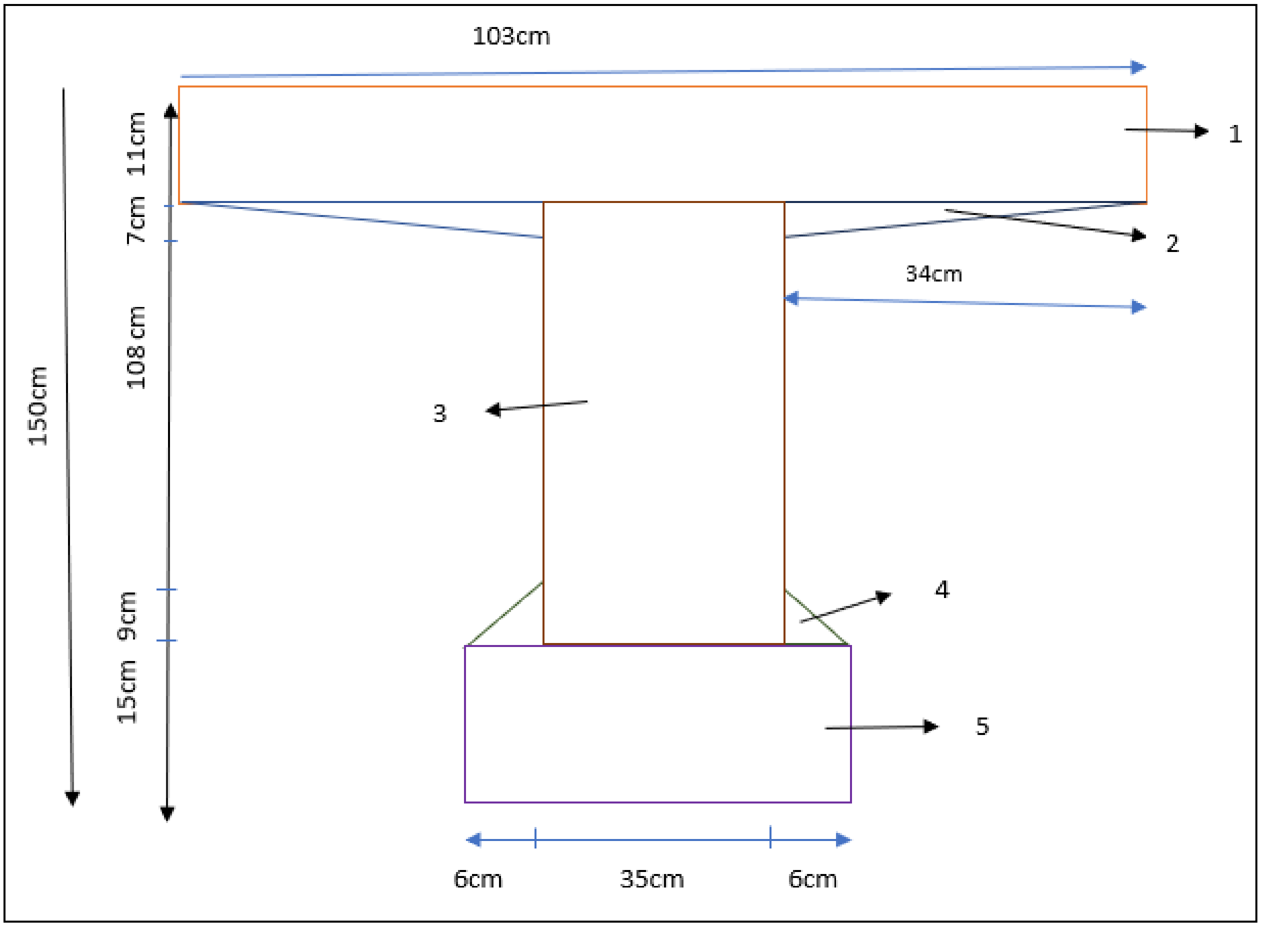

Figure 3.1: The dimensions of the beam in centimeters

The table below shows the calculation data of the geometric characteristics of the beam sections.

Table 3.1: Geometric characteristics of the beam sections

Section	Dimension	Bi (cm^2)	Zi (cm)	IG (cm^4)	Ii (cm^4)
1	103 × 11	1133	5.5	11424.41667	45697.66667
2a	34× 7/2	119	13.33	323.94	21468.92
2b	34× 7/2	119	13.33	323.94	21468.92

3	124× 35	4340	73	5560986.667	28688846.67
4a	6×9/2	27	132	121.5	470569.5
4b	6×9/2	27	132	121.5	470569.5
5	47 ×15	705	142.5	13218.75	14329125
		6470			44047746.2

$V=\frac{\sum Bi\times Zi}{\sum Bi}=\frac{433814.5}{6470}=67.05cm$

V'=h-v=150-67.05=82.95cm

IG = $\sum$(I0 + Bi x Zi2)- ($\sum Bi$ x V^2) = ($\sum$ Ii)- ($\sum Bi$ x V^2)

44047746.2- (6470×67.05^2) = 14,960551.03cm^4

$$\rho = \frac{IG}{s_B\times V\times V'_B} = \frac{14{,}960551.03}{6470\times 67.05\times 82.95} = 0.4157$$

$$\rho = 41.57\%$$

3.4.2 Geometric Characteristics of the Extreme Beam Section and the Reinforced Concrete Slab

It is necessary to consider the geometric characteristics of the beam with the inclusion of the slab.

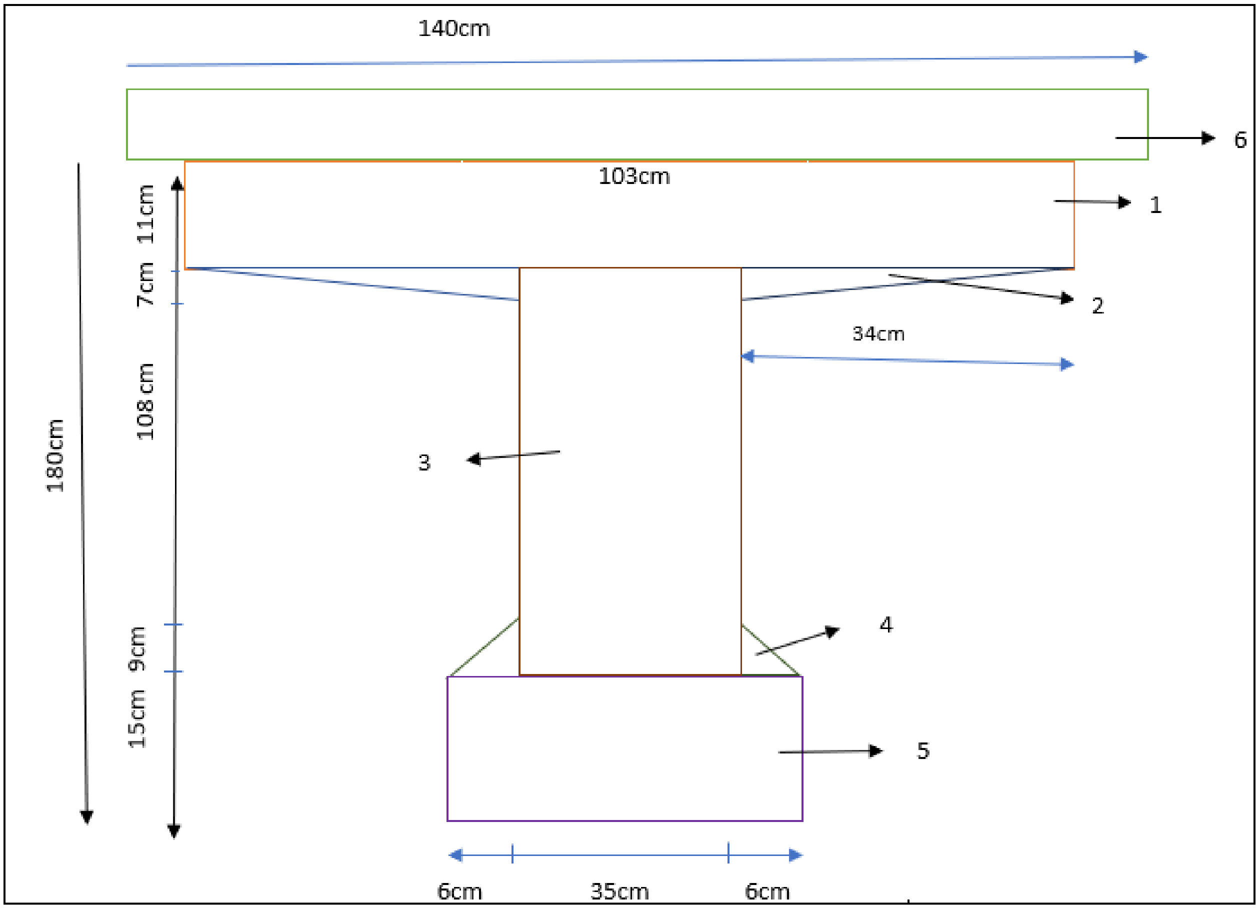

Figure 3.2: The geometric characteristics of the extreme beam including the slab

Table 3.2: The calculation of the beam characteristics including the slab

Section	**Dimension**	**Bi (cm^2)**	**Zi (cm)**	**IG (cm^4)**	**Ii (cm^4)**
1	103 × 11	1133	35.5	11424.41667	1439287.667
2a	34× 7/2	119	43.33	323.94	223745.12
2b	34× 7/2	119	43.33	323.94	223745.12
3	124 × 35	4340	103	5560986.667	51604046.667
4a	6×9/2	27	162	121.5	708709.5
4b	6×9/2	27	162	121.5	708709.5
5	47 ×15	705	172.5	13218.75	20991375

6	140×30	4200	15	315000	1260000
		10670			77159618.57

$V = \frac{\sum Bi \times Zi}{\sum Bi} = \frac{690914.5}{10670}$ = 64.75cm

V'=h-v=180-51.67=115.25cm

IG = ∑(I0 + Bi x Zi2)- ($\sum Bi$ x V^2) = (∑ Ii)- ($\sum Bi$ x V^2)

=77159618.57-($10670 \times 64.75 \times 64.75$) = 32424976.7$cm^4$

$\rho = \frac{IG}{s_B \times V \times V'_B} = \frac{32424976.7}{10670 \times 64.75 \times 115.25}$ = 0.4072

$$\rho = 40.72\%$$

Table 3.3: The general geometric characteristics details of the extreme section.

Section	**B(cm^4)**	**Is(cm^3)**	**V (cm)**	**V'(cm)**	**Ii(cm^4)**	**ρ(%)**
Beam	6470	433814.5	67.05	82.95	44047746.2	41.57
Beam + Slab	10670	690914.5	64.75	115.25	77159618.57	40.72

3.4.3 Geometric Characteristics of the Iintermediary Beam Section

Below is a figure showing the intermediary cross-section of the beam.

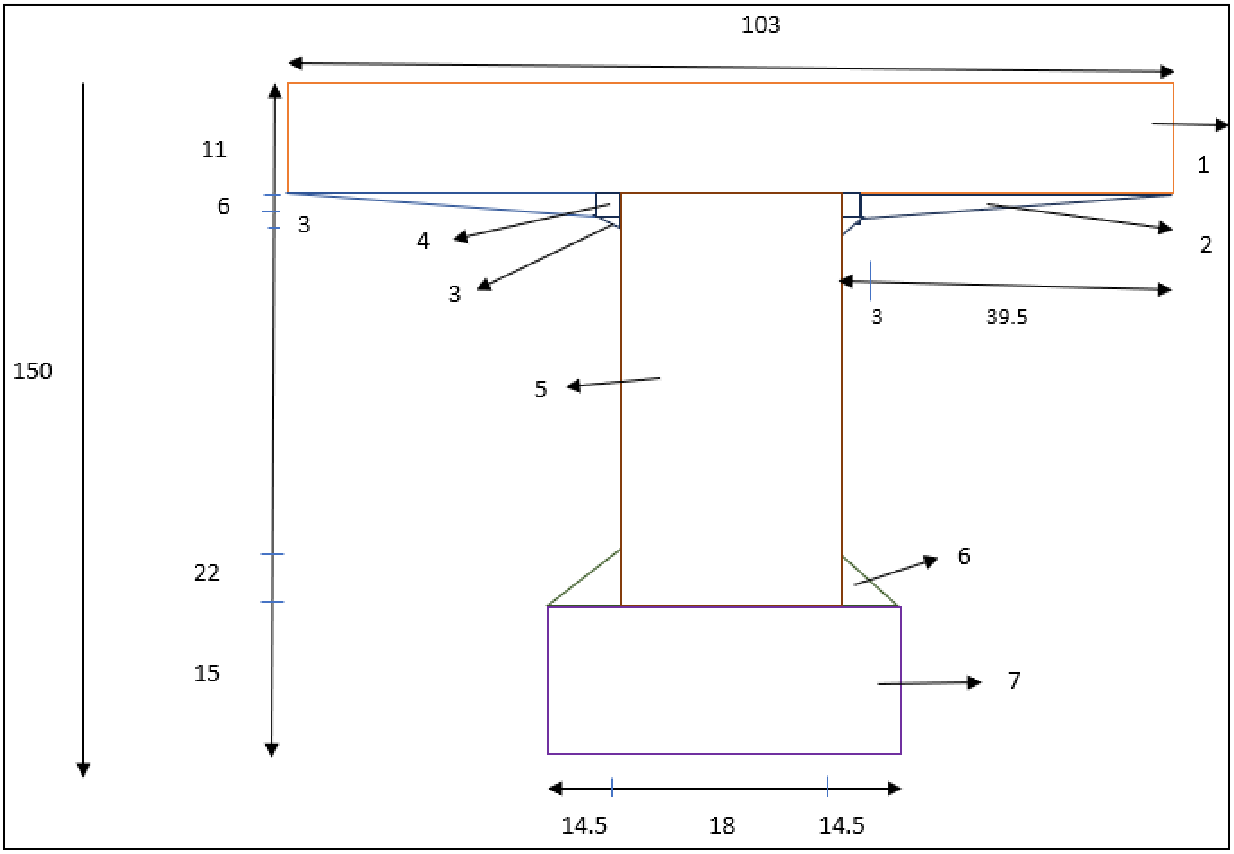

Figure 3.3.3: The cross-section of the intermediary beam section

Table 3.4: The cross-section of the intermediary beam section

Section	**Dimension**	**Bi, (cm^2)**	**Zi (cm)**	**IG' (cm^4)**	**Ii (cm^4)**
1	11× 103	1133	5.5	11424.41667	45697.66667
2a	6× 39.5/2	118.5	13	237	20263.5
2b	6× 39.5/2	118.5	13	237	20263.5
3a	3× 3/2	4.5	18	2.25	1460.25
3b	3× 3/2	4.5	18	2.25	1460.25
4a	6× 3	18	14	54	3582

4b	6×3	18	14	54	3582
5	124×18	2232	73	2859936	14754264
6a	$14.5 \times 22 /2$	159.5	127.67	4288.78	2604079.59
6b	$14.5 \times 22 /2$	159.5	127.67	4288.78	2604079.59
7	15×47	705	142.5	129778.75	14445685
		4671			34504417.3

3.4.4 Geometric Characteristics of the Iintermediary Beam Section and the Reinforced Concrete Slab

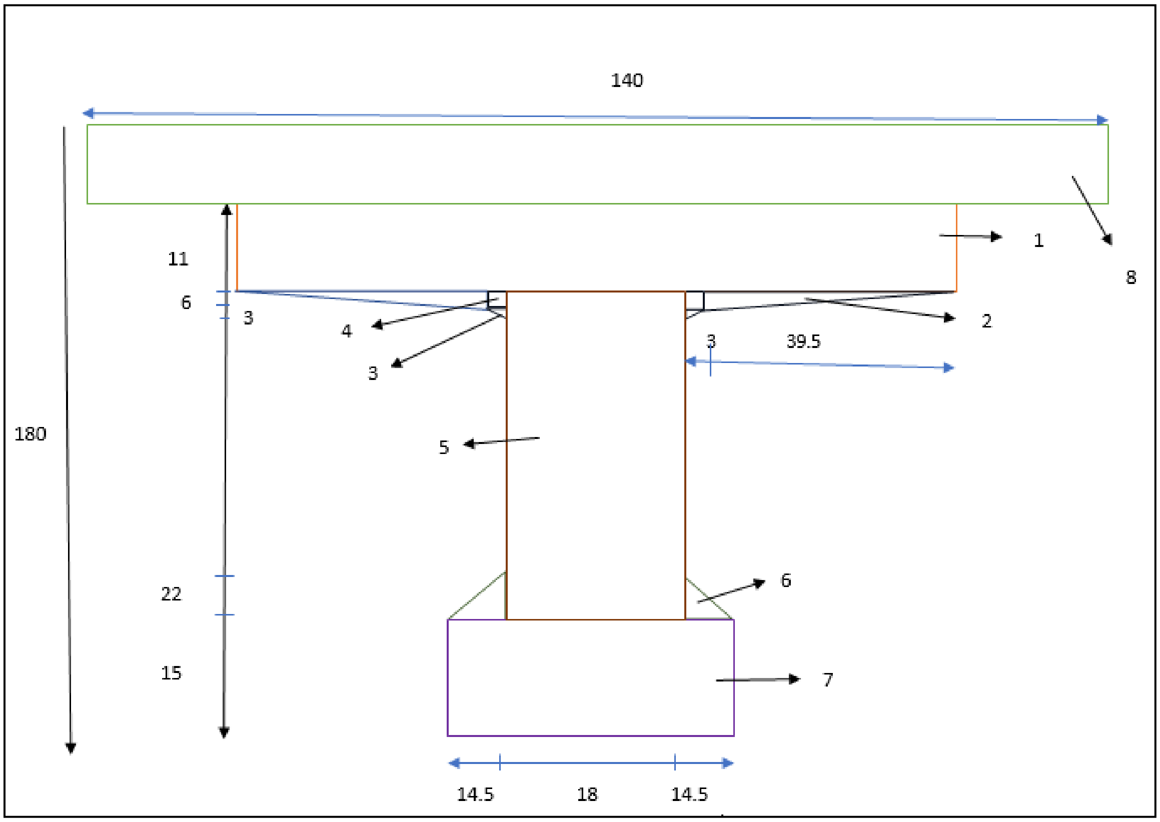

Figure 3.4: Geometric characteristics of the intermediary beam section

Table 3.5: Geometric characteristics of the intermediary beam section

Section	Dimension	Bi (cm^2)	Zi (cm)	IG (cm^4)	Ii (cm^4)
1	11× 103	1133	35.5	11424.41667	1439287.667
2a	6× 39.5/2	118.5	43	237	219106.5
2b	6× 39.5/2	118.5	43	237	219106.5
3a	3× 3/2	4.5	48	2.25	10370.25
3b	3× 3/2	4.5	48	2.25	10370.25

4a	6×3	18	44	54	34902
4b	6×3	18	44	54	34902
5	124×18	2232	103	2859936	26539224
6a	$22\times 14.5/2$	159.5	157.6667	4288.78	3969265.51
6b	$22\times 14.5/2$	159.5	157.6667	4288.78	3969265.51
7	15×47	705	172.5	4406.25	20982562.5
8	140×30	4200	15	315000	919800
$\sum$		8871			58348163

Table 3.6: The general geometric characteristics details of the intermediary section

Section	B(cm^4)	Is(cm^3)	V (cm)	V'(cm)	Ii(cm^4)	ρ(%)
Beam	4671	314103.7	67.25	82.75	34504417.3	51.47
Beam + Slab	8871	517232.7	58.31	121.69	58348163	44.78

3.5 Lowering Loads.

To verify the bridge design adopted the lowering loads calculations have to be calculated to assess the stability of the structure as a safety precaution. There exist different types of loads which are subjected to the bridge. For instance, different types of vehicles exert different amounts of loads on the bridge and these loads have to be taken into account to make sure that the structure won't collapse once it has been commissioned.

The loads are classified into;

- Permanent Loads

- Live Loads

3.5.1 Permanent Loads

The permanent loads are also known as dead loads or static loads. These loads are constant over a long period, and they rarely vary. They include the self-weight of the structure, made up of the different segments which make a bridge, such as the deck, the slab, the beams, the sidewalks, the cornices, the guide rails, the abutments, and the piers among others. The climatic loads such as wind and temperature variations are taken into account as dead loads too. The elements composing a bridge are categorized into load-bearing elements and non-bearing elements.

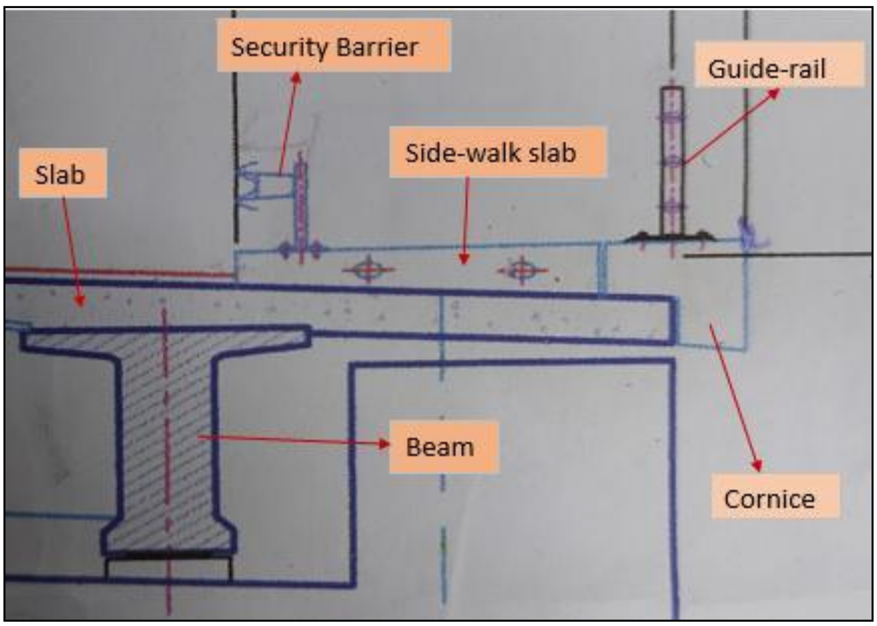

Figure 3.5 Bridge elements

3.5.1.1 Load-Bearing Elements

These elements are the dead loads from the deck only, which are composed of the reinforced concrete slab and the beams.

- **Beams**

The calculation of the self-weight of the beams taking into consideration of the two different cross-sections is as follows:

P_{s1} = 25 × 0.6470 × 3 = 48.53kn

P_{s2} = 25 × 2× (0.6470 +0.4671)/ 2 = 27.85kn

P_{s3} = 25 × 0.4671× 11.7 = 136.63kn

Thus, the self-weight of the beams is, (P_{s1}+P_{s2}+P_{s3}) × 2 =426.02kn

The self-weight of a beam: 426.02/33.4=12.76kn/ml

The self-weight of the 6 beams: 12.76×6=114.8kn/ml

G_1=114.8kn/ml

gb: volume mass

N: total number of beams

S_1: cross-section area of the beam

L: length of the beam

P_{S1}: The self-weight of the beam section on the extreme part of the beam

P_{S2}: The self-weight of the beam section on the middle part of the beam

P_{S3}: The self-weight of the beam section on the intermediary part of the beam

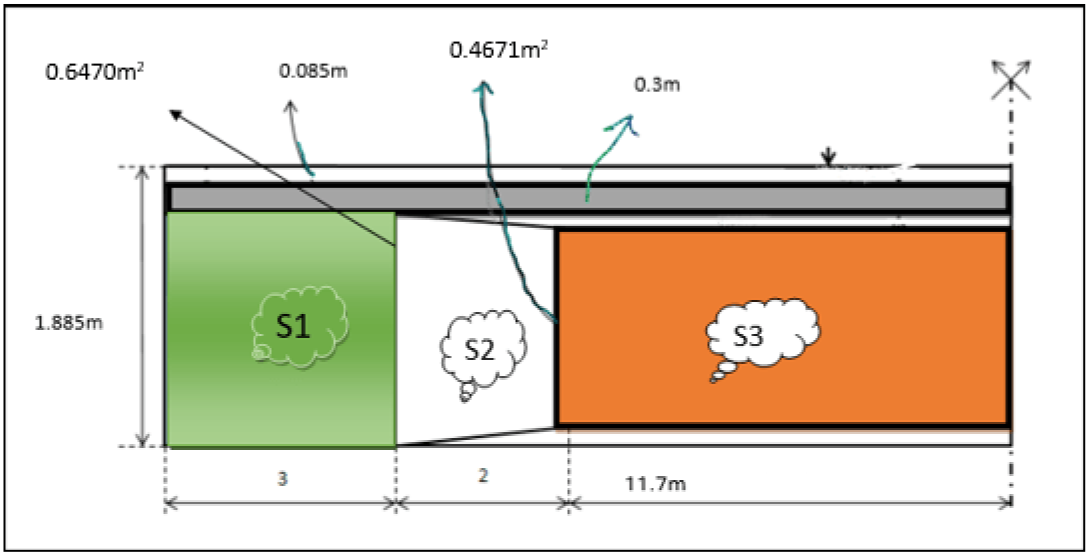

Figure 3.6: The Different beam cross-sections longitudinally

- **The Reinforced Concrete Slab**

$G2 = e_d \times L_d \times gb$

$G_2 = 0.3 \times 10 \times 25 = 75 kn/ml$

e_d: thickness of the slab

L_d: slab width

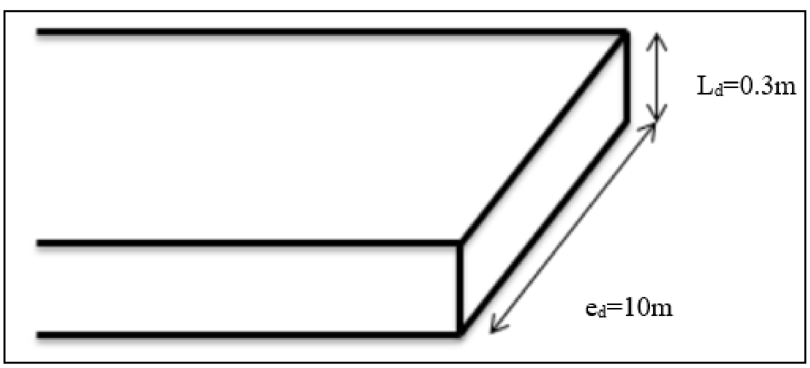

Figure 3.7: The slab

3.5.1.2 Non-Load Bearing Element

The non-load bearing elements in this project are the wearing course, the guide-rails, the sidewalk slab, the waterproofing, the safety elements and the bridge cornices.

Below is the self-weight information that was taken into account for each element.

- **Wearing Course**

$G_3 = e_r \times L_r \times gb$

$G_3 = 0.08 \times 7 \times 24 = 13.44$ Kn/ml

L_r: rollable width

e_r=thickness of the wearing course of bituminous concrete

gb: volume mass of the wearing course=24kn/m^3

- **Waterproofing Membrane**

$G_4 = e_w \times lr \times \gamma_w$

$G_4 = 0.005 \times 7 \times 22 = 0.77$kn/ml

e_w: thickness of the waterproofing membrane

γ_w: volume mass of the waterproofing membrane

- **Bridge Cornices**

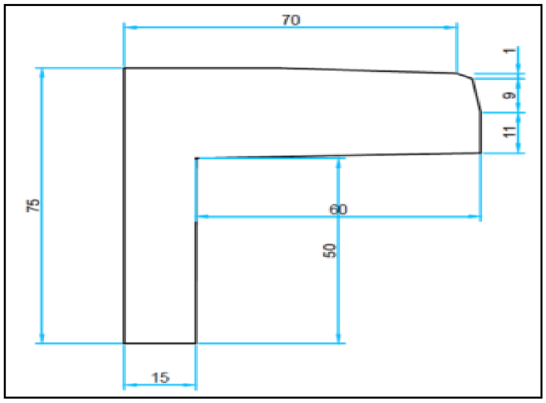

Figure 3.8: A Bridge Cornices in centimeters

The surface area of a cornice is $0.26m^2$

$G_5=0.26\times25=6.5kn/ml$

Thus, the weight of two bridge cornices is: $6.5\times2=13kn/ml$

- **Guide-rails**

In the 2^{nd} title of the 61^{st} fascicule, the weight of the guide-rails is defined as 3kn/ml

$G_6=3kn/ml$

Thus, the weight of two guide-rails is: $3\times2=6kn/ml$

- **Security Barrier**

In the 2^{nd} title of the 61^{st} fascicule, the weight of the security barriers is defined as 3kn/ml

$G_7=3kn/ml$

Thus, the weight of two security barriers is: $3\times2=6kn/ml$

- **Side-walk slab**

$G_8=Lsw\times Esw\times g_b$

$G_8=1.25\times0.3\times25=9.375kn/ml$

Lsw: width of the sidewalk

Esw: the thickness of the sidewalk

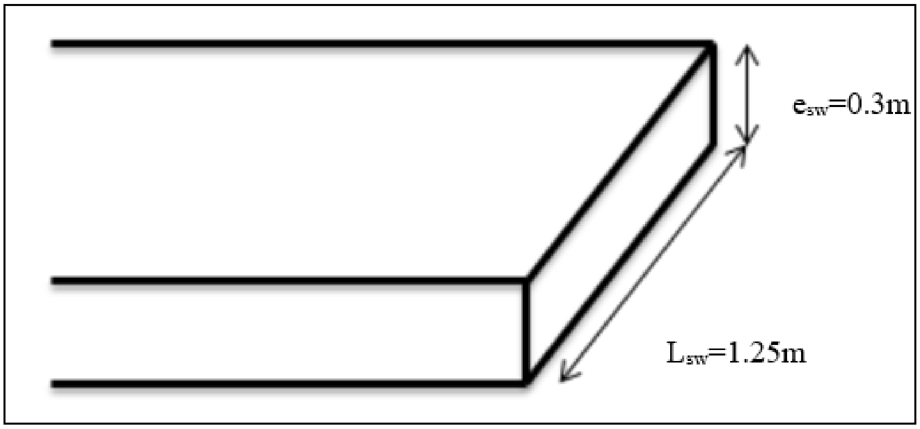

Figure 3.9: The side-walk slab

The **total dead load** of the bridge members is;

$$Gt = (G_1+G_2+G_3+G_4+G_5+G_6+G_7+G_8) \times L$$

$$= (114.8+75+13.44+0.77+13+6+6+9.375) \times 33.4$$

$$Gt = 7962.059kn$$

Table 3.7: A summary of the dead loads and their values

Dead loads	**Values in Kn/ml**
Beams	114.8
Slab	75
Cornices	13
Side-walk slab	9.375
Guide-rails	6
Security barriers	6
Wearing course	13.44
Waterproofing surface	0.77
Total Dead Loads	238.385

3.5.2 Live Loads

These loads can also be referred to as imposed loads or applied loads. They are not constant because they vary from time to time. The live loads could be people, moving or stationary vehicles among others. To dimension the deck, the 61st Fascicule, from the Technical Guideline Document "D.T. R" outlines the live loads to be considered, they include;

- Live load, A_L
- Bc system
- Bt system
- Br system
- Military live load Mc120
- Exceptional loads D240, D280
- Sidewalk live loads
- Wind and Earthquake loads
- Friction Loads
- Centrifugal force load

The bridges have to be categorized into three distinguished classes, according to the 2nd title of the 61st Fascicule which are:

Table 3.8: The Rollable width classification

Classes	**Rollable Width**
1	$Lr \geq 7m$
2	$5.50m < Lr < 7m$
3	$Lr < 5.50$

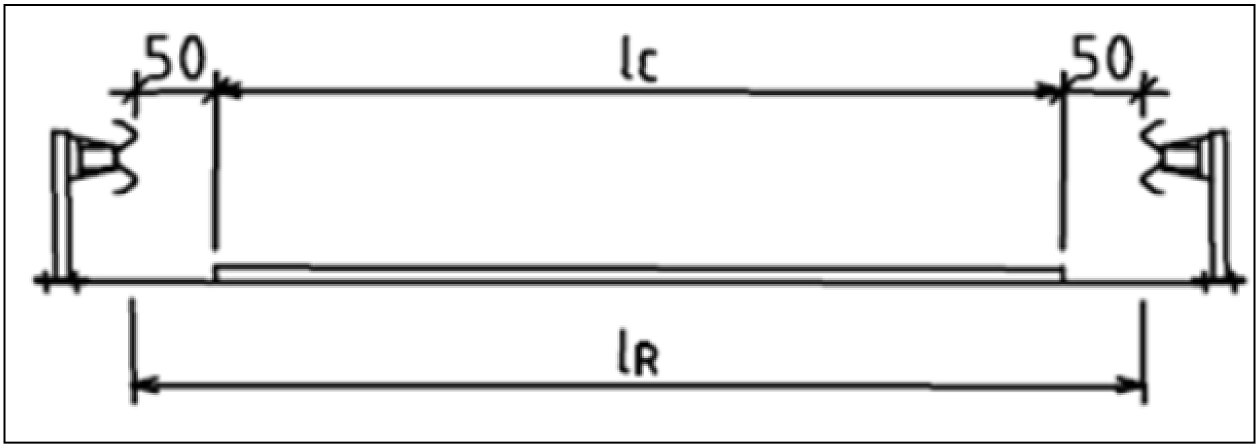

Figure 3.10: The rollable width, Lr and the loadable width, Lc in cm

In this project, the rollable width of the bridge is **7m**, thus the bridge is classified as **class1**.

a. A_L system loads

The load is uniformly distributed on the bridge pavement along the length.

$$A_L = 230+\frac{36000}{L+12}(kg/m^2)$$

L: The bridge span

$$A_L = 230+\frac{36000}{33.4+12} = 1022.95\ kg/m^2 = 10.23 kn/m^2$$

- ✓ The coefficient a1, concerning the bridge class and the given loaded lanes:

Table 3.9: The coefficient values of A_L

	Number of loaded lanes				
Classes of the bridge	1	2	3	4	5
1st	1	1	0.9	0.75	0.7
2nd	1	0.9	0.9	0.75	0.7
3rd	0.9	0.8	0.9	0.75	0.7

From the above table:

- ✓ The coefficient a1=1, because the bridge has two lanes and it's in the 1st class.

- ✓ The coefficient a2, depends on the number of lanes and the width of the loadable pavement hence; $a2=\frac{v0}{v}$

  v = Lch/Nv=6/2=3

  Nv: Number of lanes

  v: Lane width

  V_0: Lane width according to the classes of the bridge

Table 3.10: The Vo Values

1st class	2nd class	3rd class
3.5 m	3 m	2.75 m

Therefore, the coefficient $a2=\frac{3.5}{3}=1.167$

According to (LACROIX M. R et al, 1980), the formula for calculating the load A_L is;

A_L = a1 x a2 x A_L

A_L = 1 x 1.167 x 1.023=1.1935t/m^2

$Q(A_L)=1.1935\times7\times33.4=279.04t$

b. Bc System

The Bc loading system is one of the 3 separate operations found in the B-loading system and these operations loads are multiplied by an increased dynamic coefficient. It is made up of identical trucks which have three axles each. In the longitudinal direction, only two trucks are used per lane while in the transversal direction, the number of trucks depends on the number of lanes on the pavement hence, during calculations, we use the worst-case scenario. Below are figures to elaborate on the placement of the Bc loading system.

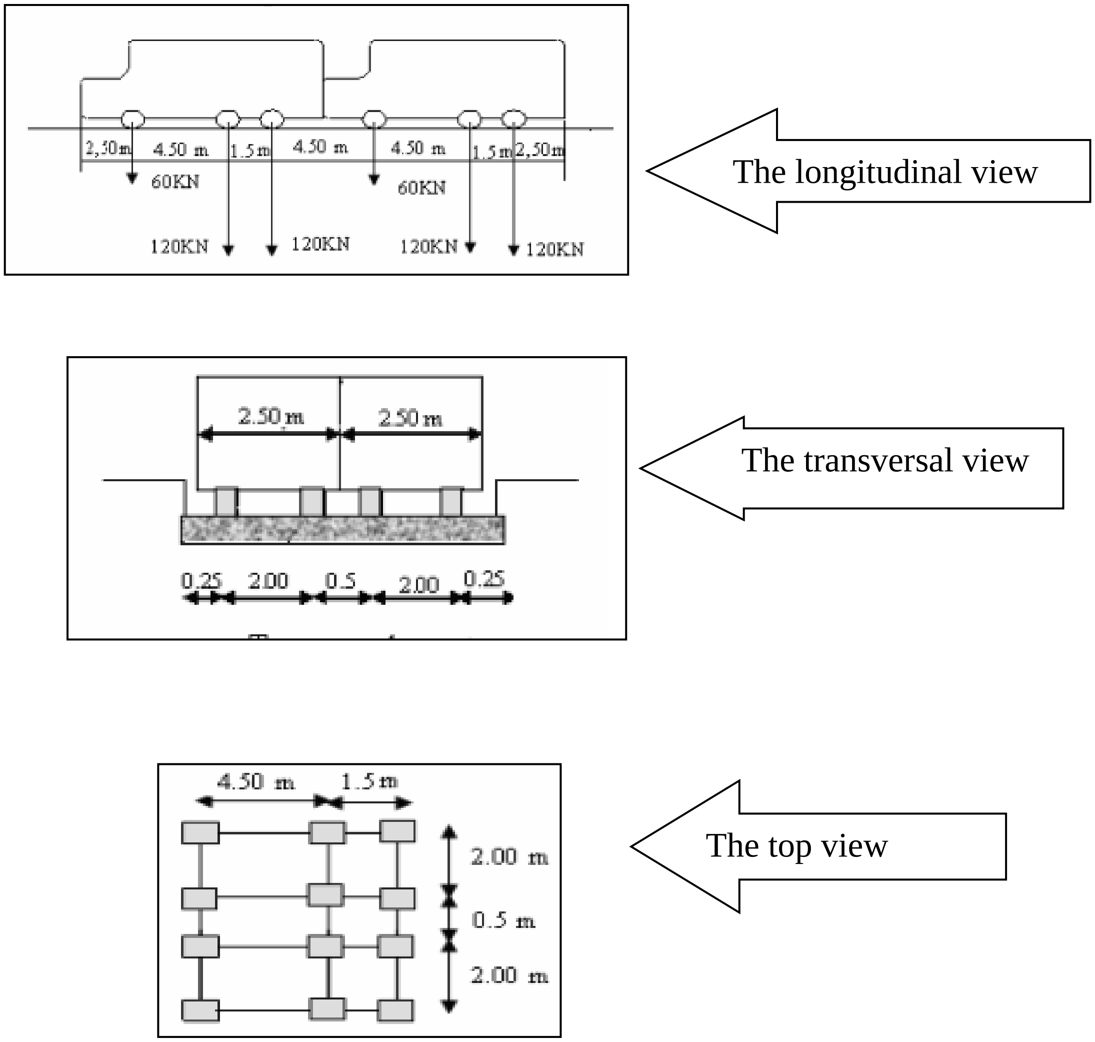

Figure 3.11: The B_c loading system

The Bc load calculated is multiplied by a transversal regression coefficient, bc, which is in function with the class of the bridge and the number of lanes on the bridge pavement. Below is a table used to find the transversal regression coefficient.

Table 3.11: coefficient of B_c loading system

Number of loaded lanes	**1**	**2**	**3**	**4**	**≥5**
Class 1	1.2	1.1	0.95	0.85	0.75
Class 2	1	1	0.95	0.85	0.75
Class 3	1	0.8	0.95	0.85	0.75

According to the table above, the **bc** coefficient is **1.1**. Two trucks are placed longitudinally and two transversally.

The weight of a truck is thirty tons. Hence, the weight of the 4 trucks is 120t.

Bc=bc ×30×2×N=120t

N: Number of lanes

The dynamic increase coefficient is: $\delta = 1 + \frac{0.4}{1+0.2L} + \frac{0.6}{1+4\frac{G}{Bc}}$

L: span length

G: total weight of dead loads

S: maximum weight of live loads which support the slabs

Table 3.12: Load Bc by Axles

Number of Lanes	**Bc**	$\boldsymbol{\delta_{bc}}$	**Loads by Axles**		
1	1.2	1.065	EAV	6×1×1.065	6.39
			EAR	12×1×1.065	12.78
2	1.1	1.076	EAV	2×6×1×1.076	12.91
			EAR	2×12×1×1.076	25.82

EAV: Front axle

EAR: Back axle

c. Bt Load System

This system consists of two tandem axles with a load of 16t each.

Below are figures to show how the BT system is placed and the distances to be respected.

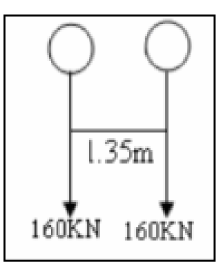

Figure 3.12: Bt loading on the transversal view

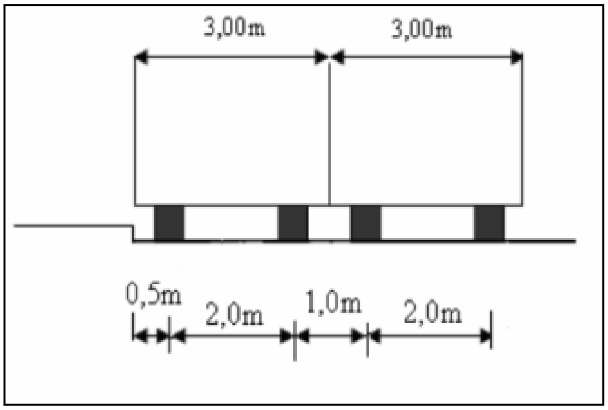

The longitudinal view

Figure 3.14: Bt loading on the Longitudinal view

From the table below, we have the transversal regression coefficient, bt, which is multiplied by the Bt.

Table 3.13: The B_t values

Class of the bridge	**I**	**II**
Value of bt	1,00	0,90

Therefore, the **bt**, of our project is equal to **1** since the bridge is in class 1.

The tandem axle weighs: 32t

Thus Bt=32×2=64t

S=64×1=64t

The dynamic increase coefficient is: $\delta = 1 + \frac{0.4}{1+0.2L} + \frac{0.6}{1+4\frac{G}{S}}$

$\delta = 1 + \frac{0.4}{1+0.2\times 33.4} + \frac{0.6}{1+4\frac{796.205}{64}}$=1.064

Bt=1.064×64=68.09t

Bt=68.09t

d. The Br Loading system

It is made up of a wheel which carries 10t. Below is an elaboration of the system.

Figure 3.13: B_t loading system

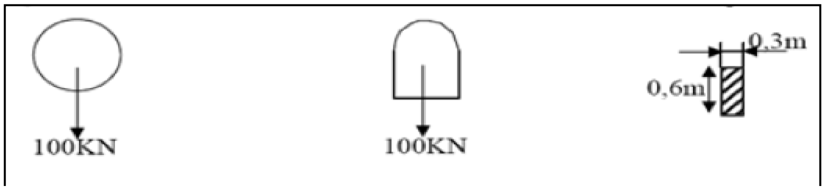

The longitudinal view The transversal view The top view

The dynamic increase coefficient is: $\delta = 1 + \frac{0.4}{1+0.2L} + \frac{0.6}{1+4\frac{G}{S}}$

S=10t

δ =1.054

Therefore, Br=10.54t

e. The Military Live load, Mc120

This load defines the weight of the military vehicles which are heavier compared to the load systems of type A and B. The Mc 120, weighs 110t, which is redistributed across its tracks.

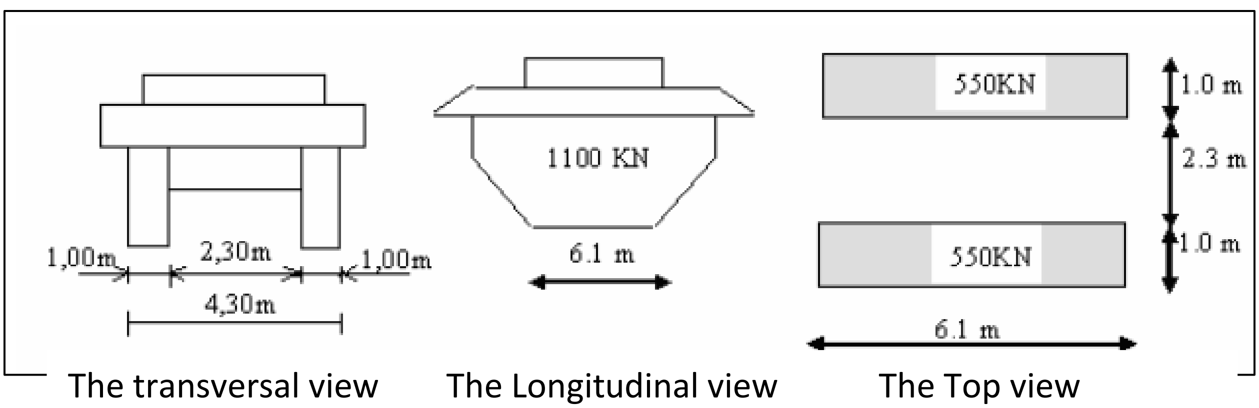

Figure 3.16: The Mc120 loading system

The dynamic increase coefficient, δ=1.135, with s=110t.

Therefore Mc120=1.135×110=124.85t

f. The Exceptional Load D240

D240

The D convoy of D240 weighs 2400t over a surface area of 18.60m longitudinally and 3.2m transversally. The D240 impact is greater that D280 therefore, in our calculations only D240 will be taken into out.

240/18.6=12.90t/ml

g. Side-walk live load

The uniformly distributed load of 150kg/m^2 of the side-walk live load is not subjected to the dynamic effect. Therefore, the side-walk live load on both sidewalks is:

2×0.15×1,25=0.375t/ml.

h. Frictional loads

The Frictional loads are due to the vehicles moving on the pavement and therefore it is necessary to use these loads to verify the stability of the abutment and the supporting devices.

- Frictional loads due to A_L load, $Hf_{(AL)}$

  $Hf_{(AL)} = \frac{Q(AL)}{20+0.0035(S)} = \frac{796.2059}{20+0.0035(6\times 33.4)} = 38.46t$

- Frictional loads due to B_C load, $Hf_{(Bc)}$

  The Frictional load developed by a truck is equivalent to the weight of the truck. Therefore, the $Hf_{(Bc)}$ =30t

i. Centrifugal Loads

The bridge is curvy and sloppy. The centrifugal loads are going to be close to insignificant because of the intersection of the roads which is near the bridge meaning that the vehicles approaching this zone and the bridge will be at a low speed.

j. Wind and Earthquake Loads

The earthquake loads are also close to insignificant because the region experiences low seismicity. The wind loads are to be included in live loads calculations because the region is prone to the sirocco winds. The sirocco wind's intensity differs with the seasons. They are strongest during autumn and spring with a highest record speed of 100km/h which is considered to be dangerous. The wind pressure generates a pressure of 2kn/m^2 for service works and 1.25kn/m^2 under construction works on the surfaces that it strikes. The wind loads were not taken into account in the calculations of this project.

k. Guard-rails loads

Horizontal forces are applied on the guide-rails therefore,

0.5(1+b) =0.5(1+1) =1kn/ml

b represents the walkable width space next to the guide-rails.

l. Thermic gradient

It is essential to take into account the thermic stresses because El Bayadh wilaya, experiences warm summer or hot days which causes a positive gradient and winters or cold nights which causes a negative gradient.

The thermal gradient of a concrete deck during the construction phase is $\pm$12 while in commissioning phase is $\pm$7.

The linear temperature difference is taken into account for the joints, because the effect is more significant on the joints.

T=$\pm$30°C

The coefficient of the expansion of the reinforced concrete=α = 1.1 × 10^{-5}C°$^{-1}$

3.6 The Manual Calculations

The shear forces and the bending moments are critical aspects that are due to the dead loads and the live loads.

3.6.1 Shear Forces

3.6.1.1 Shear Forces due to self-weights

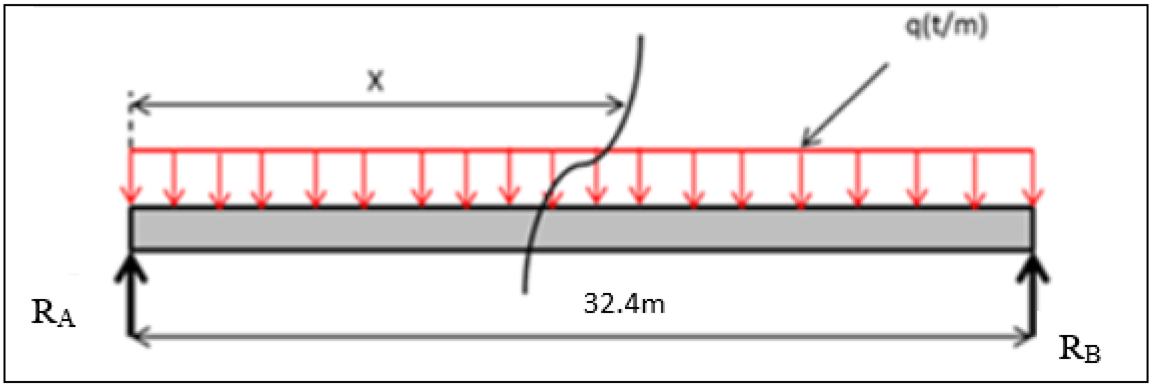

Figure 3.17: A beam under self-weight

The **self-weight** of the:

- 1 beam=12.76kn/ml
- The slab=75kn/ml

Slab weight÷number of beams=75/6=12.5kn/ml
The self-weight of the superstructures=1.455kn/ml
The self-weight of the superstructure÷number of beams=0.2425kn/ml
The total sum of the self-weight=12.76+12.5+0.2425=25.50kn/ml

The Reaction of the beam, R:
$R_A=R_B=Q.L/2=425.89$kn
To obtain the shear force:
$T(x)= R_A – Qx$

Table 3.14: Shear forces due to the self-weight of a beam

X(m)	T(t) Kn	R(t) Kn
0	425.89	425.89
L/4	212.95	/
L/2	0	/

Table 3.15: Shear forces due to the self-weight of all beams

X(m)	T(t) Kn	R(t) Kn
0	2555.34	2555.34

L/4	1277.67	/
L/2	0	/

3.6.1.2 Live Load, AL

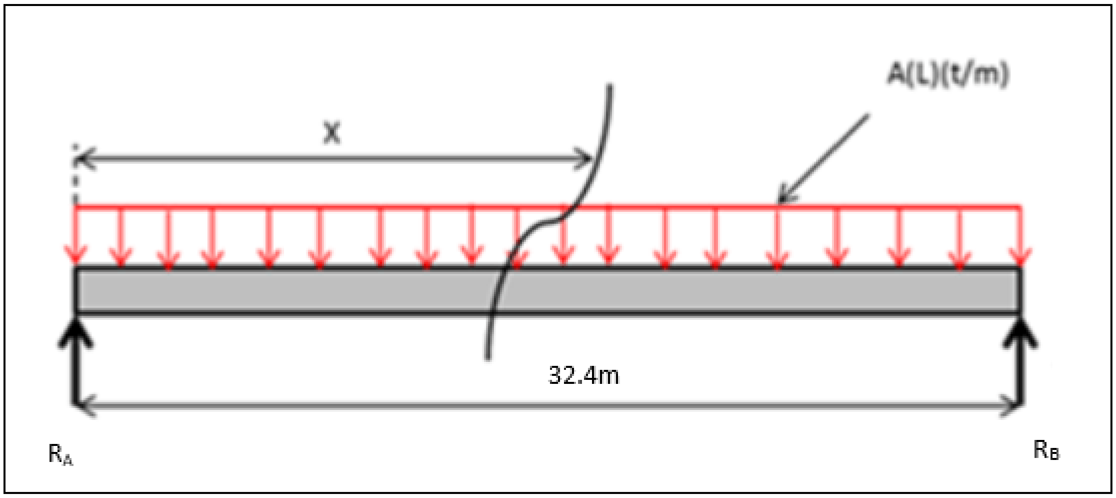

Figure 3.18: Distribution of live load, Al

The reaction by lane:

Q_{Al}=Al× 3.5 = 4.177t/m

R_A=R_B=AL.$\frac{L}{2}$= 4.177× 16.2=67.67t

The shear force is given by:

T(x) = RA - A (L) x

T (x = 0) = RA = 67.67t

T (x = 0.25L) = 67.67– 4.177× (32.4 × 0.25) /2 = 33.84 t

3.6.1.3 Live load Bc, Shear force

One Lane is loaded with the BC live load, in a manner that it will be the same for the other lane.

For x=0L

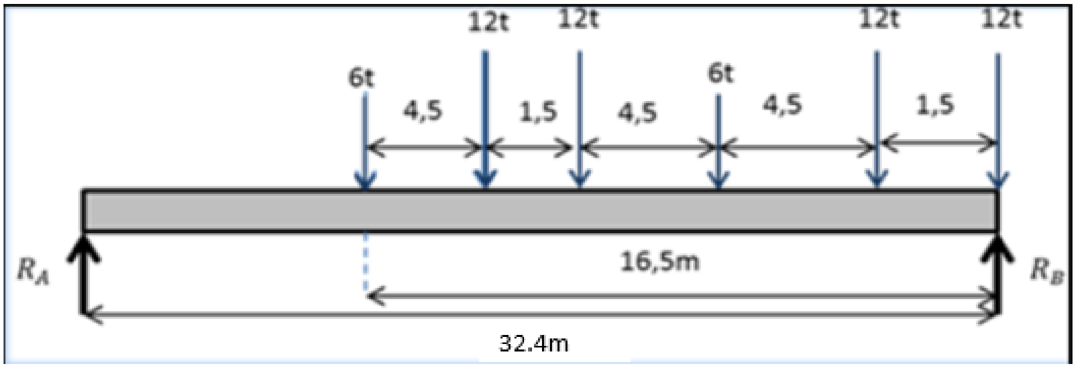

Figure 3.19: Distribution of live load Bc, 2lorries.

The solicitations calculations are as follows:

$R_A + R_B = 60t$

$\sum_B M = 0$

$12 \times 1.5 + 6 \times 6 + 12 \times 10.5 + 12 \times 12 + 6 \times 16.5 = R_A \times 32.4$

$423\ t = R_A \times 32.4$

$R_A = 13.05t$

$R_B = 60 - R_A$

$R_B = 60 - 13.06 = 46.94$

$T_0 = P_B = 46.94\tau$

$T0max = T0 \times \delta bc$

$T0max = 46.94 \times 1.076 = 50.51t$

For x=L/4

x=8.1m

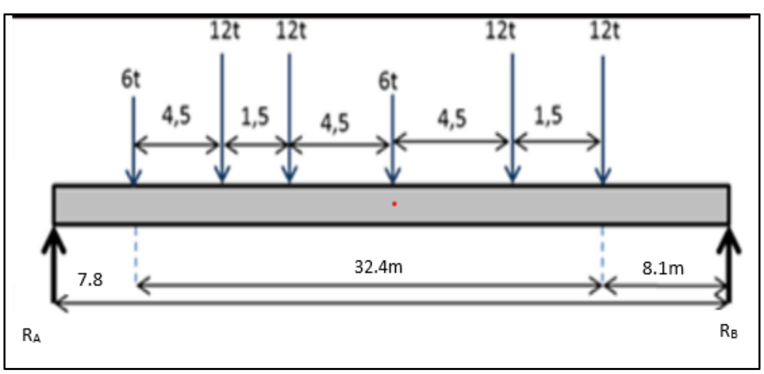

Figure 3.20:Distribution of live load Bc at x=8.1m

The solicitations calculations are as follows:

$R_A+R_B= 60t$

$\sum_B M=0$

$12 \times 8.1+12\times9.6+ 6 \times 14.1 + 12 \times 18.6 + 12 \times 20.1 + 6 \times 24.6 = R_A \times 32.4$

$909\ t = R_A \times 32.4$

$R_A=28.06t$

$R_B=60- R_A$

$R_B=60-28.06=31.94$

$T_0 = P_B = 31.94t$

$T_0\ max = T0 \times \delta bc$

$T_0\ max = 31.94\times 1.076=34.37t$

Lane	T_0, x=0L	δ_{bc}	T_{0max}, (x=0L)	T_0,x=L/4	δ_{bc}	T_{max} ,x=L/4
1	46.94	1.065	49.99	31.94	1.065	34.02
2	93.88	1.076	101.01	63.88	1.076	68.73

Table 3.16: A summary of the bc shear forces at 0L and at L/4

3.6.1.4. Bt Live Load System

The calculation for a single tandem which is similar to the other cases:

For x=0L

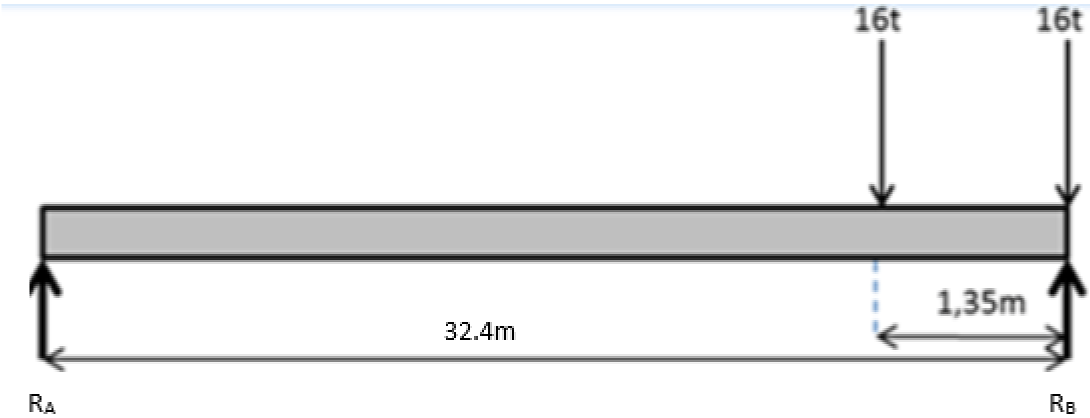

Figure 3.21: Distribution of live load Bt

Sollicitations :

$R_A + R_B = 32t$

$\sum_B M=0$

$(R_A \times 32.4) + (-1.35 \times 16) = 0$

$R_A = 0.67t$

$R_B = 31.33t$

$To = R_B = 31.33t$

$Tomax = To \times \delta_{Bt}$

$Tomax = 31.33 \times 1.058 = 33.15t$

For x=L/4

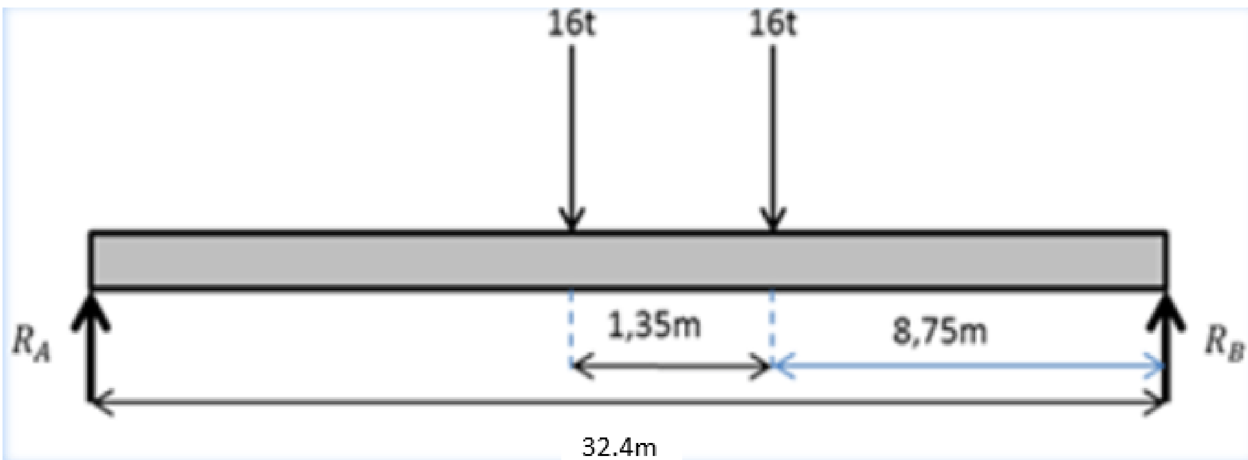

Figure 3.22: Distribution of live load Bt at x=L/4

$R_A + R_B = 32t$

$\sum_B M = 0$

$(R_A \times 32.4) + (-8.75 \times 16) + (-10.1 \times 16) = 0$

$32.4\ R_A = 301.6t$

$R_A = 9.309t$

$R_B = 22.69t$

$To = R_B = 22.69t$

$Tomax = To \times \delta_{Bt}$

$Tomax = 22.69 \times 1.058 = 24.01t$

Table 3.17: A summary of the bt live loads

Lane	T_0, x=0L	δ_{bt}	T_{0max},	T_0,x=L/4	δ_{bt}	T_{max} ,x=L/4
1 Tandem	31.33	1.058	33.15	22.69	1.058	24.01
2 Tandem	62.66	1.064	66.67	45.38	1.064	48.28

3.6.1.4 Br System

For X=0L

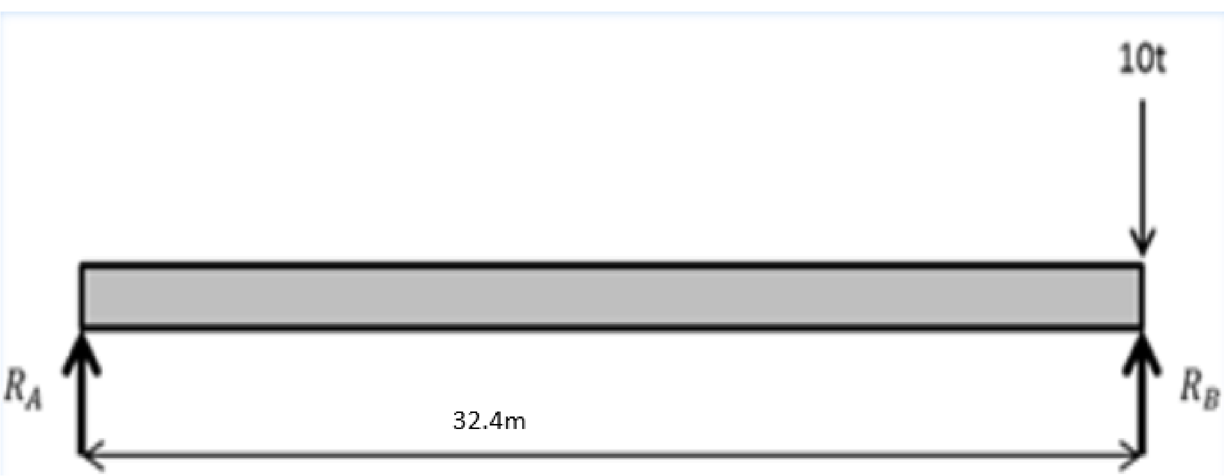

Figure 3.23: Distribution of live load, Br at x=0L

Tomax=10t

For x=L/4

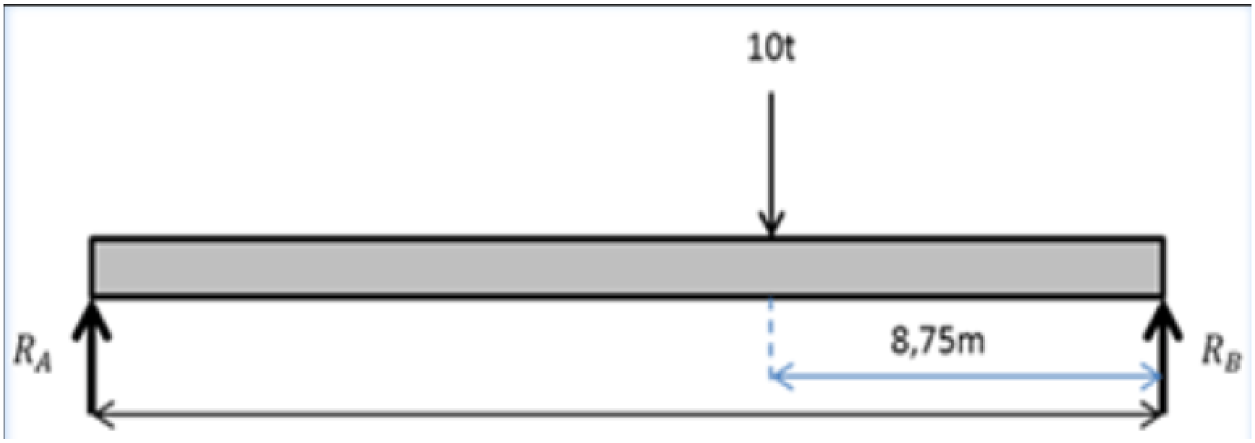

Figure 3.24: Distribution of live load, Br at x=L/4

$R_A+R_B= 10t$

$\sum_B M=0$

$32.4R_A =10\times8.75$

$R_A = 2.70t$

$R_B =10-2.7=7.30t$

$T0= R_B =7.3t$

Tmax=7.3t

3.6.1.5 MC120 System

For x=0L

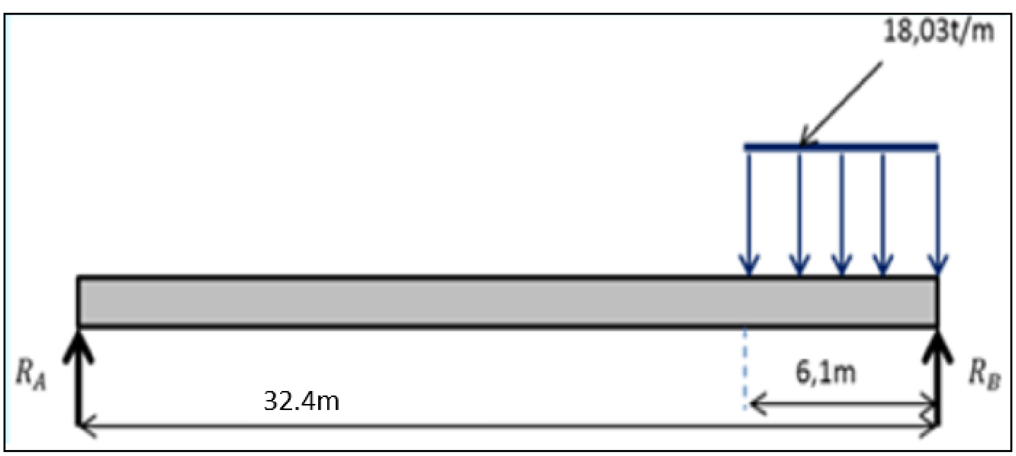

Figure 3.25: Distribution of live load, MC120 at x=0L

$R_A+R_B= 110t$

$\sum_B M=0$

$R_A \times 32.4=110 \times 6.1/2$

$R_A =10.35t$

$R_B=110-10.35=99.65t$

$T_B= R_B=99.65t$

For X=L/4

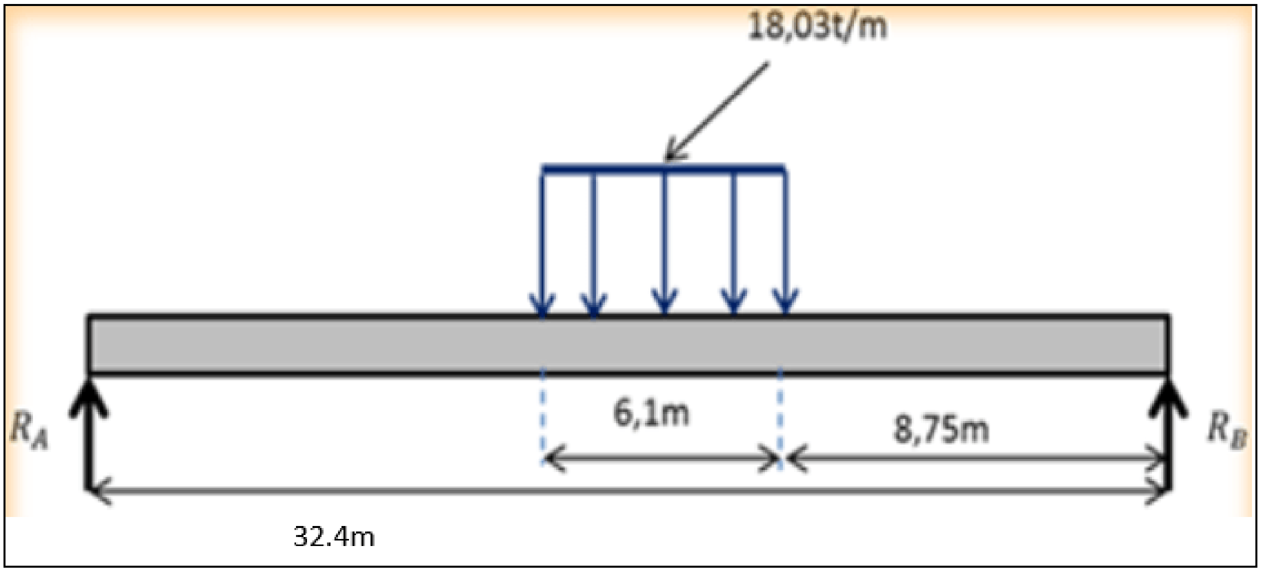

Figure 3.26: Distribution of live load, MC120 at x=L/4

$R_A+R_B= 110t$

$\sum_B M=0$

$R_A \times 32.4=110 \times (8.75+6.1/2)$

$R_A =40.06t$

$R_B=110-40.06=69.94t$

$T_B= R_B=69.94t$

The maximum Shear force is 69.94t

3.6.1.6 System D240

For **x=0L**

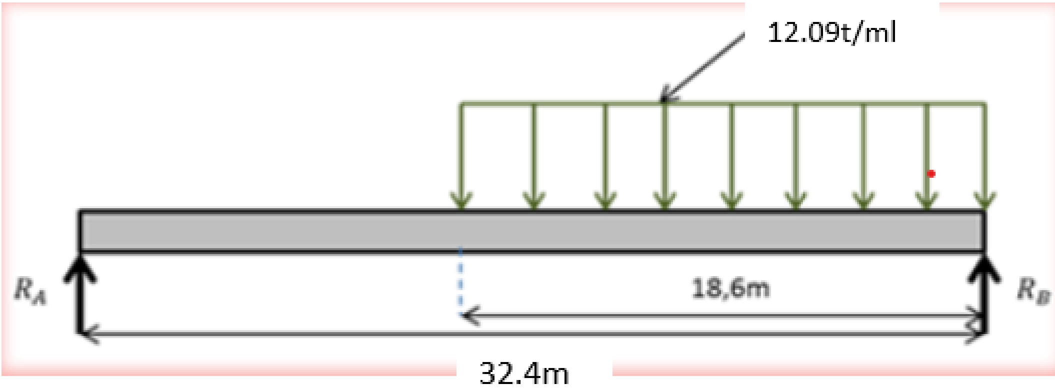

Figure 3.27: Distribution of live load, D240 at x=0L

$R_A+R_B= 240t$

$\sum_B M=0$

$R_A \times 32.4=240 \times 18.6/2$

$R_A =68.89t$

$R_B=240-68.89=171.11t$

$T_B= R_B=171.11t$

The maximum Shear force is 171.11t

For X=L/4

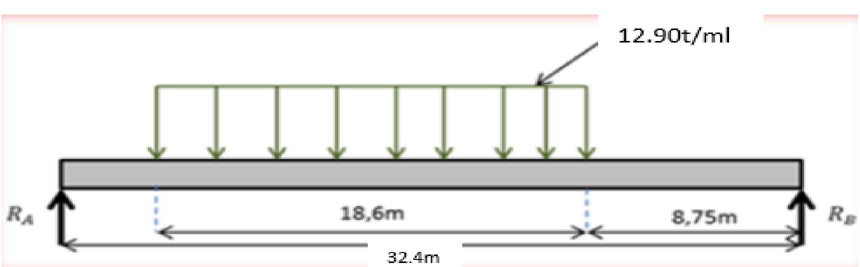

Figure 3.28: Distribution of live load, D240 at x=L/4

$R_A+R_B= 240t$

$\sum_B M=0$

$R_A \times 32.4=240 \times(8.75+18.6/2)$

$R_A =133.7t$

$R_B=240-133.7=106.3t$

The maximum Shear force is:

$T_B= R_B=106.3t$

Tmax=106.3t

Table 3.18: A summary of the shear forces from the different live load systems

Live load systems	**P in t/ml**		**X=0L**		**X=L/4**
		Tmax(t)	T0=Tmax/6	Tmax(t)	T0=Tmax/6
Al	1 lane,4.177	67.67	11.28	33.84	5.64
	2 lanes,8.354	135.35	22.56	67.67	11.28
Bc	1file, EAV=6.39	49.99	8.33	34.02	5.67
	2files, EAV=12.91	101.01	16.84	68.73	11.46
Bt	1tandem	33.15	5.53	24.01	4.00
	2tandems	66.67	11.11	48.28	8.05
Br	10	10	1.67	7.3	1.22
MC 120	18.09	99.65	16.61	69.94	11.66
D240	12.90	171.11	28.52	106.3	17.72

3.6.2 Bending Moments

3.6.2.1 Bending Moments due to self-weight

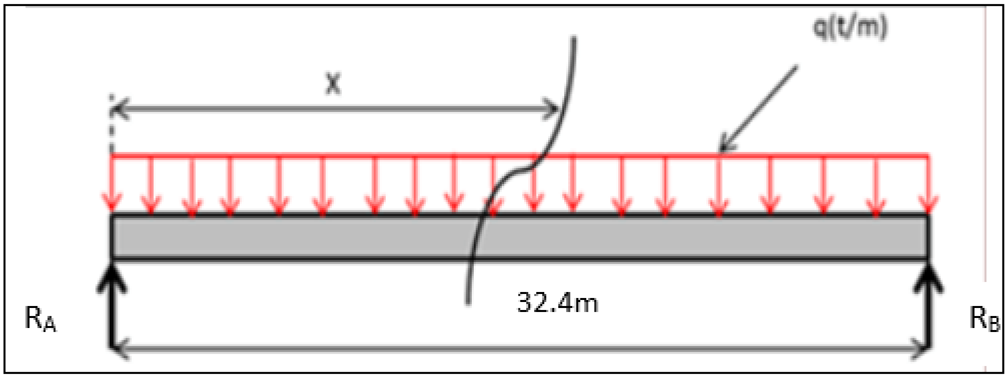

Figure 3.29: Distribution of the self-weight

To obtain the bending moments, the following expression is used:

$M(x) = qL/2(x) - qx^2/2$

q=23.84t/m

$R_A = R_B = qL/2 = 386.21t$

Table 3.19: Bending moments due to the self-weight

The section of the position	M(x) t.m	M(x)/6 t.m
X=0L	0	0
X=L/4	2346.23	391.04
X=L/2	3128.32	521.39

3.6.2.2 Moments due to live loads, Al System

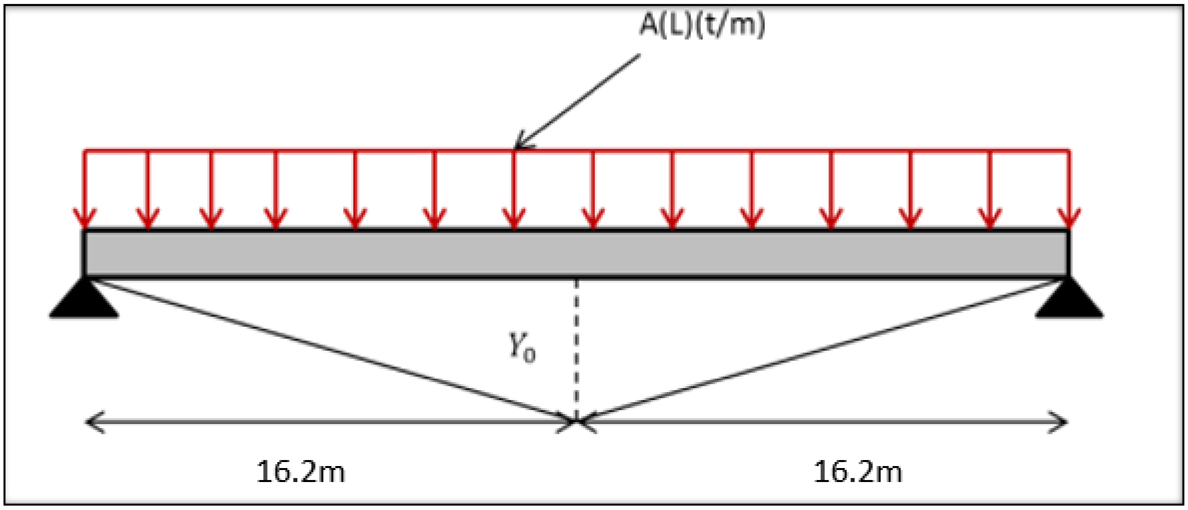

Figure 3.30: Distribution of live load Al

To determine Yo:

$$Yo=\frac{axb}{L}=8.75m$$

The area is:

$$Area=\frac{Yo\times(a+b)}{2}=\frac{8.75\times(16.2+16.2)}{2}=141.75m^2$$

The maximum moment is:

Mmax=S'× Al

S'=141.75m^2

Table 3.20: Bending moments of live load, Al

Lanes	**Al (t/ml)**	***Mmax*** **(t.m)**
1	4.177	592.09
2	8.354	1184.18

3.6.2.3 Bending Moments Due to Bc system

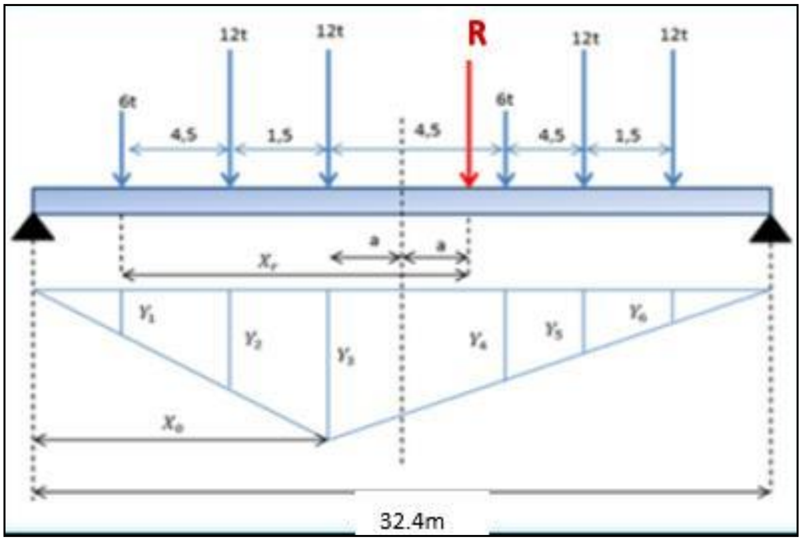

Figure 3.31: Distribution of live load Bc, case1

R = ∑ Pi = 60 t

∑M/A = 0

12 × 4.5 + 12 × 6 + 6 × 10.5 + 12 × 15 + 12 × 16.5= R × Xr

567 = 60 × Xr

Xr = 9.45 m

Thus, 2a = Xr - 6 = 3.45 m

a = 1.725 m

X0 = L/2 - a = 16.2 - 1.725 = 14.475 m

Y3 = [X0 × (L - X0)] /L

Y3 = 8.008m

Table 3.21: y values

Y_1	Y_2	Y_3	Y_4	Y_5	Y_6
4.689	**7.178**	**8.008**	**5.998**	**3.987**	**3.317**

The moments obtained from this case is:

$M1 = \sum Pi \times Yi$ = 4.689× 6 + 7.178 × 12 + 8.008× 12 + 5.998 × 6 + 3.987 × 12 + 3.317 × 12

M1 = 334. 002 t.m

Cas 2

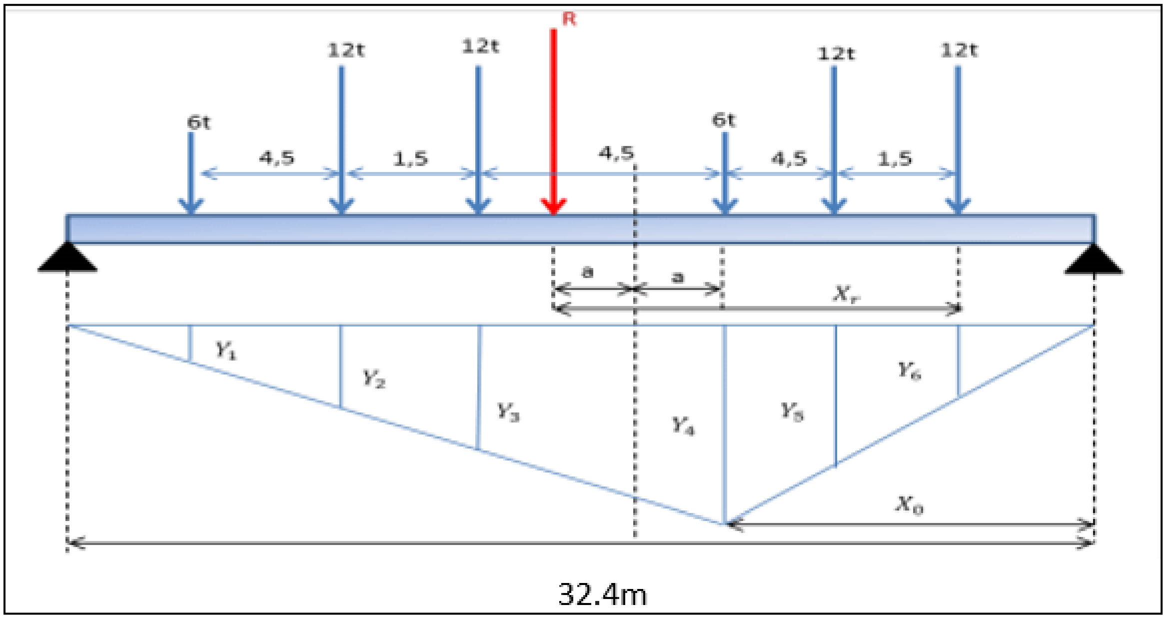

Figure 3.32: Distribution of live load Bc, case2

R = 60 t

∑M/A = 0 → 12 × 1.5 + 6 × 6 + 12 × 10.5 + 12 × 12 + 6 × 16.5 = R × Xr

423 = 60 × Xr → Xr = 7.05 m

Therefore,2a = Xr - 6 = 1.05 m

a = 0.525 m

X0 =L /2- a = 16.2 - 0.525 = 15.675 m

Y4 = [X0 × (L - X0)] /L = 8.09m

Table 3.22: y values

$\boldsymbol{Y1}$	$\boldsymbol{Y2}$	$\boldsymbol{Y3}$	$\boldsymbol{Y4}$	$\boldsymbol{Y5}$	$\boldsymbol{Y6}$
3.011	**5.188**	**5.913**	**8.09**	**5.676**	**4.993**

The moment in this case is:

M2 = 3.011 × 6 + 5.188× 12 + 5.913 × 12 + 8.09 × 6 + 5.676× 12 + 4.993 × 12

M2 = 327.85t.m

The worst-case scenario is deduced from the 1st case with a moment value of 334.002t.m which is deduced from the first case.

To obtain the maximum bending moments:

Mmax = bc × δbc × M

Table 3.23: Bending moments results from case2

Lanes	b_c	M (t.m)	δ_{bc}	M_{max} (t.m)
1	1.2	334.002	1.065	426.85
2	1.1	668.004	1.076	790.65

The bending moment by beam from the Bc system is:

$Y3 + Y6 = 11.325$m

$Y2 + Y1 + Y5 + Y4 = 21.852$m

$M = P\sum Yi = Pe$ in front $(Y1 + Y4) + Pe$ behind $(Y2 + Y3 + Y5 + Y6)$

Table 3.24: Bending Moments of live load, Bc par beam

Lanes	δbc	Axles	P (t)	Yi	Mmax (t.m)	M0=Mmax/6
1	1.065	EAV	6.39	11.35	351.77	58.63
	1.065	EAR	12.78	21.85		
2	1.076	EAV	12.91	11.35	710.69	118.45
	1.076	EAR	25.82	21.85		

3.6.2.4 Bending Moments due to live load, Bt

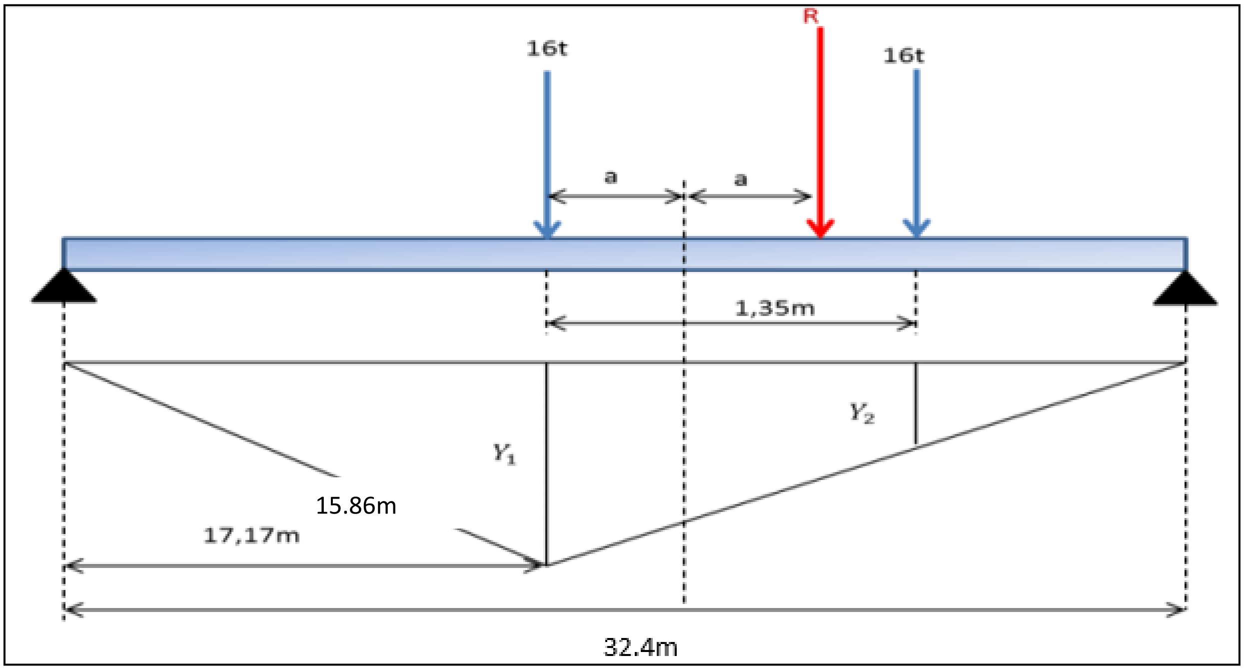

Figure 3.33: Distribution of the Bt load to obtain the bending moments

$16 \times 1.35 = 32(1.35 - 2a) \rightarrow a = 0.3375$ m

$X0 = L/2 - a = 15.86$ m

$Y1 = X0(L - X0)/L = 8.095$ m

By applying the theorem of Thales:

$Y2 = 7.434$m

$M = \sum Pi \times Yi$

$M = 16(8.095 + 7.434) = 248.47$ t. m

$Mmax = bt \times \delta bt \times M$

Table 3.25: Bending Moments of Bt system

Number of Tandems	Bt	δbt	M (t.m)	Mmax (t.m)
1	1	1.058	248.47	262.88
2	1	1.064	496.94	528.74

3.6.2.5 Bending Moments due to the Br System

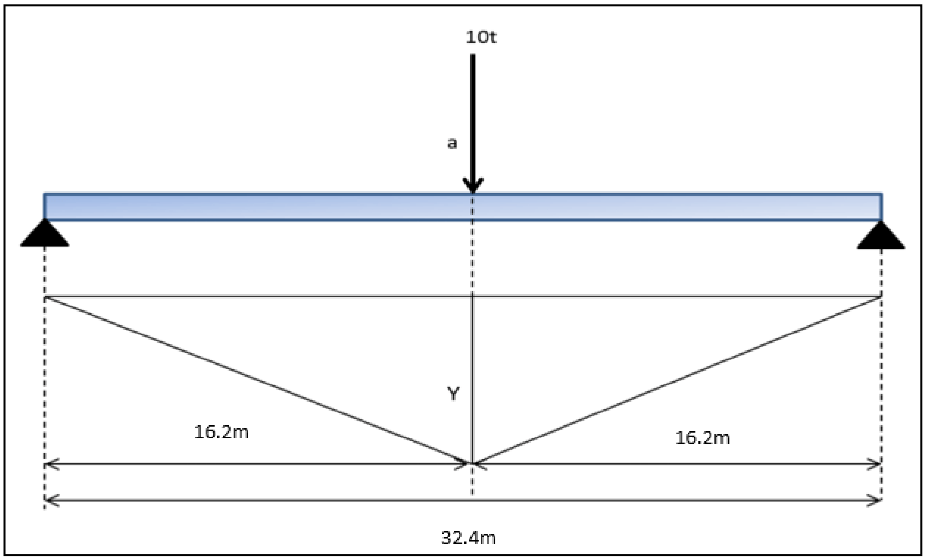

Figure 3.34: Distribution of Bt live load

$Y=\frac{(L/2)^{\wedge}2}{L}=8.1m$

$Mmax=10\times Y=81t.m$

3.6.2.6 Bending Moment of live load MC120.

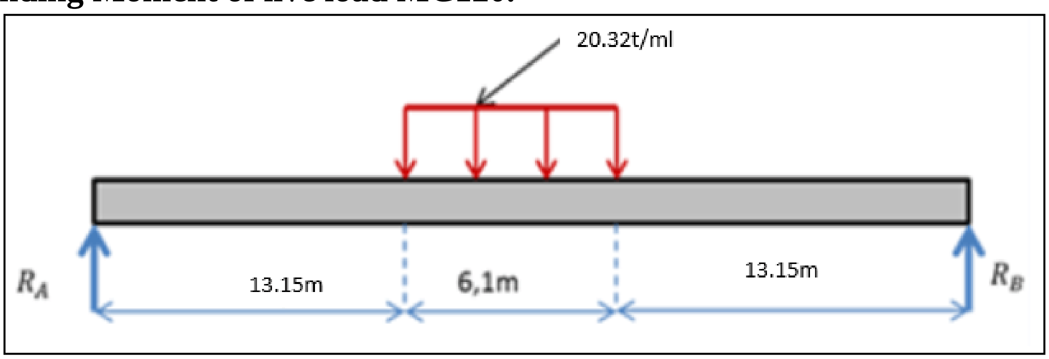

Figure 3.35: Distribution of live load MC120

$R_A = R_B = (\delta_{Mc120} \times 110)/2 = 61.99$ t

$Mmax = R_{Ax} – q\ (3.05^2/2) = 61.99 \times 16.2 – 20.32(3.05^2/2) = 909.72$t. m

$\boldsymbol{Mmax} = 909.72$ t.m

3.6.2.7 Bending Moment of live load, D240

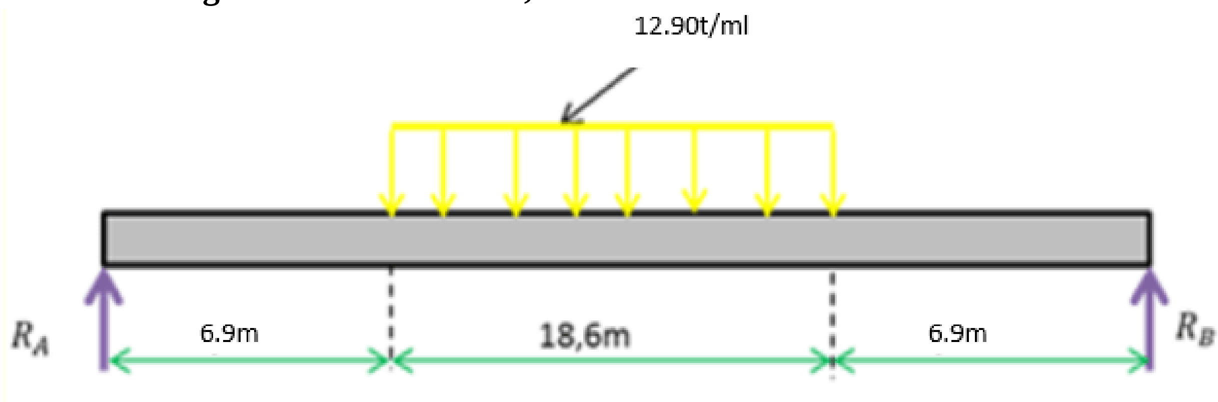

Figure 3.36: Distribution of D240

$R_A = R_B = (12.90\times18.6/2) = 119.97t$

$M_{max} = R_{Ax} – q\,(9.3^2/2) = 119.97\times 16.2 – 12.90(9.3^2/2) = 1385.65t.\ m$

$\boldsymbol{Mmax} = 1385.65t.\ m$

Table 3.26: A summary of the bending moments from the live loads

Live-loads			P (t/ml)	Mmax (t.m)	M0=Mmax/6 (t.m)
Al	**1 lane**		4.177	592.09	98.68
	2 lanes		8.354	1184.18	197.37
Bc	**1 file**	**EAV**	6.39	351.77	58.63
		EAR	12.78		
	2 files	**EAV**	12.91	710.69	118.45
		EAR	25.82		
Bt	**1 tandem**			262.88	43.81
	2 tandems			528.74	88.12
Br			**10**	81	13.5
MC120			**20.32**	909.72	151.62
D240			**12.90**	1385.65	230.94

Using SAP2000vs14.0.0, the moments of the dead load and live loads were generated with respect to the loads placed on one beam with a slab.

Table 3.27: SAP obtained values

	Moment Obtained (KN.m)	Loads (KN/m or KN)	Distances on which the loads are placed on the beam span
Gslab + Gbeam	3052.177	10.5+12.76	0m to 32.4m
Al	1879.94	83.55	0m to 32.4m
BC case1	5730	60, 120, 120	From the extreme 0m to 16.m
BC case 2	6578	60, 120, 120	6m to 22.5m
BC case 3	6670	60, 120, 120	7.95m to 24.45m
D240 case1	3873.2	2400	0m to 18.6m
D240 case 2	6024.33	2400	6.9m to25.5m
Br case1	607.50	100	at 8.1m
Br case 2	810.00	100	At 16.2
Bt	2160	160	9.45m to 10.85m
	2232	160	10.85m to 12.15m
	2394	160	12.15m to 13.50m
	2457	160	13.50m to 14.85m
	2484	160	14.85m to 16.20m
	2485	160	15.86m to 17.21m

3.7 Conclusion

We can conclude that the sizing of the beam is done concerning the different civil engineering guidelines, for instance, the S.E.T.R.A guide. The geometric characteristics of the beam are imperative to the calculation of the beam's yield. The lowering of loads on the beam varies concerning the permanent loads yielded by the bridge itself and the live loads which act now and then on the bridge apron. Hence the study of this chapter is essential to ensure the safety and the stability of this project.

Chapter 4:
The Prestressed Study

4

4.1 Introduction

In the year, 1928, a French structural and civil engineer, Sir Eugene Freyssinet pioneered the invention of prestressed concrete by using concrete of high quality and steel of high strength. The invention has ever since been in use in the civil engineering world. Therefore, prestressed concrete revolutionized the use of concrete especially, on bridges with longer spans.

4.2 The Prestressed Principle

Since concrete is strong under compression but weak under tensile stresses, prestressed concrete, therefore, permits us to create internal compressive stresses in the concrete using stress cables, wires, or rods which are high in tensile stresses to counter or balance the external stresses which are due to the applied loading. The main aim of prestressing is to make sure that we have low or zero tensile stresses in the concrete to minimize cracks especially on the lower fibre when the beam is under the bending solicitation. The prestressed principle allows the structure to be more stable due to the increased load-bearing capacity. Below is a figure demonstrating the prestressed principle.

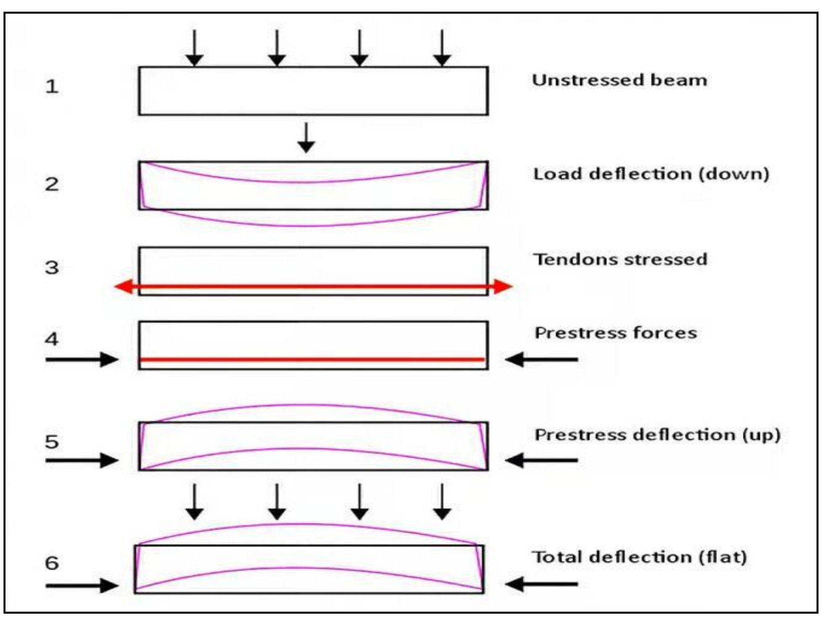

Figure 4.1: The prestressed principle

4.3 Types of Prestressed

In prestressing, we have two main categories which are:

- Pre-tensioning
- Post-tensioning

4.3.1 Pre-Tensioning

This prestressed technique is disguisable by the fact that the stressed cables or wires are placed first before casting of the concrete. Once casting takes place and concrete dries up, the stressed cables are released, thus creating a compressive force which is the prestressed force.

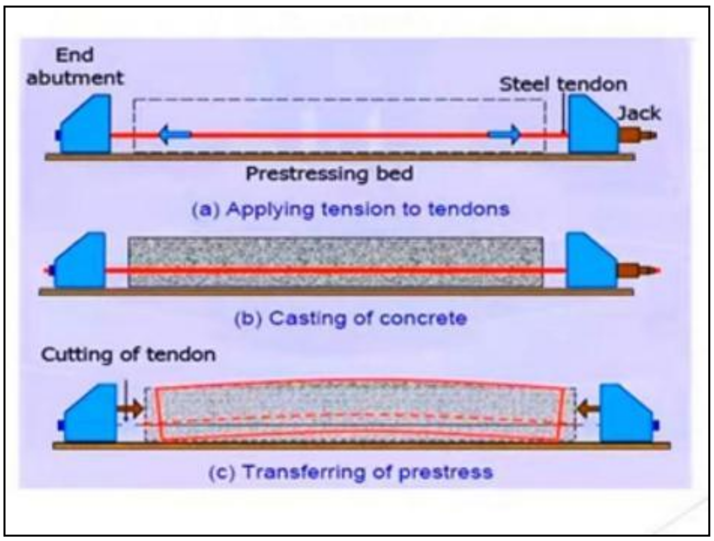

Figure 4.2: Pre-tensioning process

4.3.2 Post-Tensioning

In this project, the post-tensioning prestressed technic was used in the construction process. Predominantly, this technic introduces the prestressed later, after the casting of the concrete of the beam section has taken place by leaving an empty duct within the section. Later on, after the casted concrete dries up and after it has attained a certain resistance, the steel cables are inserted in the duct and tensioned at a certain percentage, for instance, 50% to create the internal compressive stresses. The equipment used to tension the steel cables can be a Stressing Jack or a Stressing Pump. After tensioning, the steel cables are anchored, with precision.

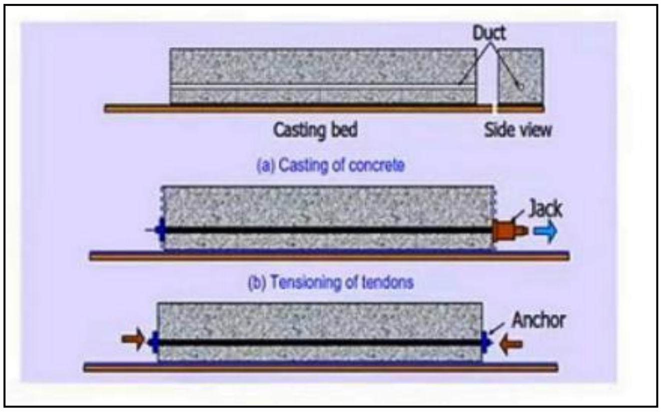

Figure 4.3: Post-tensioning process

4.4 The Prestressed Force Calculation

According to the B.P.E.L guidelines, it states that the prestressed force is equivalent to the most unfavourable of two values which are:

- The maximum prestressing, P_{sup}= P supercritical
- The minimum prestressing, P_{sub}= P subcritical

  $P=\max(P_{sup}, P_{sub})$

These two values depend on whether the passage segment of the steel cables invades the covering zone or not, therefore the section is said to be over-critic, critic or under-critic. Thus, during prestressing the two main factors to be considered are: the sufficient coating zone and the passage segment for the steel cables.

4.4.1 Under-Critical Section

When the passage section of the steel cables, does not interfere with the coverage zone, then the beam section is said to be under-critic.

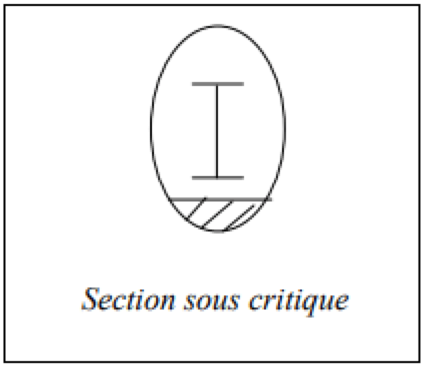

Figure 4.4:Sub-critical section

With: the shaded region=coating zone.

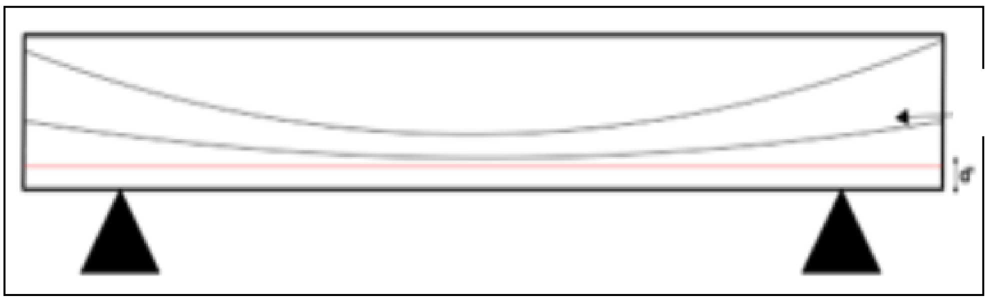

Figure 4.5: Sub-critical section in a longitudinal view

The formula below is used to calculate the sub-critical section:

$$\mathbf{Psub} = \frac{\mathbf{\Delta M}}{\boldsymbol{\rho} \cdot \mathbf{h}} + \frac{\mathbf{s}}{\mathbf{h}}(\boldsymbol{\sigma}_{\mathbf{ti}} \cdot \mathbf{v} + \boldsymbol{\sigma}_{\mathbf{ts}} \cdot \mathbf{v}')$$

With;

Psub: Sub-critical Prestressing force

ΔM: Mmax – Mmin=MQ

Mmax: Moments due to the dead loads and live loads

Mmax=MQ+MG

Mmin: Moments due to dead loads

Mmin=MG

ρ: geometric yield

h: height of the beam

s: beam's section

σ_{ti}: permissible tensile stresses on the lower fibre

σ_{ts}: permissible tensile stresses on the upper fibre

MQ=6.024 Mn.m due to live-load D240.

MG=3.052 Mn.m

$$\text{Psub} = \frac{6.024}{0.4478 \times 1.8} + \frac{0.8871}{1.8}((-2.4) \times 0.5831 + (-3.6) \times 1.2169)$$

Psub=4.6249Mn

4.4.2 Critical Section

When the passage section of the steel cable can be minimized into a point, then the section is said to be critical.

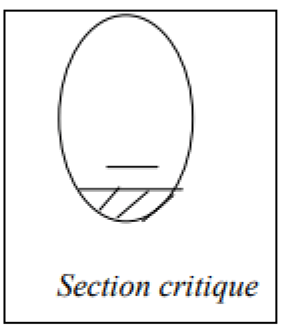

Figure 4.6: Critical section

4.4.3 Over-Critical Section

When the passage section of the steel cables, interferes with the coverage zone, the beam section is said to be over-critic.

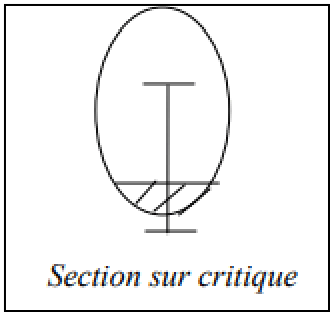

Figure 4.7: Super-critical section

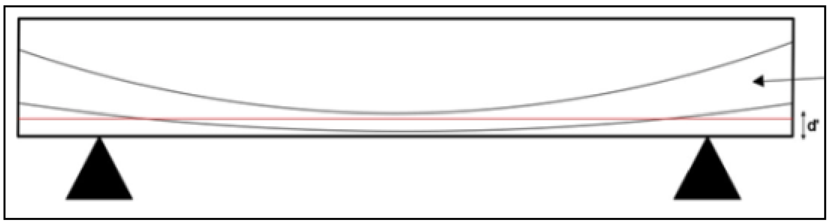

Figure 4.8: Super-critical section on longitudinal view

The formula below enables us to find the super-critical prestression.

$$\mathbf{Psup} = \frac{\mathbf{Mmax + s.\rho.v.\sigma ti}}{\mathbf{\rho \cdot v + v' - d'}}$$

With d': is the distance between the centre of gravity and the lower fibre.

d'=10cm

$$\text{Psup} = \frac{9.076 + 0.8871 \times 0.4478 \times 0.5831 \times (-2.4)}{0.4478 \times 0.5831 + (1.2169 - 0.10)}$$

Psup=6.183Mn

P=max (Psub, Psup) = max (Psub=4.6249Mn, Psup=6.183Mn)

Therefore, the section is super-critical and 6.183Mn.

To verify that the section is indeed super-critical, the equation below is used.

$\frac{I}{v} \geq \frac{\rho Ph}{\bar{\sigma}_{max}+\frac{v}{v'}\bar{\sigma}_{min}}$ = 0.4834≥ 0.2973

The condition is **verified**, and we can conclude that the section is **super-critical**.

4.5 Estimated Prestressing

The estimated prestressing is done using a percentage of estimated prestressing losses which are:

- 25% at 14 days.
- 20% at 28 days.

The prestressing losses reduce gradually, hence higher prestressing losses occur in the earlier days of concrete and prestressing.

According to the B.P.E.L, prestressing is the average of the Psub and Psup.

Hence, P = $\frac{Psup+Psub}{2} = \frac{4.6249+6.183}{2}$ = 5.404Mn

P1 and P2 are then deduced from the average Prestressing obtained with a factor,λ=0.1.

P1= (1+ λ) P=7.961Mn

P2= (1- λ) P= 6.513Mn

The fictive permissible stresses are:

$\bar{\sigma}'^{f}_{max} = \frac{\bar{\sigma}'_{max}}{1+\lambda}$ =16.36MPa ci

$\bar{\sigma}'^{f}_{min} = \frac{\bar{\sigma}'_{min}}{1-\lambda}$ =-2.667MPa ti

$\bar{\sigma}^{f}_{max} = \frac{\bar{\sigma}_{max}}{1-\lambda}$ =20MPa cs

$\bar{\sigma}^{f}_{min} = \frac{\bar{\sigma}_{min}}{1+\lambda}$ =-3.273MPa ts

The fictive moments are:

$M^{f}_{max} = \frac{M_{max}}{1-\lambda}$ =10.084 Mn.m

$M^{f}_{min} = \frac{M_{min}}{1+\lambda}$ =2.775 Mn.m

$\frac{I}{V} = \frac{\Delta M^f}{\Delta \bar{\sigma} f} = \frac{10.084-2.775}{20} = 0.3655m^3$

$\frac{I}{V\prime} = \frac{\Delta M^f}{\Delta \bar{\sigma}\prime f} = \frac{10.084-2.775}{16.36} = 0.4468m^3$

Using the new fictive values:

P^Nsup=6.8695MPa

P^Nsub=6.34MPa

Hence, the section is still super-critical.

4.6 Determining the Number of Cables Required

To calculate the number of cables, with P being the maximum prestressed force from the fictive values.

$N = \frac{\text{Max}\ (\mathbf{PNsup}, \mathbf{PNsub})}{\sigma p_0 \times A_P}$

N: number of cables

σp_0: Original stress: min= (0.8fprg; 0.9f_{peg})

fprg: guaranteed constraint to ruin

fpeg: elastic guaranteed constraint

We will use a cable of T15 hence,

f_{prg}: 1860MPa

f_{peg} :1640MPa

Area of 1Toron=139mm^2 thus,19strands=2641mm^2

σp_0 =Min (0.8× 1860 ; 0.9× 1640)= 1476MPa

P=1476×2641×10^{-6}= 3.898MN

N=6.8695/3.898= 1.7623=2 cables

With the **2 cables**, the admissible stresses were not verified. Therefore, there was a need to increase the number of cables to **4 cables**, which verified the admissible stresses.

The real prestressing value:

P0=N×P=4×3.898=15.592Mn

Maximum Prestressing (MN)	Eccentricity	Number of cables 19T15	Initial Prestressing, P0 (MN)
6.8695	1.0669	4	15.592

Figure 4.9: A Summary of Prestressed Values

4.6.1 The Verification of the Tensioning at SLS

$P1=11.971\times0.25\times 1.1$

$\mathbf{P1=3.292MN}$

$P2=65.49\times0.9\times0.2$

$\mathbf{P2=11.789MN}$

The execution of this project during its construction and commissioning was done in 4 main operational phases with the tensioning verification at SLS done at 14 days and 28 days.

Phase 1

During the 1st phase, the concrete was cast to make the prefabricated beam for 7 days. At the age of 7 days, the concrete gained a notable strength.

Phase 2

After 14 days, the concrete had dried up and the duct spaces were created, to facilitate the passage for the steel tendons and to allow tensioning of the cables from the 1st family at 50%. The prefabricated beam was placed on the supports and thus the beam was under a solicitation. It is at this stage that the slab of 30cm thickness is poured on the beams to create a uniform surface The strength resistance of the concrete went higher too after 14 days.

During the tensioning of the steel cables of the first family, the stresses have to meet the permissible stress conditions as shown below.

$$\frac{P1}{B} - \frac{P1.e}{I/V} + \frac{MG}{I/V} \geq \overline{\sigma}_{st}$$

$$\frac{P1}{B} + \frac{P1.e}{I/V\prime} - \frac{MG}{I/V\prime} \geq \overline{\sigma}_{ci}$$

Table 4.1: Phase 2 verification

P1			
$\frac{P1}{B}$	$\frac{-P1.e}{I/V}$	$\frac{MG}{I/V}$	Results
3.711	-7.267	6.314	2.758MPa
$\frac{P1}{B}$	$\frac{P1.e}{I/V'}$	$-\frac{MG}{I/V\prime}$	Results
3.711	15.165	-13.178	5.698MPa

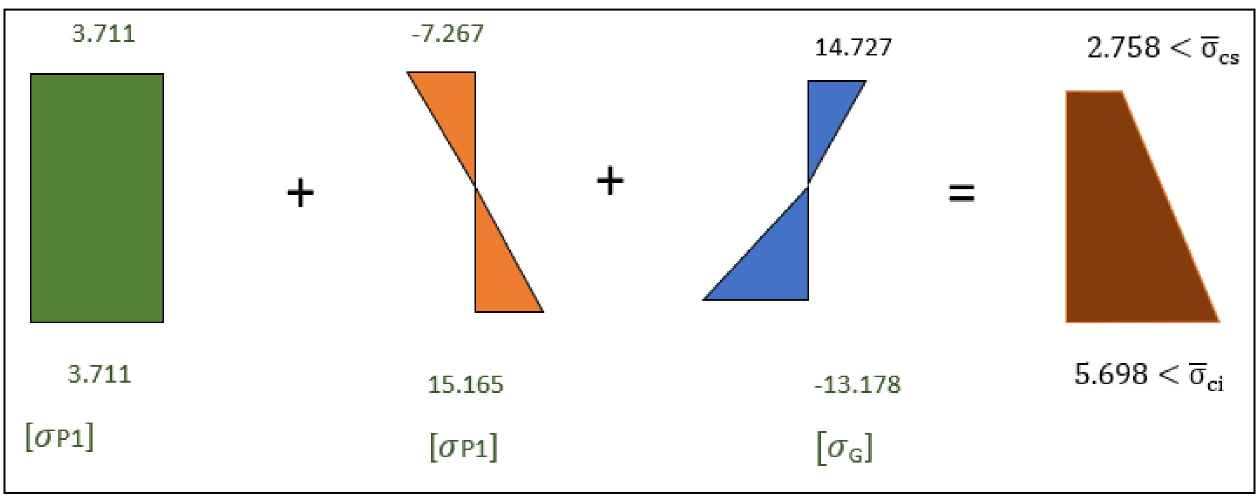

Figure 4.10: The stress diagram

The conditions are **verified**.

Phase 3

After 28 days, the rest of the dead loads like the side-walk were added and the live-loads were also taken into consideration at this stage. At this stage, the steel cables are tensioned again at 100%.

$$\frac{P2}{B} - \frac{P2.e}{I/V} + \frac{MG}{I/V} + \frac{Ms}{I/V} + \frac{Mq}{I/V} \geq \overline{\sigma}_{st}$$

$$\frac{P2}{B} + \frac{P2.e}{I/V'} - \frac{MG}{I/V'} - \frac{Ms}{I/V} - \frac{Mq}{I/V} \geq \overline{\sigma}_{ci}$$

Table 4.2: Rare Combination at 28days

P2					
$\frac{P2}{B}$	$\frac{-P2.e}{I/V}$	$\frac{MG}{I/V}$	$\frac{Ms}{I/V}$	$\frac{Mq}{I/V}$	Results
13.289	-21.633	5.792	7.8974	11.43	16.78MPa
$\frac{P2}{B}$	$\frac{P2.e}{I/V'}$	$-\frac{MG}{I/V'}$	$\frac{Ms}{I/V'}$	$\frac{Mq}{I/V'}$	Results
13.289	39.422	-10.555	-15.032	-20.834	6.29MPa

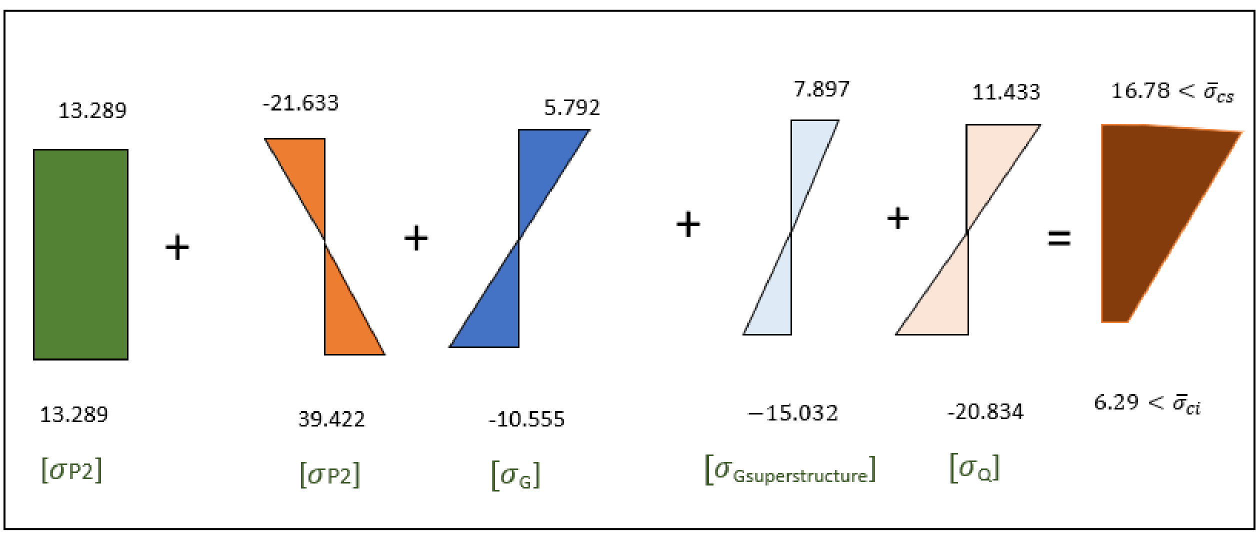

Figure 4.11: The stresses at 28 days

- The conditions of the permissible stresses are verified.

Phase 4

The tensioning of the cables of the 2nd family takes place here, whereby, the steel cables are tensioned at 100%. The bridge is ready to be commissioned after superstructures and the exploitation loads are verified and after the bridge meets all the stability checks.

4.6.2 Verification of the Bending Moments at SLU

The following calculations are done according to the B.P.E.L formulas

Ultimate moments, Mu = 1.35 G + 1.35 Q

$G = G_{beam} + G_{slab} + G_{superstructures} = 12.76 + 10.5 + 31$

G = 54.26 KN/ml = 0.054 Mn/ml

$$M_G = G \cdot \frac{L^2}{8} = 0.054 \times \frac{32.4}{8} = 7.12\mathrm{Mn} \cdot \mathrm{m}$$

$$MQ = 6.024\mathrm{Mn} \cdot \mathrm{m}$$

$$Mu = 1.35G + 1.35Q$$

Thus, Mu=1.35(7.12) +1.35(6.024) = 19.224 Mn.m

Resistant moments of the table

$$\overline{\sigma}_{bcu} = \frac{0.85fc28}{\gamma b} = \frac{0.85 \times 30}{1.5} = 17\mathrm{MPa}$$

$$F_{bc} = (b - b_0)h_0 \cdot \overline{\sigma}_{bcu} = (1.4 - 0.8)0.5 \times 17$$

$$F_{bc} = 10.37\mathrm{MN}$$

$$\mathrm{Leverarm}, z = h - d' - \frac{h_0}{2} = 1.8 - 0.15 - \frac{0.5}{2} = 1.4\mathrm{m}$$

Resistant moment, $M_r = F_{bc} \cdot z = 10.37 \times 1.4 = 14.518\mathrm{Mn} \cdot \mathrm{m}$

$M_r < M_u$ therefore, the neutral fiber is located in the flange

$\mathbf{M_r} = 14.518\mathrm{Mn \cdot m} > \mathbf{Mu} = 9.076\mathrm{Mn \cdot m}$

Hence it is considered rectangular section (bxh) because Mn =Mu, with Mn being the moments due to the dead loads and live loads.

The reduced moments, μ.

$$\mu = \frac{\mathrm{Mn}}{\mathrm{b} \times \mathrm{d}^2 \times \mathrm{f_{bc}}} = \frac{9.076}{1.4 \times 1.65^2 \times 17} = 0.14$$

$$\alpha = 1.25\left(1 - \sqrt{(1 - 2\mu)}\right) = 0.1894$$

With the knowledge of the position of the neutral fibre, we can deduce a relation between the elongation of steel, "$\Delta\varepsilon_3$" and the shortening of concrete,"ε_b".

$$\Delta\varepsilon_3 = \varepsilon_b\left(\frac{1 - \alpha}{\alpha}\right) = 3.5\left(\frac{1 - 0.1894}{0.1894}\right)$$

$$\Delta\varepsilon_3 = 14.98\ ‰ > 10‰$$

Therefore, $\Delta\varepsilon_3$ is limited to 10 ‰

Determination of σ_1 and ε_1

According to Henry Thornier,

$$\sigma_1 = \frac{P1 + P2}{Ap}$$

$$\frac{P_1 + P_2}{2} = \frac{3.292 + 11.789}{2} = 9.1865MN$$

$$\sigma_1 = \frac{9.1865}{4 \times 19 \times 139 \times 10^{-6}} = 869.6Mp_a$$

$$\sigma_{1 < \frac{0.9 \text{ x fpeg}}{\gamma_b}} = \frac{0.9 \times 1640}{1.15} = 1283.48\mathrm{MPa}$$

This means it is in the elastic domain

$\varepsilon_1 = \frac{\sigma_1}{E_p} = \frac{869.6}{190000} = 0.00457 = 4.57\%$

Determination of σ_2 and ε_2

$\sigma_2 = \sigma_1 + \Delta\sigma_2 = \sigma_1 + 5\sigma c$

σc: concrete stress due to the dead loads

$\sigma_c = 7.119\text{MPa}$

$\Delta\sigma_2 = 5\sigma c = 5 \times 7.119 = 35.595\text{MPa}$

$\sigma_2 = 869.6 + 35.595 = 905.195\text{MPa}$

$\sigma_{2<\frac{0.9 \text{ x fpeg}}{\gamma_b}} = 1283.48\text{MPa}$

Thus, it is in the elastic domain.

Therefore,

$$\varepsilon_2 = \frac{\sigma_2}{E_p} = \frac{905.195}{190000} = 0.004764 = 4.76\%$$

Determination of the σ_3

$\varepsilon_3 = \varepsilon_2 + \Delta\varepsilon_3 = 4.764‰ + 10‰ = 14.764‰$

$\varepsilon_3 = \frac{\sigma_3}{E_p} + 100\left(\frac{\gamma_b.\sigma_3}{\text{fpeg}} - 0.9\right)^5 = 0.014764 = \frac{\sigma_3}{190000} + 100\left(\frac{1.15\sigma_3 - 0.9}{1640}\right)^5$

$\varepsilon_3 = 1493.398MPa$

$p_3 = 1 \cdot 493.398 \times 76 \times 139.10^{-6} = 15776\text{MN}$

The resultant compression of the table

$F_t = (b - b_0)h_0 \cdot \bar{\sigma}_{bc} = (14 - 0.18)0.5 \cdot 17 = 10.37\text{Mn}$

The verification of the reinforcement of the rectangular section:

$\text{Ap} \geq \frac{F_t}{\sigma_3} = \frac{10.37}{1493.398} = 0.00694\text{m}^2$

$\text{Ap} = 4 \times 19 \times 139 \times 10^{-6} = 0.010564\text{m}^2$

Thus, $\text{Ap} \geq \frac{F_t}{\sigma_3}$ is verified.

4.7 Constructive Arrangement of Cables

In the first family of cables, 1 cable was prestressed at 14 days and the other 3 cables were prestressed at 28 days.

B.P.E.L recommends a spacing greater than 0.36m between the successive cables with respect to the height. For the positioning of the cables according to SETRA, d is fixed in a manner that the application point of the resultant prestressing forces exiting on the end face of the extreme section of the beam must coincide with the centre of gravity of the section.

Knowing that moments on the support are zero, we can deduce the $\sum M_F=0$.

$P1\times d+P2(Sc+d)+P3(2Sc+d)+P4(3Sc+d)=4\times P0\times V'$

$P1=P2=P3=P4=P0$

$P0(4d+6Sc)=4P0v'$

$d=\frac{4v'-6Sc}{4}=\frac{4\times 85.95-6\times 36}{4}$

$d=28.95cm$

d: the space distance from the bottom part of the beam to where the first cable is positioned on the extreme section of the beam.

Sc: Spacing distance between cables

P1, P2, P3, P4: The prestressing force for each cable.

Below is Figure 4.12, showing an elaborate arrangement of the cables and their distances on the extreme beam cross-section.

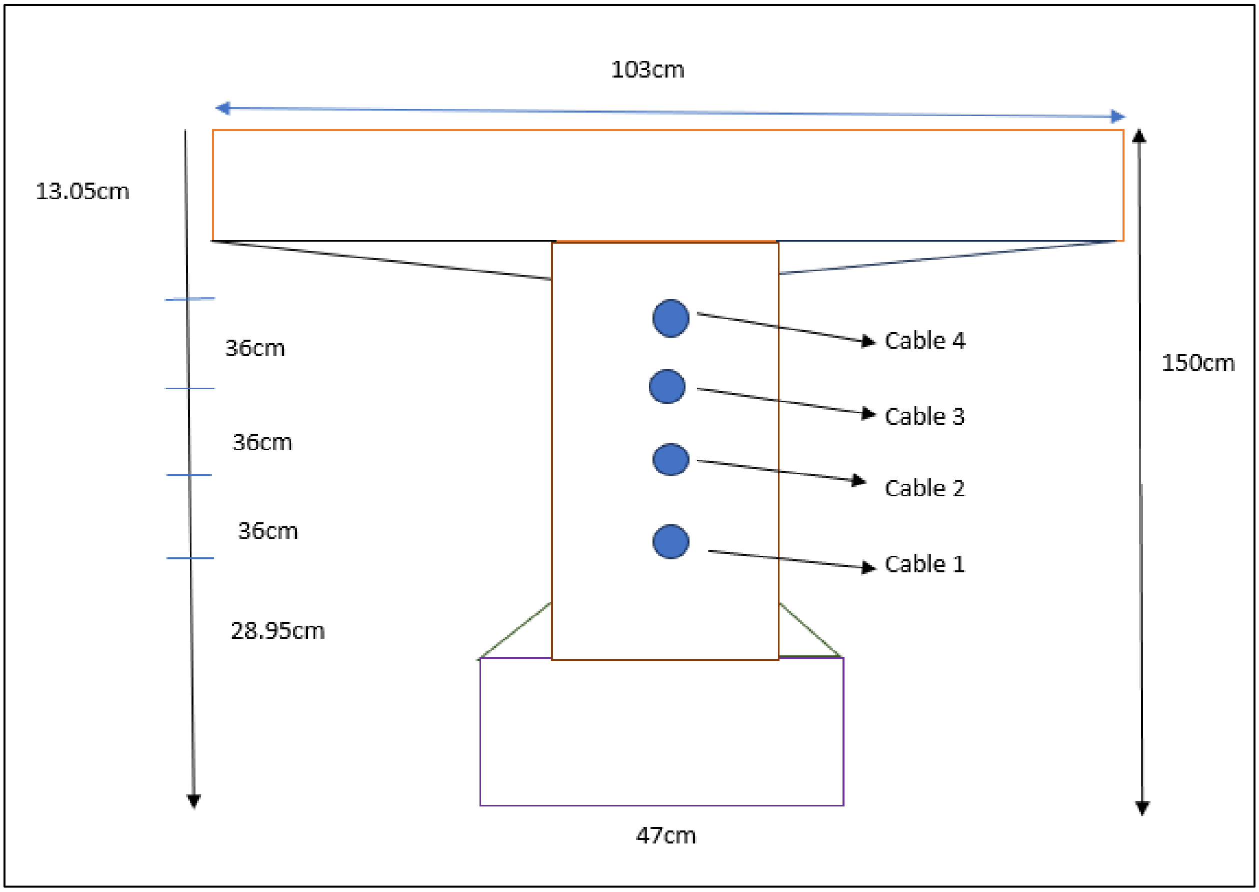

Figure 4.12: The positioning of the cables on the extreme section of the beam

For the disposition of cables on the **intermediary beam cross-section:**

d the coating distance, is equivalent to 15cm**.**

∅ is the diameter of the cable which is 100mm.

C1: Cable1

C2:Cable2

C3:Cable3

C4:Cable4

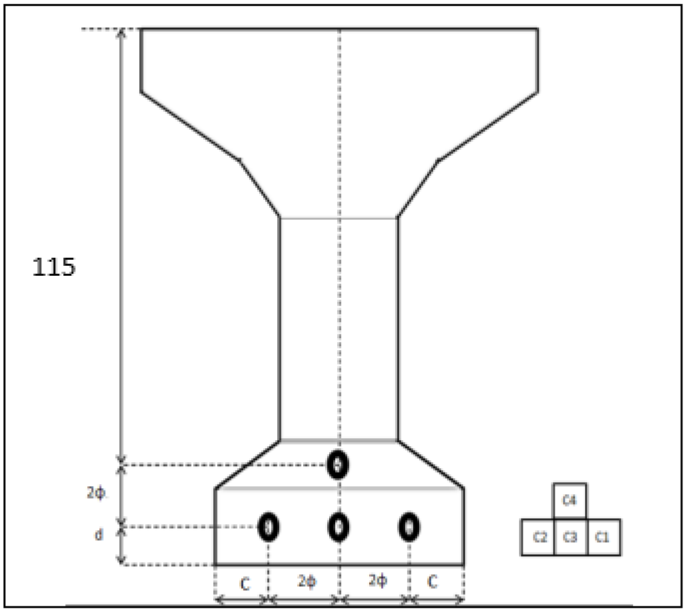

Figure 4.13: showing the disposition of cables in the intermediary section

4.7.1 The Cable Passage Zone

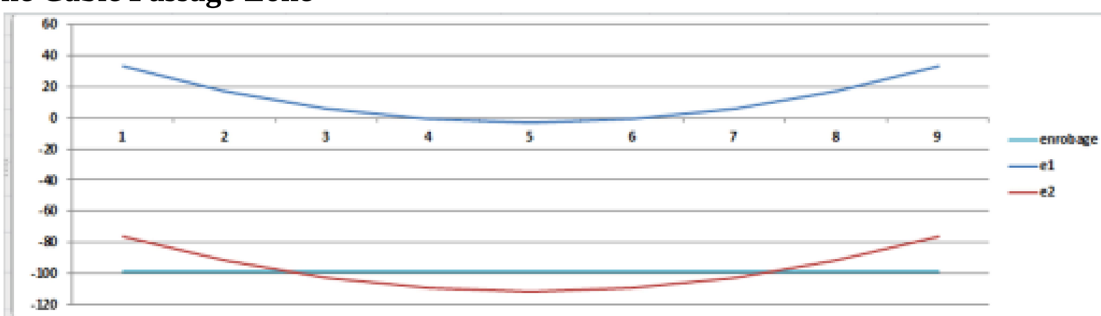

Figure 4.14: The figure shows the limit passage of the cables in red and blue.

The table in **(Figure 4:15)** shows the values that were used to draw the eccentricity 1 and 2 and their coating, "enrobing" in **(figure 4:14)**

		Fuseau de passage								
		L=0	L/8	L/4	3L/8	L/2	5L/8	3L/4	7L/8	L
	x	0	405	810	1215	1620	2025	2430	2835	3240
	Mmin	0	133532,7525	228913,29	286141,6125	305217,72	286141,6125	228913,29	133532,753	0
	Mq	0	0	0	0	0	0	0	0	0
	Mmax	0	133532,7525	228913,29	286141,6125	305217,72	286141,6125	228913,29	133532,753	0
	ρv	26,43683597	26,43683597	26,436836	26,43683597	26,43683597	26,43683597	26,436836	26,436836	26,43683597
	ρv'	-55,17790659	-55,17790659	-55,1779066	-55,17790659	-55,17790659	-55,17790659	-55,17791	-55,1779066	-55,17790659
e1 (classe I)	$\rho v-M_{max}/P$	26,43683597	10,70560463	-0,53098918	-7,272945466	-9,520264228	-7,272945466	-0,530989	10,7056046	26,43683597
e2 (classe I)	$\rho v'-M_{min}/P$	-55,17790659	-70,90913793	-82,1457317	-88,88768803	-91,13500679	-88,88768803	-82,14573	-70,9091379	-55,17790659
	$(M_{max}+\rho v S_g \sigma'_{...})/P$	-6,630834887	9,100396448	20,3369903	27,07894655	29,32626531	27,07894655	20,33699	9,10039645	-6,630834887
	$(M_{min}-\rho v' S_g \sigma_{...})/P$	20,75942003	36,49065136	47,7272452	54,46920146	56,71652022	54,4[illegible]920146	47,727245	36,4906514	20,75942003
	e1	33,06767085	17,33643952	6,09984571	-0,642110579	-2,889429342	-0,642110579	6,0998457	17,3364395	33,06767085
	e2	-75,93732662	-91,66855796	-102,905152	-109,6471081	-111,8944268	-109,6471081	-102,9052	-91,668558	-75,93732662
	enrobage	-99,19398414	-99,19398414	-99,1939841	-99,19398414	-99,19398414	-99,19398414	-99,19398	-99,1939841	-99,19398414

Figure 4.15: Shows elaborate values used to draw the passage of the cables.

4.7.2 The Tilting Angle

The cables have a titling angle which is derived from the following expression.

$$\text{ArcSin}\frac{VM-V}{P} \leq \alpha \geq \text{ArcSin}\frac{Vm-V}{P}$$

With,

Vm: The minimum shear forces on the supports due to the self-weight. Vm=0.42585MN

VM: The maximum shear forces on the supports due to the most `unfavourable load combination which is (G+D240). VM=1.1968MN

The limit shear force on the extreme beam section is expressed as:

$V=\tau \times bn \times 0.8h$

Whereby,

h: The total height of the beam and the slab

bn: The web width knowing that: bn=bo-n×k× ∅

∅: the diameter of the sheath. ∅=0.1m

k: coefficient for post-tensioning with cement grouting injection. k=0.5

n: number of sheaths per row. n=1

b0=0.35m

Thus, bn=0.35-(1×0.5×0.01) =0.3m^2

τ: tangential stress limit at SLS=$(0.4\times ftj(ftj+\frac{2}{3}\sigma_x))^{0.5}$

Whereby,

ftj=ft28=2.4MPa

σ_x=P/Bn

P=n $\times(1-\Delta P)$ ×P0=4×0.7×3.898=10.9144MN

Bn=b0-$\frac{2\pi\emptyset\emptyset}{4}$=1.067-$\frac{2\pi\times0.1\times0.1}{4}$=1.0513m^2

σ_x=10.9144/1.0513=10.382MPa

τ=2.99

V=2.99×0.3×0.8×1.8=1.2923MN

The limits for the cable slope are, therefore, **-0.5° $\leq \boldsymbol{\alpha} \geq$9.06°**

The optimal angle is determined by: αopt=arcsin$\frac{VM+Vm}{2P}$=4.26°

4.7.3 The Cable Layout

The 4 cables are traced in a parabolic form concerning: Y=AX^2+B+C. The cables have this layout to reduce the prestressing on the end sections of the beams by being raised at a certain angle. This helps to reduce excess stresses on the lower fiber which results in a reduction of the shear force as stated in the SETRA guidelines. It's also important to note that the cables are only parabolic on the end sections and straight on the other remaining sections.

Cable 1

Y=Ax^2+Bx+C

If x=0, then Y=C, thus Y=C=0.2895m

x=16.7m, then 0.15=278.89A+16.7B+0.2895

Y'=2Ax+B

If x=0, then 0=2A (16.7) +B, thus A=-B/33.4

Therefore, the parabolic equation for cable 1 is **Y=0.0005002x^2-0.0167x+0.2895**

Cable 2

$Y=Ax^2+Bx+C$

If x=0, then Y=C, thus Y=C=0.6495m

x=16.7m, then 0.15=278.89A+16.7B+0.6495

Y'=2Ax+B

If x=0, then 0=2A (16.7) +B, thus A=-B/33.4

Therefore, the parabolic equation for cable 2 is $\mathbf{Y=0.001791x^2-0.0598x+0.6495}$

Cable 3

$Y=Ax^2+Bx+C$

If x=0, then Y=C, thus Y=C=1.0095m

x=16.7m, then 0.15=278.89A+16.7B+1.0095

Y'=2Ax+B

If x=0, then 0=2A (16.7) +B, thus A=-B/33.4

Therefore, the parabolic equation for cable 3 is $\mathbf{Y=0.00308x^2-0.1029x+1.0095}$

Cable 4

$Y=Ax^2+Bx+C$

If x=0, then Y=C, thus Y=C=1.3695m

x=16.7m, then 0.35=278.89A+16.7B+1.3695

Y'=2Ax+B

If x=0, then 0=2A (16.7) +B, thus A=-B/33.4

Therefore, the parabolic equation for cable 4 is $\mathbf{Y=0.003656x^2-0.1221x+1.3695}$

Table 4.3: The disposition of the cables according to the parabolic equations

	Cable1	Cable2	Cable3	Cable4
X(m)	Y(m)	Y(m)	Y(m)	Y(m)
0	0.2895	0.6495	1.0095	1.3695
1	0.2733	0.591491	0.90968	1.251056
2	0.2581	0.537064	0.81602	1.139924
3	0.2439	0.486219	0.72852	1.036104
4	0.2307	0.438956	0.64718	0.939596
5	0.2185	0.395275	0.572	0.8504
6	0.2073	0.355176	0.50298	0.768516
7	0.1971	0.318659	0.44012	0.693944
8	0.1879	0.285724	0.38342	0.626684
9	0.1797	0.256371	0.33288	0.566736
10	0.1725	0.2306	0.2885	0.5141
11	0.1663	0.208411	0.25028	0.468776
12	0.1611	0.189804	0.21822	0.430764
13	0.1569	0.174779	0.19232	0.400064
14	0.1537	0.163336	0.17258	0.376676
15	0.1515	0.155475	0.159	0.3606
16	0.1503	0.151196	0.15158	0.351836
16.7	0.150055	0.150332	0.150051	0.350052
17	0.1501	0.150499	0.15032	0.350384
18	0.1509	0.153384	0.15522	0.356244
19	0.1527	0.159851	0.16628	0.369416
20	0.1555	0.1699	0.1835	0.3899

21	0.1593	0.183531	0.20688	0.417696
22	0.1641	0.200744	0.23642	0.452804
23	0.1699	0.221539	0.27212	0.495224
24	0.1767	0.245916	0.31398	0.544956
25	0.1845	0.273875	0.362	0.602
26	0.1933	0.305416	0.41618	0.666356
27	0.2031	0.340539	0.47652	0.738024
28	0.2139	0.379244	0.54302	0.817004
29	0.2257	0.421531	0.61568	0.903296
30	0.2385	0.4674	0.6945	0.9969
31	0.2523	0.516851	0.77948	1.097816
32	0.2671	0.569884	0.87062	1.206044
33	0.2829	0.626499	0.96792	1.321584
33.4	0.2895	0.650148	1.008565	1.369847

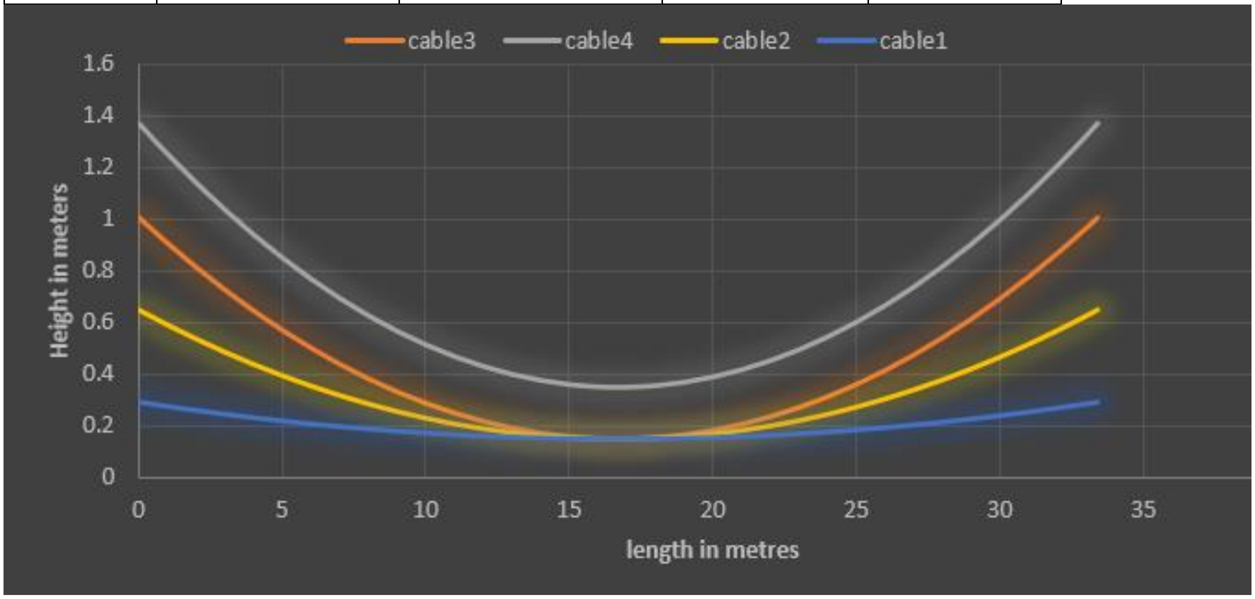

Figure 4.16: Showing the parabolic curves of the cables

4.8 Calculations of Prestressed Losses

The prestressed force that is used to tension the steel tendon to a certain length to induce the pre-compression in the concrete which counters the tensile stresses reduces with time. This reduction of the prestressed force that was applied to the steel tendons is referred to as the prestressed losses. The losses stabilize with time, which results in the final prestressed force which also is known as the effective prestressed force (Walter 1969).

The prestressed losses occur at a given time and point after the prestressing force has been applied. Therefore, there exist two types of prestressed losses which are the instantaneous losses and the deferred losses.

The instantaneous losses in the post-tensioning are a result of:

- The tendon friction
- The anchorage slips
- The elastic deformation of concrete.

The deferred losses resulting from the post-tensioning prestressed are:

- The relaxation of steel,
- The concrete creep,
- The shrinkage of concrete.

4.8.1 The Instantaneous Losses

These losses accrue from:

a) Losses due to the tendon friction, $\Delta\sigma_{fr}$**.**

The friction between the different materials, which is the duct concrete surface and the steel tendons results in a diminution of the prestressed force that was initially applied on the ends by jacking. It is also referred to as the wobbling effect or the length effect. The curvature of the steel tendons also results in prestressed losses.

Below are calculations according to the B.P.E.L to $\Delta\sigma_{fr}$.

$$\sigma_{po}(x) = \sigma_{po}\, e^{-f\alpha-\varphi x}$$

With:

$\sigma_{po}(x)$: The initial prestressed force during tension, $\sigma_{po}(x)$=1476MPa

x: The distance from the considered section to the tensioning elements

α: The angular deviation over distance x f: The friction coefficient in a curve, f=0.18 rd^{-1}

φ: The tension loss coefficient per unit length, φ=0.002 m^{-1}

The friction loss is equivalent to:

$\Delta\sigma_{fr}=\sigma_{po}(x) - \sigma_{pf}(x)$

From the parabolic equations of the cables, $\sigma_p(x)$ can be derived as:

$\sigma_{p(x)} = \sigma_{po}^{\ (1 - (f \times \alpha(x) + \varphi \times x);\ (_e{}^{-x} = 1 - x)}$

Thus,

$\Delta\sigma_{f(r)} = \sigma_{po} \times (f \times \alpha(x) + \varphi \times x) = 1476(0.18 \times \alpha + 0.002 \times x)$

Table 4.4: The friction Losses resulting from the cables.

	X(m)	0	8.35	16.7
Cable 1	α	0.02793	0.02793	0.02793
	$\Delta\sigma_{fr}$ (MPa)	7.42	32.07	56.72
Cable 2	α	0.06248	0.062483	0.062483
	$\Delta\sigma_{fr}$ (MPa)	16.60	41.25	65.9
Cable 3	α	0.09687	0.09687	0.09687
	$\Delta\sigma_{fr}$ (MPa)	25.74	50.39	75.03
Cable 4	α	0.13105	0.13105	0.13105
	$\Delta\sigma_{fr}$ (MPa)	34.82	59.47	84.12

b) Losses due to the anchorage slips, $\Delta\sigma_{as}$.

During anchoring of the steel tendons to the anchorage device, a slip might occur which results in a loss. Thus, the slippage percentage loss in shorter lengths will be high compared to the longer lengths.

Below are calculations to obtain the anchorage slip losses.

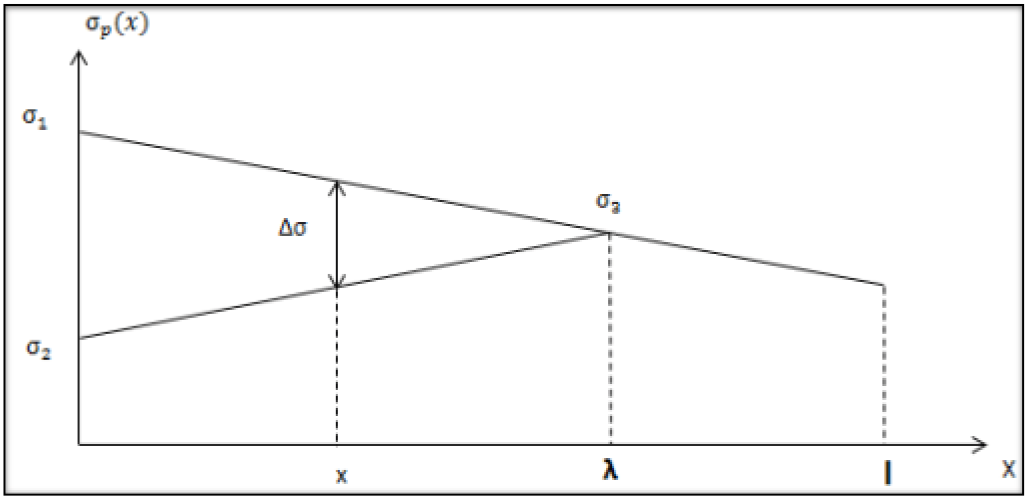

Figure 4.18: Diagramme representing the principle of prestress losses

Figure 4.19: Diagramme representing the principle of prestress losses

The slope symmetry:

$\Delta\sigma 0 = \sigma 1 - \sigma 2 = 2(\sigma 1 - \sigma 3) = 2 \times \psi \times \lambda \times \sigma 1$

The x coordinates:

$\Delta\sigma o = \sigma 1 - \sigma 2((\lambda - x)/\lambda) = 2 \times \psi \times \sigma o \times (\lambda - x)$

With:

$\psi = f\ (\alpha/l\ ) + \varphi$

If λ<x, prestressing losses exist

λ>x, prestressing losses are inexistent.

$$\lambda = \sqrt{\frac{g x E_P}{\sigma_0 x \psi}}$$

λ: Anchoring setback length

g: Anchoring recoil intensity, g=6mm.

E_P: Steel's modulus elasticity, E_p=190000MPa.

Table 4.5: The anchorage slips loss details.

	X(m)	0	8.35	16.7

Cable1	λ	18.33	18.33	18.33
	ψ	0.0023	0.0023	0.0023
	α	0.02793	0.02793	0.02793
	$\Delta\sigma_{as}$ (MPa)	124.45	67.76	11.07
Cable 2	λ	16.91	16.91	16.91
	ψ	0.0027	0.0027	0.0027
	α	0.06248	0.062483	0.062483
	$\Delta\sigma_{as}$(MPa)	134.78	68.23	1.67
Cable 3	λ	16.05	16.05	16.05
	ψ	0.0030	0.0030	0.0030
	α	0.09687	0.09687	0.09687
	$\Delta\sigma_{as}$(MPa)	142.14	68.19	0
Cable 4	λ	15.07	15.07	15.07
	ψ	0.0034	0.0034	0.0034
	α	0.13105	0.13105	0.13105
	$\Delta\sigma_{as}$(MPa)	151.25	67.45	0

c) Losses due to the elastic deformation of the concrete, $\Delta\sigma_{ed}$.

It is also referred to as the elastic shortening of concrete. These losses mainly are a result of the non-simultaneous post-tensioning of the cables. The post-tensioning prestressing of a cable affects the adjacent cables in a manner that the first cable to be tensioned, experiences the most losses while the last cable to be tensioned experiences close to zero losses.

Below are calculations for the losses.

$\Delta\sigma_{ed}(x)=[(n\text{-}1)\ Ep/2n\times Eij]\times\sigma b(x)$

n: number of sheaths

Ep: steel modulus elasticity

Eij: instantaneous modulus elasticity of concrete at “j” e.g.

$Ei28 = 11000 3\sqrt{fc28} = 34179.56 MPa$

$\sigma_{b(x)}$: concrete stress

$\sigma b(x) = P/Bn + Mg(x).\, e(x)/Ign + Pe(x)^2/Ign$

$P = n\, Ap\, (\,\sigma po - \Delta\sigma recul - \Delta\sigma frot(x)\,)$

$e(x)$: eccentricity of post-tensioned cables

$\Delta\sigma ed\ (x) = (Ep/2Eij) \times \sigma b(x)$: According to the BPEL.

Table 4.6: The elastic shortening entries.

Cables	X(m)	0	8.35	16.7
1	P(MN)	3.32	3.40	3.48
	e_x	0.00	0.8565	1.25
	Mg (Mn.m)	0.00	3.91	5.21
	Section m^2	0.6156	0.8569	0.8569
	In(m^4)	0.3952	0.5072	0.5072
	σ_b(MPa)	5.39	16.31	25.48
	$\Delta\sigma_{ed}$ (MPa)	14.99	45.34	70.81
2	P(MN)	3.27	3.38	3.48
	e_x	0.00	0.8565	1.25
	Mg (Mn.m)	0.00	3.91	5.21
	Section	0.6156	0.8569	0.8569
	In(m^4)	0.3952	0.5072	0.5072
	σ_b(MPa)	5.31	16.25	25.48
	$\Delta\sigma_{ed}$ (MPa)	14.76	45.18	70.81
3	P(MN)	3.23	3.35	3.46
	e_x	0.00	0.8565	1.25
	Mg (Mn.m)	0.00	3.91	5.21
	Section m^2	0.6156	0.8569	0.8569
	In(m^4)	0.3952	0.5072	0.5072

	σ_b(MPa)	5.25	16.17	25.41
	$\Delta\sigma_{ed}$ (MPa)	14.59	44.94	70.62
Cable 4	P(MN)	3.19	3.33	3.45
	e_x	0.00	0.8565	1.25
	Mg (Mn.m)	0.00	3.91	5.21
	Section m^2	0.6156	0.8569	0.8569
	In(m^4)	0.3952	0.5072	0.5072
	σ_b(MPa)	5.18	16.11	25.37
	$\Delta\sigma_{ed}$ (MPa)	14.39	44.78	70.51

The total sum of the instantaneous losses= $\Delta\sigma_{ed} + \Delta\sigma_{as} + \Delta\sigma_{fr}$

Cable	X(m)	0	8.35	16.7
1	$\Delta\sigma_{as}$ (MPa)	124.45	67.76	11.07
	$\Delta\sigma_{fr}$ (MPa)	7.42	32.07	56.72
	$\Delta\sigma_{ed}$ (MPa)	14.99	45.34	70.81
	$\Delta\sigma_{inst}$ (MPa)	146.86	145.17	138.6
2	$\Delta\sigma_{as}$ (MPa)	134.78	68.23	1.67
	$\Delta\sigma_{fr}$ (MPa)	16.60	41.25	65.9
	$\Delta\sigma_{ed}$ (MPa)	14.76	45.18	70.81
	$\Delta\sigma_{inst}$ (MPa)	166.14	154.66	138.38
3	$\Delta\sigma_{as}$ (MPa)	142.14	68.19	0
	$\Delta\sigma_{fr}$ (MPa)	25.74	50.39	75.03
	$\Delta\sigma_{ed}$ (MPa)	14.59	44.94	70.62
	$\Delta\sigma_{inst}$ (MPa)	182.47	163.52	145.65
4	$\Delta\sigma_{as}$ (MPa)	151.25	67.45	0
	$\Delta\sigma_{fr}$ (MPa)	34.82	59.47	84.12
	$\Delta\sigma_{ed}$ (MPa)	14.39	44.78	70.51

	$\Delta\sigma_{inst}$ (MPa)	200.46	171.7	154.63

4.8.2 The Deferred Losses

These losses accrue from

a) **Losses due to the shrinkage of concrete, $\Delta\sigma r$.**

This type of loss occurs due to the reduction of moisture in the concrete which results in the steel tendons losing their stretch.

The BPEL states that the effective prestressed from the shrinking of the concrete is:

$\Delta\sigma r = \mathcal{E}r \times Ep$

With:

$\mathcal{E}r$: The total shrinking of the concrete from a dry climate, $\mathcal{E}r$=0.0003

Ep: Steel's modulus elasticity, Ep=190000MPa

Thus, $\Delta\sigma r$ = 0.0003 × 190000=57MPa

b) **Losses due to the relaxation of steel, $\Delta\sigma\rho$.**

It is also referred to as the creep in steel. This type of loss occurs when the tensioning in the steel tendons is greater than half of the elastic limit stress.

These losses are calculated as follows:

$\Delta\sigma\rho = 6\times \rho_{1000}(\frac{\sigma pi(x)}{fprg}\text{--}\mu 0)\ \sigma pi(x)$

The coefficient $\mu 0$=0.43 for the reinforcements that are very lowly relaxed, TBR which were used in this project.

σpi(x): The initial stress of the reinforcement after the instantaneous stresses, $\sigma pi(x) = \sigma 0 - \sigma inst$.

$\sigma 0 = 1476(\text{MPa})$

fprg: guaranteed breaking limit of stress, fprg=1860MPa

ρ_{1000}: the creep in steel at 1000 hours is equivalent to 2.5%.

Table 4.7: The relaxation of steel

Cables	X(m)	0	8.35	16.7
1	σpi(x) in MPa	1329.14	1330.83	1337.4
	$\Delta\sigma\rho$ inMPa	56.74	56.99	57.98
2	σpi(x) in MPa	1309.86	1321.34	1337.62
	$\Delta\sigma\rho$ inMPa	53.88	55.58	58.02
3	σpi(x) in MPa	1293.53	1312.48	1330.35
	$\Delta\sigma\rho$ inMPa	51.50	54.26	56.92
4	σpi(x) in MPa	1275.54	1304.3	1321.37

	$\Delta\sigma\rho$ inMPa	48.94	53.07	55.58

c) Losses due to the creep of concrete, $\Delta\sigma$cc.

Creep in concrete, will be evident in this project because the project's location is considered to be a dry region with low chances of humidity. It's important to note that the age of concrete, plays a significant role too in the creeping of concrete.

To calculate the losses due to the creep of the concrete:

$\Delta\sigma_{cc}= (\sigma_b+\sigma_{max})\frac{Ep}{Eij}$

σ_b: Final stress

σ_{max}: Maximum stress

If the $\sigma_{max} < 1.5\ \sigma_b$ as stated in the BPEL, then $\Delta\sigma_{cc}= 2\times\sigma_b\times \frac{Ep}{Eij}$

Table 4.8: The creep in concrete result values

Cables	X(m)	0	8.35	16.7
1	σb in MPa	5.39	16.31	25.48
	$\Delta\sigma cc$ in MPa	50.93	154.13	220.98
2	σb in MPa	5.31	16.25	25.48
	$\Delta\sigma$cc in MPa	50.18	153.56	208.98
3	σb in MPa	5.25	16.17	25.41
	$\Delta\sigma$cc inMPa	49.62	152.82	184.98
4	σb in MPa	5.18	16.11	25.37
	$\Delta\sigma$cc inMPa	48.95	152.24	154.148

The BPEL, states that the equation for the total deferred losses is:

$\Delta\sigma diff = \Delta\sigma r + \Delta\sigma\rho + \frac{5}{6}\Delta\sigma cc$

Table 4.9: The deferred losses for each cable at a given length

Cables	X(m)	0	8.35	16.7
1	$\Delta\sigma$diff in MPa	156.18	242.43	299.128
2	$\Delta\sigma$diff in MPa	152.70	240.55	289.168
3	$\Delta\sigma$diff in MPa	149.85	238.61	268.068
4	$\Delta\sigma$diff in MPa	146.73	236.94	266.728

The sum of the deferred losses and the instantaneous losses is equivalent to the total prestress losses, $\Delta\sigma_{tot}$.

The effective prestress, σ_{eff} is equivalent to:
$\sigma_{eff}=(n\times \sigma_0)- \Delta\sigma_{tot}$
n: number of cables.
σ_0: initial prestress force
The percentage of the losses is expressed as follows:
$\%\Delta\sigma_{tot} = 100 \times [(4\times\sigma_o - \sigma_{eff})/(4\times\sigma_0)]$

Table 4.10: The total losses, effective stress and the %

Cable	X(m)	0	8.35	16.7
1	$\Delta\sigma_{tot}$ in MPa	280.63	387.6	437.728
2	$\Delta\sigma_{tot}$ in MPa	318.84	395.21	427.548
3	$\Delta\sigma_{tot}$ in MPa	332.32	400.46	413.718
4	$\Delta\sigma_{tot}$ in MPa	347.19	408.64	421.358
$\sum \Delta\sigma tot$		1278.98	1591.91	1700.352
σ_{eff}		4625.02	4312.09	4203.648
%		21.66	26.96	28.80

The percentage of prestressing losses is highest in the middle of the span. The losses percentage are less than 30% hence the condition is verified.

4.9 Reinforcement of the Beam

4.9.1 Longitudinal Passive Reinforcements

In prestressed structures, we consider two types of passive reinforcements which are:

- Skin reinforcements
- Longitudinal reinforcements in the tense areas.

The skin reinforcements

The primary purpose of this reinforcement is to minimize possible cracks on the beam by evenly distributing the stresses on the beam's cross-section and also by increasing the load-carrying capacity of the beam.

Asmin≥max (3cm^2/ml of the perimeter: 0.1% of the beam's section)

Asmin≥max (3×(0.47+1.5) ×2=11.82: 0.1%×6156=6.156)

Therefore As=11.82cm^2

We take 8T16=16.08 cm^2

The longitudinal reinforcements in the tense areas

Since there's no tensioned area on the concrete, the skin reinforcement is adequate hence minimum reinforcement will be used. As=6.23cm^2.

4.9.2 Justification of Tangential Constraints

These calculations are done to ensure that:

- The steel rods don't crush
- The transversal reinforcements don't break

The skin transversal reinforcement

They serve to support the longitudinal reinforcements. The steel bars, $2cm^2/ml$ are placed around the perimeter of the beam and parallel to the center of gravity. Hence three HA10 or 2HA12 frames are used in each facing.

The minimum transversal reinforcement

St ≤ min (0.8h; 3b; 1m) = min (1.2; 1.41; 1) = 1m.

With:

h: height of the beam

b: width of the beam's heel

St: spacing of steel bars

The minimum transversal reinforcement is given by:

$\frac{At}{St \times br} \times \frac{fe}{\gamma s} \geq 0.4$

At=2.26cm^2 for 1HA12

St<0.5m

Thus, the spacing for the intermediary of the beam is 35cm and 15cm on the extreme.

Justification of the transversal reinforcement

It ensures that the tensed areas made up of the trellis of concrete rods and frames are resistant enough.

$\tau red.u \leq \bar{\boldsymbol{\tau}}\mathrm{u} = Atfe1.15Stbn \times cotg(\beta u) + \boldsymbol{ftj3}$

$\tau red.u = \frac{vred.u \times S}{Ih \times Bh}$

vred. u=Vmax-Psin (α)

β: inclination angle of the concrete rods, $\beta < 30°$

The condition is verified.

Justification of the connecting concrete rods

The following has to be verified: $\tau red.u \leq \frac{fcj}{4\times\gamma b}=\frac{30}{4\times1.5}=5MPa$

The condition is verified.

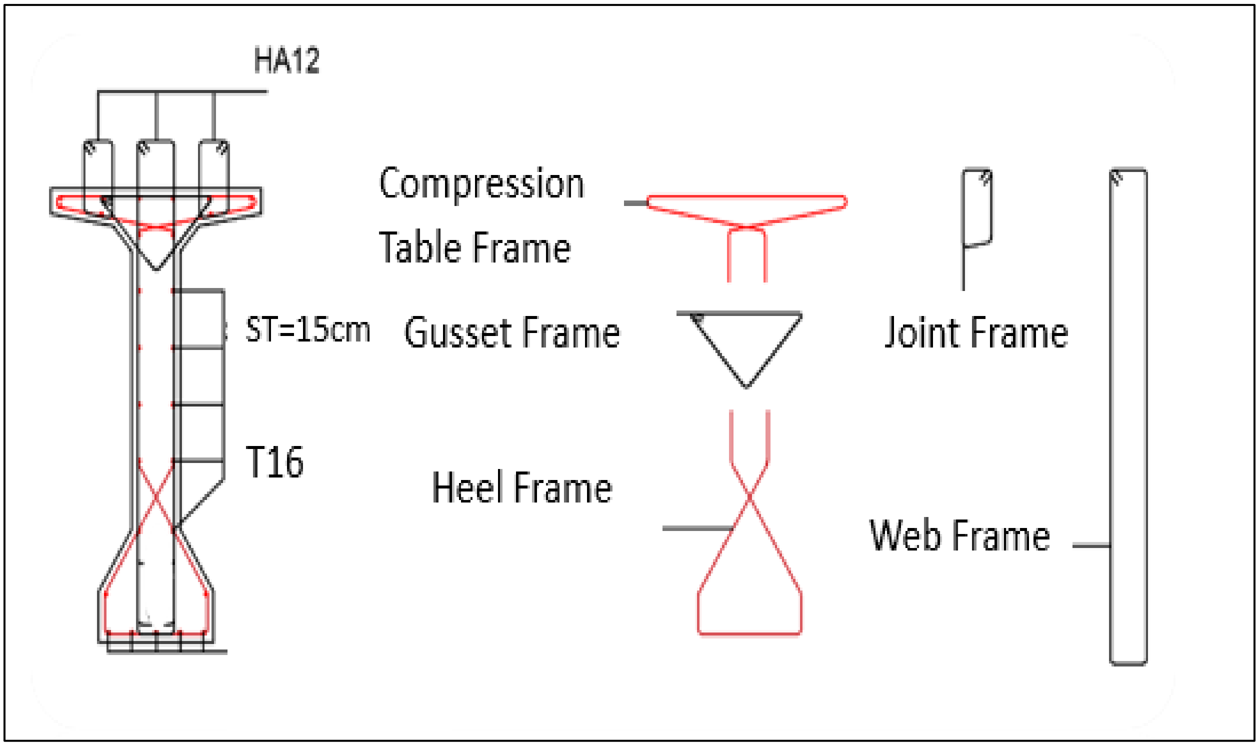

Figure 4.20: The Reinforcement of the Extreme beam section

4.10 Conclusion

Using the civil engineering guidelines, the beam's post-tensioning prestressing was verified taking into account the age of the concrete, the losses, the loads and the reinforcement of the beam among other factors. All conditions need to be verified where necessary to ensure the integrity of the structure

Chapter 5:
The Slab Study

5

5.1 Introduction

The slab is a vital component of bridge construction, providing the primary surface for traffic and contributing to the overall strength and stability of the bridge structure. The slab which is a part of the deck, carries the loads applied on it and distributes them to the beams. In this study, the analysis of the various aspects of slab design, material composition, and construction techniques shall be considered to ensure the structural integrity and longevity of bridges.

5.2 Type of Slab

It is important to note that, there exist different types of slab designs in the bridge construction. They include solid slabs, hollow slabs, pre-stressed slabs and composite slabs. Thus, a layer of concrete was cast-in-site on the beams and cured on-site to form a solid slab which was used in this project's bridge construction.

5.3 Pre-sizing of the Slab

In this project, a slab of a total thickness of 0.3m was used, with a width of 10m and a length of 33.4m. The thickness of the slab under compression has to be between the following bounds of $0.20m \leq ed \leq 0.30m$ using the S.E.T.R.A guide.

5.4 Evaluation of Loads on the Slab

The dead loads applied on the slab are:

- The self-weight of the slab
- The side-walk concrete slab
- The security barriers
- The guide-rails
- The cornices
- The wearing courses
- The waterproofing surface

The live-loads applied on the slab are:

- Live load, A_L
- Bc system
- Bt system
- Br system
- Military live load Mc120
- Exceptional loads D240

- Side-walk live-loads

The combinations are taken into account

Table 5.1:The slab load combination cases and their coefficients

G+Al	**1.35G + 1.6A(L)**	**G + 1.2 A(L)**
G+Bc	1.35G + 1.6Bc	G + 1.2 Bc
G+Mc120	1.35G + 1.35Mc120	G + Mc120
G+D240	1.35G + 1.35D240	G + D240

5.5 Bending Moments

The slab undergoes traversal moments on its width and longitudinal moments on its length.

According to the B.A.E.L method:

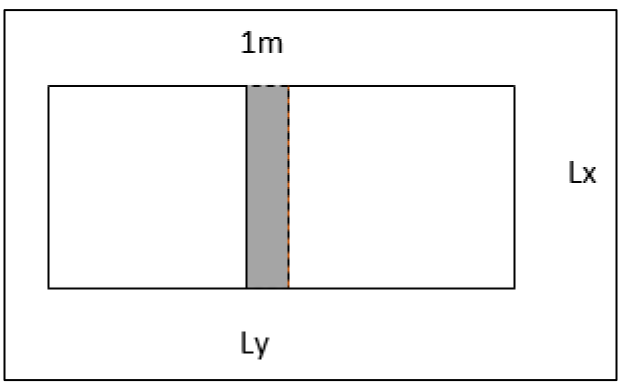

Figure 5.1: The slab area

Lx: the width of the slab which is also the shortest side of the slab in terms of dimensions.

Ly: the length of the slab which is also the longest side of the slab.

$$\frac{\mathrm{Lx}}{\mathrm{Ly}} = \frac{10\mathrm{m}}{32.4\mathrm{m}} = 0.31 < 0.4$$

The ratio of the shortest length to the longest length of the slab helps us to determine that our slab is a **one-way slab** meaning that the bending moments occur in **one direction only** along the shortest length.

The beams in this case act as the supports of the slab on the two edges and the steel reinforced is along the shortest length while the longest side is reinforced with minimum steel reinforcements according to the civil engineering guidelines.

The self-weight of the slab: 0.3×1×25=7.5KN/ml

The weight of the superstructures: 31KN/ml

$\sum$ G=38.5KN/ml

Q=129.03KN/ml

In SLU, Qu=1.35(38.5+129.03) =226.16 KN/ml

The moments in SLU are therefore, Mu= $\frac{Qu\times L^2}{12}$ =0.22616×1.4²/12= 0.03694 MN.m

The moments in SLS are therefore, Ms=$\frac{Qs\times L^2}{12}$ = 0.16753×1.4²/12= 0.02736 MN.m

5.6 Slab's Steel Reinforcement

In **SLU:**

$f_{bu}=\frac{0.85fc28}{\gamma b}=\frac{0.85\times 30}{1.5}=17MPa$

d=0.9h=0.9×0.3=0.27m

$\mu=\frac{Mu}{b\times d\hat{}2\times fbu}=\frac{0.03694}{1.4\times 0.27\hat{}2\times 17}$ = 0.021<0.392 thus the section has simple reinforcements

$\alpha=1.25(1-\sqrt{1-2\mu})=0.0269$

Z=d (1-0.4α)=0.267

fsu= $\frac{fe}{\gamma s}=\frac{400}{1.15}$ = 347.82MPa

At = $\frac{Mu}{z\times fsu}=\frac{0.03694}{0.267\times 347.82}=3.976\times 10^{-4}m^2$

Therefore, we adopt a reinforcement of 8T20, with an of 25.13cm^2

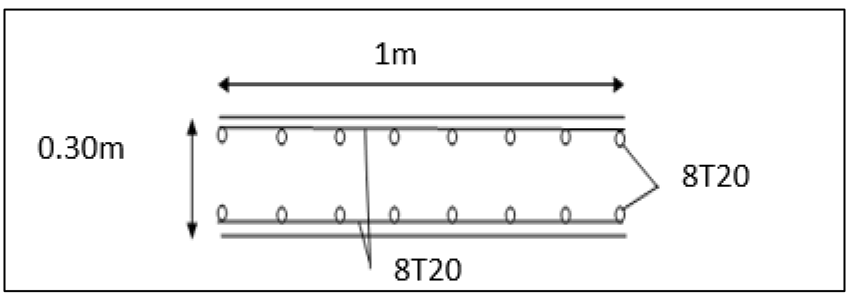

Figure 5.2: The Slab Steel Reinforcement on the Slab

Below is a figure that shows the passive steel reinforcement on the supports.

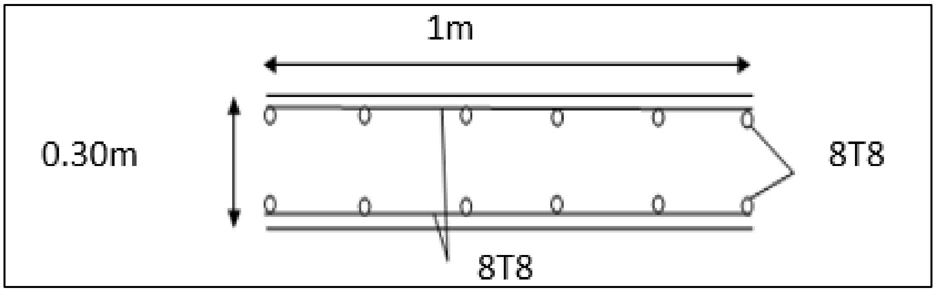

Figure 5.3: The Steel Reinforcements on the Supports

In **SLS:**

Ms= 0.02736 MN.m

Determination of the neutral axe:

$$\frac{bx^2}{2} + n \times Asc(x - d') - n \times Ast \times (d - x) = 0 \ldots\ldots\ldots\ldots..1$$

With;

Asc=0

n is the equivalence coefficient of 15

x= 0.0966m

$I=\frac{bx^3}{3} + n \times Ast \times (d - x)^2 = 1.554 \times 10^{-3} m^4$

Determining the stresses

$$\sigma_{bc} = \frac{Ms \times x}{I} = \frac{0.02736 \times 0.0966}{1.554 \times 10-3} = 1.7MPa$$

Therefore, $\sigma_{bc} = 1.7MPa$

$\bar{\sigma}_{bc}=0.6f_{c28}=0.6\times30=18MPa$

$\sigma_{bc} < \bar{\sigma}_{bc}$ …...The condition is verified

$$\sigma_{st} = n \times \frac{Ms \times (d-x)}{I}$$

$$\sigma_{st} = 15 \times \frac{0.02736 \times (0.27 - 0.0966)}{1.554 \times 10-3} = 45.79MPa$$

$$\bar{\sigma}_{st} = \min\left(\frac{2}{3}fe; \max\left(0.5fe, 110\sqrt{\eta.ft28}\right)\right)$$

$$\bar{\sigma}_{st} = \min\left(\frac{2}{3} \times 400 = 266.67; \max\left(0.5 \times 400 = 200, 110\sqrt{1.6 \times 2.4} = 215.56\right)\right)$$

$\sigma_{st} < \bar{\sigma}_{st}$ ..... The condition is verified

5.7 Verification of the Shear Forces

The steel reinforcements are disposed of at an angle of 90°.

Transversally

Tu= 97.95kn

$\tau u = \frac{Tu}{b \times d}$

$\tau u = \frac{Tu}{b \times d} = \frac{0.09795}{1 \times 0.27}$ =0.36MPa

τ_{adm}=min($\frac{0.15fc28}{\gamma b}$;4MPa)

τ_{adm}=min(3.91MPa;4MPa)

τ_{adm}=3.91MPa

$\tau u = 0.36\text{MPa} \leq \tau_{adm}$=3.91MPa thus the condition is verified.

Longitudinally

Tu= 83.77KN

$\tau u = \frac{Tu}{b \times d} = \frac{0.08377}{1 \times 0.27}$ =0.31MPa

τ_{adm}=min($\frac{0.15fc28}{\gamma b}$;4MPa)

τ_{adm}=3.91MPa

The condition is verified

5.8 Non-Fragile Condition

$A_{min} \geq 0.23 \times b \times d \times \frac{f_{t28}}{fe}$

A_{min} =3.974×10^{-4}m^2 $\geq 0.23 \times 1 \times 0.27 \times \frac{2.4}{400}$ =3.726×10^{-4} m^2

The condition is verified.

5.9 Verification of Punching

Punching occurs when there's a punctual load, *such as Br*, acting on the slab surface hence, in our case, there's a need to verify the risk of punching of the slab.

The condition to be verified is:

$$Qu = \frac{0.045 \times Uc \times h \times fcj}{\gamma b}$$

With,

Qu: design load at SLU

Uc: outline the perimeter at the level of the middle sheet

h: the total thickness of the slab

fcj: characteristic compressive strength of concrete at 28days

U=V=u+h+2hr

hr: coating height

U=V=30+30+2×8.5=68.5cm

Qu=1.5× $\delta_{br} \times Q$

Q=10, δ_{br}= 1.054, thus Qu= 15.81t

Uc=2×(U+V) =274cm

h=30cm

f_{c28}=30MPa

Qu=15.81t < $\frac{0.045 \times Uc \times 0.3 \times 3000}{1.5}$ =73.98t

Therefore, there's no risk of punching.

5.10 Conclusion

It is necessary to have a good comprehension of the slab study, taking into consideration the bending moments of the slab and the steel reinforcements according to the bridge construction guidelines and standards to make sure that the structure is durable.

General Conclusion

Throughout this thesis study, an extensive comprehensive detailed study was done from the presentation of the project to the final study of the slab to make sure that the structure met all the necessary safety precautions. Doing this project has been more enriching since I got to learn a lot about the technical aspects of a bridge, putting into practice most of the knowledge gained in class and mainly learning how to manually calculate the bending moments and shear forces using the different vehicular live loads among many other calculations in this thesis study. All these calculations were done with respect to the civil engineering guidelines and standards. Therefore, it is commendable for a student to have all this knowledge.

The focal points of this study were the dimensioning, lowering of loads and the prestressing of the beams which ensures economical material use, cost of the project and the safety of the structure. The structure has to be durable and stable; this is elaborated by respecting the admissible stresses and limits in all stages and where applicable.

The knowledge and skills acquired from this thesis study will play a significant role in my professional career as a young civil engineer who intends to work in the line of bridges and road designs and other related construction works.

Afric Mémoire. (2015-2024). Chapitre i : généralités sur les ponts. Retrieved March 28, 2024, from https://www.africmemoire.com/part.2-chapitre-i-generalites-sur-les-ponts-1121.html

CCTG. (1991b). Règles techniques de conception et de calcul des ouvrages et constructions en béton précontraint suivant la méthode des états limites ((fascicule n°62 - titre i - section ii) ou (bpel 91révisé 99)). Paris, France : ministère de l´équipement, des transports et du logement secrétariat d´état au logement secrétariat d´état au tourisme.

C Miki, K Homma, and T Tominaga, (2002). High strength and high performance steels and their use in bridge structures, Journal of Constructional Steel Research, Volume 58,Issue1,2002,Pages320,ISSN0143974X,https://doi.org/10.1016/S0143974X(01)000281.

Designing Buildings ltd. (2022, April 5). *Dead loads - Designing Buildings*. Designing Buildings Wiki. Retrieved July 7, 2024, from https://www.designingbuildings.co.uk/wiki/Dead_loads

Designing Buildings ltd. (2022, November 15). *Bridge structures - Designing Buildings*. Designing Buildings Wiki. Retrieved July 7, 2024, from https://www.designingbuildings.co.uk/wiki/Bridge_structures

Document technique réglementaire D.T.R règle parasismiques applicable au domaine des ouvrages d'art RPOA 2008. Ministre des travaux publics.

ENG-TIPS.COM. (2017, February 3). *Post Tensioning Cable Slope - Concrete Engineering general discussion*. Eng-Tips. Retrieved July 7, 2024, from https://www.eng-tips.com/viewthread.cfm?qid=420562

ESC Group (2023, March 26). *A Basic Guide to Steel Bridges: An Engineering Marvel*. ESC Group. Retrieved July 7, 2024, from https://www.escglobalgroup.com/post/a-basic-guide-to-steel-bridges-an-engineering-marvel

Ferdinand, R. (2024). *Modulus of Elasticity Formula | Calculating Steel, Concrete & Aluminum - Lesson*. Study.com. Retrieved July 7, 2024, from https://study.com/academy/lesson/modulus-of-elasticity-steel-concrete-aluminum.html

Hafnaoui Mohammed Amin, Madi Mohammed, Benmalek Ahmed and Ben Said Mosbah (2022, September 28). Floods in El Bayadh City: Causes and Factors. Volume 19, Number3,Pages 127-142. https://www.asjp.cerist.dz/en/article/204156.

Karima Belaroui, Houria Djediai et Hanane Megdad (2014) The influence of soil, hydrology, vegetation and climate on desertification in El-Bayadh region (Algeria), Desalination and Water Treatment, 52:10-12, 2144-2150, DOI: 10.1080/19443994.2013.782571

LACROIX.M. R et all., 1980 : Conception, calcul et épreuves des ouvrages d´art, programmes de charges et épreuves des ponts-routes. Fascicule N° 61 titre II

Mishra, G. (2010, September 23). *Types of Losses in Prestress of Prestressed Concrete*. The Constructor. Retrieved July 7, 2024, from https://theconstructor.org/concrete/prestress-losses-prestressed-concrete/3287/

Oussadit, D. et Hadj, S. (2016) Etude d’un pont a poutres indépendantes en béton précontraint sur oued essam wilaya de Naama, Masters Thesis, Defended in 2016, Tlemcen, Algeria, 148p.

Setra. (1996). Ponts à poutres préfabriquées précontraintes par post-tension : guide de conception. Bagneux-cedex, France: Setra.

Shushkewich, K. W. (2012). Eugène Freyssinet—Invention of Prestressed Concrete and Precast Segmental Construction. *Structural Engineering International*, *22*(3), 415–420. https://doi.org/10.2749/101686612X13363869853338

Soliman, E. (2011, June). *Characteristics of prestressing, nonprestressing, and post-tensioning... | Download Table*. ResearchGate. Retrieved July 7, 2024, from https://www.researchgate.net/figure/Characteristics-of-prestressing-nonprestressing-and-post-tensioning-strands-for-CFCC_tbl1_256463091

Team Xometry. (2023, April 15). *Elastic Modulus: Definition, Values, and Examples*. Xometry. Retrieved July 7,2024,from https://www.xometry.com/resources/materials/modulus-of-elasticity/

TMG Global Pte Ltd. (2013-2018). *Prestressing*. Post Tensioning System. Retrieved July 7, 2024, from https://www.tmgglobals.com/prestressing

Thonier, h. (1985). Le béton précontraint aux états-limites (3ème éd). Paris, France : presses de l'école nationale des ponts et chaussées.

Understanding the losses in prestressing. (n.d.). PCI.org. Retrieved July 7, 2024, https://www.pci.org/PCI_Docs/Publications/PCI%20Journal/1969/October-1969/Understanding%20the%20Losses%20in%20Prestressing.pdf

Walter, P, Jnr. (1969). Understanding the losses in prestressing. Published on October 1969,14,43-53. *https://www.pci.org/PCI_Docs/Publications/PCI%20Journal/1969/October-1969/Understanding%20the%20Losses%20in%20Prestressing.pdf*

Yazid, a. (2005). Béton précontrainte- cours et exercices. Bechar, Algérie : centre universitaire de Bechar.